ALMA MATER STUDIORUM
UNIVERSITÀ DI BOLOGNA

DOTTORATO DI RICERCA IN

BIOLOGIA CELLULARE E MOLECOLARE

Ciclo 36

Settore Concorsuale: 05/D1 - FISIOLOGIA

Settore Scientifico Disciplinare: BIO/09 - FISIOLOGIA

KETOGENIC SUPPLEMENTATIONS FOR AGC1 DEFICIENCY: INVESTIGATING EPIGENETIC AND METABOLIC PATHS TO RECOVER PROLIFERATION AND DIFFERENTIATION OF OPCS AND NSCS IN VITRO MODELS

Presentata da: Giorgia Babini

Coordinatore Dottorato

Vincenzo Scarlato

Supervisore

Barbara Monti

Co-supervisore

Francesca Massenzio

Esame finale anno 2024

Index

1. ABSTRACT 5
2. INTRODUCTION 6
2.1 AGC1 deficiency 6
2.2 AGC1 carrier in Central Nervous System 7
2.3 Neurogenesis: embryonic and adult 9
2.4 Oligodendrogenesis 13
2.4.1 External Stimuli 14
2.4.2 Internal stimuli 15
2.4.2.1 Epigenetic regulation of OPCs proliferation and differentiation 16
2.5 Oligodendrocytes myelination and metabolism 18
2.5.1 Fatty acids synthesis pathway 22
2.6 Crosstalk between epigenetics and metabolism 25
2.6.1 Ketogenic diet 28
3. AIM 31
4. MATERIALS and METHODS 33
4.1 Cell cultures 33
4.1.1 Oli-Neu 33
4.1.2 Neurospheres 33
4.2 Supplementations 35
4.3 Livecyte proliferation analysis 35
4.4 Incucyte proliferation analysis 36
4.5 Western Blot 37
4.6 Immunofluorescence and BrdU Analysis 38
4.7 DNA extraction and PCR 40
4.8 RNA extraction and Real-Time PCR 42
4.9 RNA-seq 44
4.10 ATAC-seq 45
4.11 Quantitative metabolites concentrations 45
4.12 iPSC-derived Neural Progenitor Cells 46
4.13 Statistical Analysis 47
5. RESULTS 48
5.1 RNA-seq and *in vitro* analysis reveals alterations of fatty acids synthesis pathways in OPCs and neurospheres AGC1 deficiency models 48
5.2 ATAC-seq confirms the altered epigenetic landscape of siAGC1 Oli-Neu cells 54
5.3 Metabolic and epigenetic alterations in AGC1 deficiency models 56
5.4 BCAAs and KBs supplementations improve proliferation in AGC1 deficiency models 63

5.5 BCAAs and KBs supplementations restore the differentiation defects seen in Oli-Neu and neurospheres AGC1 deficiency models 73

5.6 Histone epigenetic modifications could explain the effects of KBs and BCAAs supplementations on OPCs model of AGC1 deficiency 82

5.7 Preliminary experiments on iPSC-derived Neural Precursor Cells confirm presence of proliferation defects 90

6. DISCUSSION 92

7. CONCLUSION 103

8. REFERENCES 105

1. ABSTRACT

AGC1 deficiency is an ultra-rare demyelinating disease caused by mutations in the *SLC25A12* gene, which encodes for isoform 1 of the mitochondrial aspartate-glutamate carrier (AGC1). The main pathological features are brain atrophy, growth retardation and secondary hypomyelination, along with impaired proliferation of brain cells. As demonstrated in patients, the abnormal myelin production is due to a reduced synthesis of N-acetyl-aspartate (NAA), from which the acetyl groups mainly derive. This, in turn, leads to epigenetic alterations in the brain precursor cells and resulting in transcriptional dysregulation, causing proliferation and differentiation defects, as demonstrated by previous data on our *in vitro* AGC1 deficiency models of our laboratory (precursor cells of mouse oligodendrocytes -OPCs- where *SLC25A12* is silenced by a shRNA and neurospheres by mouse model of AGC1 deficiency).

Along with epigenetic alterations, lower production of NAA leads specifically to reduced levels of acetyl-CoA, involved in many biological activities, including the synthesis of fatty acids, major components of the myelin sheath. Thus, an alteration of their production causes hypomyelination. This is confirmed by RNA-seq analysis and *in vitro* validation on OPCs and on neural stem cells model, which show altered expression of transcriptional factors and enzymes involved in the fatty acid synthesis pathway. Meanwhile, metabolomics analysis shows altered concentrations of many metabolites, as TCA cycle intermediates, amino acids and cofactors (NAD^+, CoA); whereas ATAC-seq confirmed the presence of abnormal epigenetic landscape, which could affect genes involved in many biological pathways.

To try to rebalance the epigenetic and metabolic alterations, supplementations with ketogenic compounds, as branched-chain amino acids and ketone bodies, will be carried out on OPCs and neurospheres, to induce a potential recovery of differentiation/proliferation defects, through epigenetic modifications restoration.

2. INTRODUCTION

2.1 AGC1 deficiency

AGC1 deficiency, also called Early Epileptic Infantile Encephalopathy 39 (EEIE39), is an ultra-rare demyelinating disease, caused by mutations in *SLC25A12* gene, encoding for Aspartate-Glutamate carrier 1 (AGC1/Aralar). Although the rare frequency of the disease, few cases were reported worldwide, with the first one in 2009 by (Wibom et al. 2009). The patient showed a non-functional AGC1 protein due to c.1769A → G transition in exon17 and, in turn, a Q590R substitution. Many other patients were identified, with different mutations on AGC1 carrier, some causing specific structural alterations (Pfeiffer et al. 2020), others affecting the binding site, as for Q590R, a highly conserved residue in the sequence of the protein. Despite these intrinsic differences, the main characteristics of the disease show up at early stage of infancy and comprise developmental delay, hypotonia, epilepsy and psychomotor activities deficits. Another important feature is an age-correlated hypomyelination, with progressive brain atrophy, especially concerning cortex and ventricles (Fig. 2.1). In parallel, reduction of N-acetyl-Aspartate (NAA) was detected through Magnetic Resonance Images (MRI); whereas an increase in lactate blood levels indicate a mitochondrial dysfunction in AGC1 deficiency patients (Falk et al. 2014).

At this time, no cure is still available, just ketogenic diet brought some psychomotor and myelination improvements. The first trial was for 6 years old AGC1 patient, in which carbohydrates restriction and high-fat and protein rate diet regimen was followed (Dahlin et al. 2015). After 20 months from the start of the treatment, patient showed motor skills improvements, as movements of arms and legs, together with a more intense interaction with external environment. From MRI, overall myelination increase was detected, too (Dahlin et al. 2015).

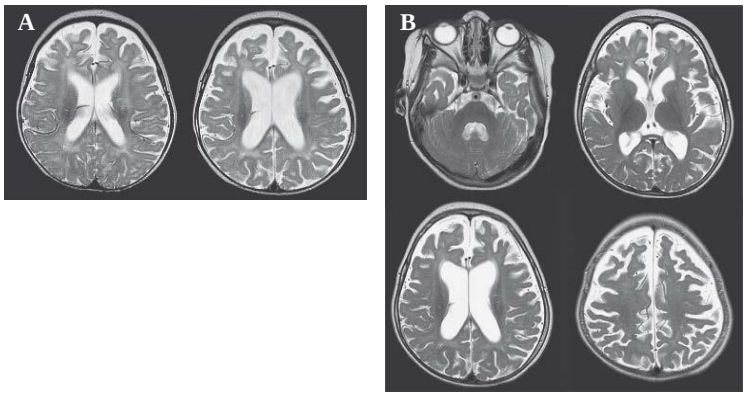

Fig. 2.1 AGC1 deficiency patient MRI. A) 8-month and 16-month MRI brain images. B) patient's MRI images at 2 years and 9 months of age. Images show ongoing hypomyelination, pale globe and putamen decrease in volume. Together with progressive reduction in brain volume and formation of prominent cortical sulci and ventricle enlargement (Wibom et al. 2009)

To study this pathology, different *in vivo* models were created. The first was by Jalil et al. (2005), a homozygous mouse model of AGC1 deficiency (Aralar $^{-/-}$) in which gene trapping techniques induced

formation of a truncated protein, through the presence of premature stop codon at exons 13-14 of the *SLC25A12* gene, in SVJ129/C57BL mice. This model showed up no embryonic lethality but after birth, the Aralar $^{-/-}$ mice had growth retard, lower lifespan, tremors and motor coordination defects, along with hypomyelination. In addition, *in vivo* and *in vitro* extracted neuronal cultures demonstrated an impairment of NAA production, suggesting a possible role of AGC1 carrier for this metabolite synthesis in the central nervous system (Jalil et al. 2005). This, in turn, could hamper the myelin formation, since acetyl moieties derived from NAA, are generally used for myelin lipids synthesis. One clear example is the galactocerebroside, the main myelin precursor, also seen reduced in the AGC1$^{-/-}$ mouse (Jalil et al. 2005). A quite similar model was obtained also by Sakurai et al., (2010), in which stop codon was inserted at exon 1, creating a fully inactive protein. Likewise, this model showed up growth retardation, tremors and shorter lifespan. In addition, neuronal and myelin abnormalities were identified *in vivo* but also in *in vitro* Oligodendrocyte Precursor Cells (OPCs) in which AGC1 was silenced. This reinforces the hypothesis of AGC1 involvement in myelination, which can be hampered not only through neuronal NAA synthesis defects (Satrústegui, Pardo, and del Arco 2007; Jalil et al. 2005; Ramos et al. 2011), but also via OPCs/oligodendrocytes developmental alterations, upon carrier mutations (Sakurai et al. 2010).

Defects regarding glial and neural cell precursors were also identified in Petralla *et al*., (2019) mouse model of AGC1 deficiency. They performed same gene trapping techniques but on different exon and genetic background (C57BL6/N), which firstly caused the embryonic mortality of homozygous AGC1 mice. Thus, AGC1 $^{+/-}$ were used and characterized, which better resembles pathophysiological characteristics of patients with partial AGC1 loss. This mouse didn't show morphological neither behavioural alterations respect to wild-type ones, but proliferation and differentiation defects were detected on neuronal and oligodendrocyte precursor cells, with reduced Olig2 positive cells (Petralla et al. 2019). This stresses the role of glial and neuronal crosstalk in the study of this pathology, suggesting a more complex pathogenetic mechanism, not only regarding the altered AGC1 activity in neuronal cells.

2.2 AGC1 carrier in Central Nervous System

As ATP-Mg/Pi transporters, AGCs are Calcium-binding Mitochondrial Carriers (CaMCs) consisting of three distinct domains: N-, C-terminal and an intermembrane one. The C-terminal domain has six transmembrane alpha-helices, whereas hydrophilic N-terminal contains several EF-hand motifs, in the intermembrane space, that are the site for the Ca-dependent regulation (Pebay-Peyroula and Brandolin 2004). However, of this site, just the first three EF-motifs are responsible for the carrier activity, inducing -upon Calcium binding- a conformational change in the other domains that allows

the passage of solutes. Instead, the remaining motifs are involved in the dimerization process, and channel opening/closing (Fig. 2.2; Thangaratnarajah, Ruprecht, and Kunji 2014; Palmieri et al. 2001).

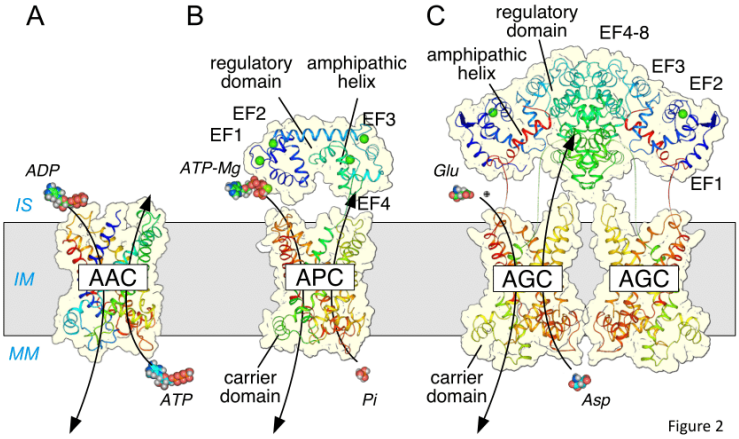

Fig. 2.2 General structures of mitochondrial carriers. AGC1 (c) is the only dimer (Kunji et al. 2020)

SLC25A12 gene belongs to the SLC25 family, together with *SLC25A13*. Indeed, two distinct isoforms of this carrier exist, AGC1 and AGC2, with different expression pattern but 77,8% sequence homology (L. Palmieri et al. 2001; Amoedo et al. 2016). The first, AGC1/Aralar is mainly expressed in excitable tissues (skeletal muscles and central nervous system); the second, AGC2/Citrin, was found in liver, kidney, and heart (del Arco and Satrústegui 1998; F. Palmieri 2013); even though they perform same functions. Despite this functional similarity, mutations on the two genes cause different pathologies: the demyelinating AGC1 deficiency for *SLC25A12* gene and the adult-onset type 2 citrullinemia (CTLN2) for *SLC25A13*, which in more severe cases can manifest as the neonatal intrahepatic cholestasis (NiCCD). These diseases are characterized by ammonia and citrulline high levels in blood, which cause confusion, hyperactivity, pancreatitis, hepatic steatosis, and comatose state in adults. While, in infants, enlarged liver, with low blood sugar are present, along with bilirubinemia and cirrhosis, but in this case, the disease tends to disappear with growth or evolves into T-2 citrullinemia (Amoedo et al. 2016; Kunji et al. 2020).

Functionally speaking, AGCs transport a molecule of aspartate from mitochondria to intermembrane space, in exchange of one molecule of glutamate and one proton (F. Palmieri 2013). In CNS, it was mainly found the AGC1 isoform, especially in neurons. Indeed, neuronal aspartate, once reached the cytosol, it's converted to N-Acetyl-Aspartate (NAA) by N-acetyl transferase (Asp-NAT), which adds a molecule of Acetyl-CoA. Then, through trans axonal transport, NAA is delivered to oligodendrocytes, via Na^+-dependent high-affinity dicarboxylate transporter (NADC3). Here, it undergoes another chemical reaction by Aspartoacylase (ASPA), which regenerates aspartate and acetate. This last will be used by cells to produce fatty acids and complex lipids, essential for myelin

synthesis (Urenjak et al. 1993; Wiame et al. 2010). For this reason, the correct functioning of this carrier is crucial to maintain the myelination process in CNS.

In addition, AGC1 belongs to the Malate-Aspartate Shuttle (MAS). It's one of the most important shuttles in cells that allows to balance the NADH levels between mitochondrial matrix and cytoplasm. It's composed by two carriers, AGC1 and OGC (oxoglutarate carrier) and two pairs of cytosolic and mitochondrial enzymes, glutamate oxaloacetate transaminases (GOT) 1 and 2, and malate dehydrogenases (MDH) 1 and 2, respectively. Since the mitochondrial membrane is impermeable to $NADH/NAD^+$, a coordinated activity among all these players is essential to transfer the reducing equivalents, produced by glycolysis in the cytosol, to the mitochondria. This ensures the proper redox balance within the cell; it's important, not only to speed up glycolysis in cytoplasm and OXPHOS (oxidative phosphorylation) in mitochondria, but also for many other cell functions, as signal transduction and protection against oxidative stress (Fig. 2.3; Broeks et al. 2021; Pardo et al. 2022). For this reason, alterations upon AGC1 expression or function can hamper different biological pathways.

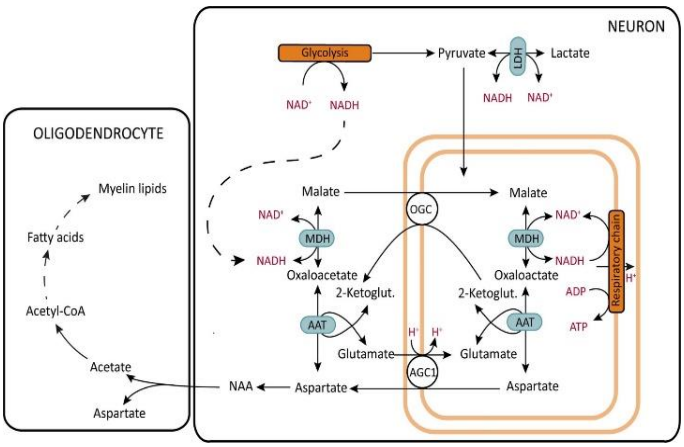

Fig. 2.3 AGC1 function in Central Nervous System. Here, neuronal Aspartate is exported to cytoplasm where it's converted to NAA, a precursor of myelin lipids in oligodendrocytes (Dahlin et al. 2015)

2.3 Neurogenesis: embryonic and adult

Neurogenesis is the process by which multipotent Neural Stem Cells (NSCs) can form different brain cells – neuronal, glial or ependymal. In fact, NSCs can divide, maintaining their stemness (self-renewal or symmetric division) or differentiate into different neural lineages (asymmetric division), forming the specific progenitors which then, migrate and maturate completely. In mammals, neurogenesis mainly happens during embryonic development, even though there're some neurogenic niches also in adult brain (Pino et al. 2017).

During embryonic development, three layers of cells constitute the basis for all tissues and organs formation: ectoderm, endoderm and mesoderm. From the outer or more dorsal layer, ectoderm, CNS

will be formed. Indeed, the neural plate, a thickening of ectoderm, starts to invaginate creating the neural tube, through neurulation process. Its growth proceeds caudally and rostrally, forming spinal cord and three brain vesicles (fore, mid and hindbrain), respectively (de Lahunta, Glass, and Kent 2016). Within wall of neural tube, the pseudostratified neuroepithelium -constituted of neuroectodermal cells- forms the ventricular zone (VZ). This is the primary embryonic neurogenic niche, from which CNS develops, also postnatally. This layer will give rise to all neuronal and glial progenitors and cells, following symmetrical and asymmetrical divisions, in a series of growth and differentiation processes (Silbereis et al. 2016; Darnell and Gilbert 2017). Specifically, at the beginning, their divisions are symmetric to ensure an abundant pool of stem cells for self-renewal, but then, they start to restrict their stemness, following a specific commitment of differentiation, upon presence/absence of different stimuli. At ninth embryonic day (in mice) or 5-6 gestation week (in humans), NSCs start to become Radial Glial Cells (RGCs), which have many astrocyte-specific markers. Indeed, they express Glial Fibrillar Acidic Protein (GFAP), astrocyte-specific glutamate transporter (GLAST), Brain Lipid-Binding Protein (BLBP), and Tenascin C (TN-C). However, similarly to NSCs, they have an apical-basal polarity, with long processes, extended from VZ, where their cell bodies reside, to pial and neocortical surface. In addition, they maintain their multipotency and express Nestin marker (A. R. Kriegstein and Götz 2003; Beattie and Hippenmeyer 2017). These characteristics allow to perform amplification -maintaining a pool of RGCs- but also asymmetric division, which produces a new RG but also IPC (Intermediate Progenitor Cell). These last express pro-neural genes, Neurog2 and Pax6, highlighting a neuronal commitment and differentiation, and generally migrate along RG processes, towards a region, the Sub-Ventricular Zone (SVZ), which will become a new neurogenic niche (A. Kriegstein and Alvarez-Buylla 2009). Depending on localization, time and morphogens exposition, RG can produce different neuronal types (Hochstim et al. 2008), which then migrate through an inside-out mechanism, to form 6 layers of cortex. Specifically, the cells in the deeper layers are the first to be produced and have the highest ability to produce all other 6-layers cell types, whereas the most external are the younger and have a more reduced spectrum (Noctor, Martínez-Cerdeño, and Kriegstein 2008; Noctor et al. 2004; Nowakowski et al. 2016). Once arrived in their position, all neurons start to create junctions and express adhesion molecules to create functional unit (Darnell and Gilbert 2017).

At the end of neuronal production, RGCs can detach from VZ and move toward cortex/subcortical regions, where activation of astrocytic genes (GFAP, Nfia) induce differentiation into astrocytes, with multipolar morphology; whereas others remain there, in an undifferentiated state, proliferating in CNS (Fig. 2.4; Noctor, Martínez-Cerdeño, and Kriegstein 2008).

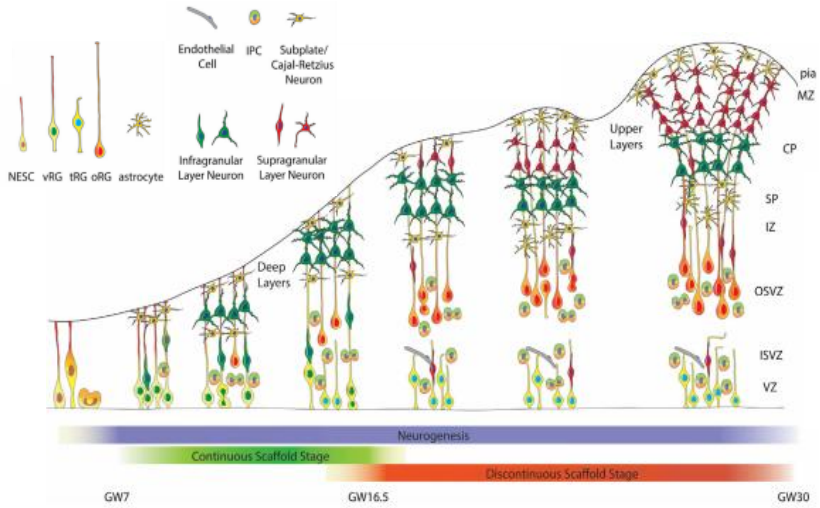

Fig. 2.4 Cortical development. VZ, ventricular zone; NESC, neuroepithelial stem cell; ISVZ, inner subventricular zone; OSVZ, outer subventricular zone; IZ, intermediate zone; SP, subplate; CP, cortical plate; MZ, marginal zone; IPC, intermediate progenitor cell; vRG, ventricular radial glia; tRG, truncated radial glia; oRG, outer radial glia (Nowakowski et al. 2016)

Beside previous knowledges, also adult brain has neurogenic niches, in two distinct areas: the Dentate Gyrus (DG) and Sub-Ventricular Zone. From first region, resident RGCs can origin the dentate gyrus granule cells, starting from asymmetric division, which generates daughter cells with a high proliferative capacity. Upon migration from sub granular zone to the granule cell layer, they completely differentiate into granule neurones (Fig. 2.5; Cope and Gould 2019). These obtained neurons are mainly involved in memory and learning systems (Kumar et al. 2019).

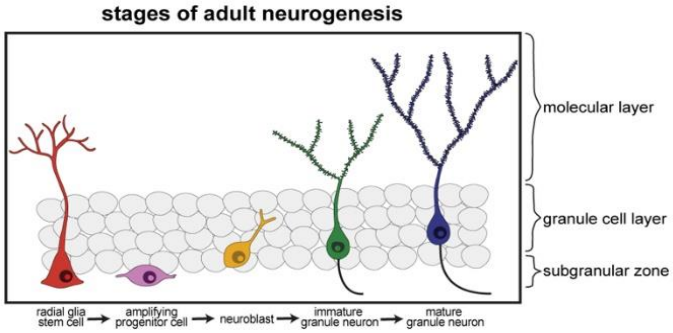

Fig. 2.5 Adult neurogenesis in Dentate Gyrus. From Radial Glial cells to mature granule neuron, through neuroblast (Cope and Gould 2019)

For what concerning neurogenesis in SVZ, it's thought to be essential for olfaction and olfactory bulb circuitries (Kumar et al. 2019; Bergmann et al., 2015). Here, resident NSCs -called B1 cells- are placed within lateral ventricles walls and maintain some characteristics of astrocytes: GFAP, GLAST and BLBP expression; alongside contacts with blood vessels, but, as RGCs, they can be quiescent or actively proliferating. In this case, they express Nestin, and can give rise to TAC (Transit-Amplifying Cells, or type C cells). In turn, TACs symmetrically divide to generate neuroblasts (type A cells), which migrate to the olfactory bulb (Fig. 2.6; Lim and Alvarez-Buylla 2016).

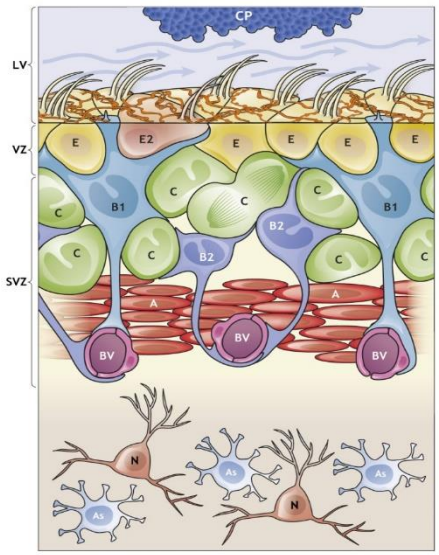

Fig. 2.6 Neurogenesis in lateral ventricles (LV). B1 cells (light blue) act as NSCs, giving rise to TAC (C cells; green). They, in turn, originate young neurons (A cells; red). Cerebrospinal fluid (CSF; blue arrows); Choroid Plexus (CP; blue); Ependymal Cells (E/E2 cells); mature neurons (N; orange); astrocytes (As; pale blue; Obernier and Alvarez-Buylla 2019)

The B1 cells can origin different types of interneurons depending on their location, but they can also give rise to glial cells – oligodendrocytes and astrocytes (Obernier and Alvarez-Buylla 2019). Indeed, clue of their multipotency was identified firstly by Menn et al. (2006) together with ability to produce oligodendrocytes or astrocytes, after brain injury (Lim and Alvarez-Buylla 2016). This suggests a role of these cells during brain trauma and a possible use for regenerative medicine. For this reason, SVZ neurogenesis and B1 cells are more studied than DG neurogenic process, also thanks to their ease to manipulation, and the possibility to create *in vitro* cultures (Obernier and Alvarez-Buylla 2019). One clear example are the neurospheres. They are floating 3D cultures of NSCs and neural progenitors, at different differentiation stages, mainly derived by SVZ of mice. Reynolds and Weiss, in 1992, were the first to discover and describe neurospheres as a pool of neural stem cells (Ahmed 2009). They maintain *in vitro* their stemness, with a high proliferative capacity, when plating with mitogens (EGF and FGF-2), in suspension. Instead, upon passage on adhesive matrixes (as fibronectin), they start to differentiate and originate neuron, oligodendrocytes or astrocytes (Fig. 2.7; Gil-Perotín et al. 2013).

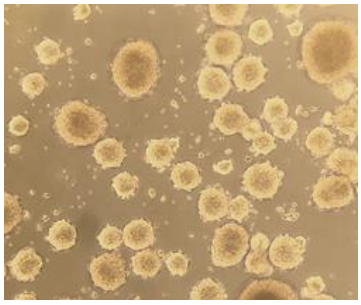

Fig. 2.7 Neurospheres culture, obtained from SVZ. The Image was acquired through optical microscopy ad 40X objective

Since they better resemble *in vivo* physiological environment, mimicking the extracellular matrix components and maintaining their stemness, neurospheres are widely use to study proliferation, differentiation and self-renewal processes of NSCs. Such applications span from study of molecules and treatment on neurogenic niches, through basic analysis of proliferation/differentiation processes in pathological conditions, to cell replacement therapy, overcoming the ethical and limited availability of fetal tissues-deriving cells (Jensen and Parmar 2006).

2.4 Oligodendrogenesis

Despite the central role of neurons in the study of nervous system, nowadays, researchers are starting draw attention to glial cells, too. Indeed, within CNS, they are as important as neurons, for the correct functioning of all biological processes. Even though at preliminary stages, much has been discovered about glial cell production, and particularly oligodendrogenesis.

Oligodendrocytes are cells of CNS responsible for myelin formation and axonal myelination. This ensures, not just the correct electric impulses propagation and speed, but also metabolic and trophic support to neurons (Antontseva and Bondar 2021). Oligodendrocytes production starts lately respect to neuronal and astrocytic ones, during final stages of embryonic development and they are fully generated after birth, postnatally (Malatesta, Hartfuss, and Götz 2000). All derive from OPCs (Oligodendrocyte Precursor Cells) which give rise from RDGs, upon Sonic Hedgehog (Shh) expression, a morphogenic transcription factor with the highest concentration in the ventral area (Rowitch and Kriegstein 2010). The OPCs are small uni/bipolar cells, expressing NG2 (proteoglycan) and PDGFRα (platelet-derived growth factor receptor alpha), in addition to SOX10, O4 antigen, Olig1, Olig2 (basic helix–loop–helix transcription factors) and Nkx2.2 (homeodomain transcription factor; Amaral et al. 2016; Fancy, Zhao, and Franklin 2004). They populate the brain parenchyma with myelinating OLs following specific waves of OPCs production and differentiation, namely three, along the entire CNS development. A first one occurs during E12,5 in mice, starting from ventral area, then second and third waves arise from caudal and cortical regions, after birth (El Waly et al. 2014). At the beginning of oligodendrogenesis, OPCs generally divide producing two OLs, to create excess of cells, which then, upon competition for growth factors (as PDGF-α; IGF-1, Insulin Growth Factor-1 and FGF-2, Fibroblast Growth Factor-2) are reduced through apoptosis (Antontseva and Bondar 2021). Instead, since OPCs persist also throughout adulthood, in mature brain, their division gives rise to two OPCs or one OPC and one OL, reducing the ability to produce myelinating oligodendrocytes (Nishiyama et al. 2021). The presence of OPCs in adults allows the re-myelination process after brain trauma or injury, but also for myelin turnover (Elbaz and Popko 2019).

Thank to their high migratory ability, OPCs move towards all developing brain regions, where differentiate into mature OLs and this characteristic is maintained also during adulthood, where quiescent OPCs start to migrate upon specific stimuli to induce remyelination. This migration is guided by different types of stimuli (Tsai et al. 2016): intrinsic, as the proteoglycan NG2, which is essential to induce cell polarization and changes in soma morphology for polarization and migration (Biname et al. 2013) but also, PDGF-α. Its active form is composed as homo/heterodimers of A and B chains, where the PDGF-A is mainly released by neurons and astrocytes, whereas PDGF-B from endothelial cells. To exert their different functions, they bind to PDGFR-α and PDGFR-β, on cells surface and controls many different biological pathways, as migration but also proliferation (Fruttiger et al. 1999; Sugimoto et al. 2001).

After reaching their site in brain parenchyma, OPCs exit form cell cycle and start to differentiate, mainly through the activity of TGFβ (Transforming Growth Factor β) signalling. This cascade involved two different receptors, TGFβR-I and TGFβR-II, to which TGFβ1 binds and activates, causing the SMAD2/3 stimulation. This, in turn, induces expression of cyclin-dependent kinase inhibitors (p15, p21 and p27), via Fox01 and Sp1. The activity of these CdKi brings to repression of the pro-mitotic transcription factor, c-Myc, which immediately stops the proliferation (Palazuelos, Klingener, and Aguirre 2014). This suggest an opposite action of TGFβ respect to PDGFα, which instead is a potent mitogen, and their well-controlled balance in OPCs maturation (Dutta et al. 2014). To complete differentiation, Olig1 and MRF transcription factors are expressed and they activate the myelin genes and mature OLs markers, as MAG (Meylin Associated Glycoprotein), PLP (Proteolipid Protein) and CNPase. After that, myelinating OLs can wrap around axons and create the myelin sheet (Barateiro and Fernandes 2014).

Since OLs persist in adult brain, the regulation of OPCs proliferation and differentiation needs to be tightly controlled and balanced. Alterations upon them can induce severe defects in terms of brain development and myelination. Thus, different types of stimuli, intrinsic and extrinsic, regulate these processes.

2.4.1 External Stimuli

Among the external stimuli, we find ligands and molecules expressed by axons, which guides the myelination, thus OPCs differentiation and maturation. Clear examples are Lingo-1, Jagged, which interact with Notch receptor on oligodendrocytes precursors surface, inhibiting cell maturation. In addition, also the Wnt/β-catenin canonical pathway was found to have complex role in OPCs maturation, since its activity, together with its effectors Tcf4/Tcf7l2, generally are downregulated in mature OLs, suggesting a possible regulatory mechanism on proliferation (Emery 2010; Fancy, Zhao,

and Franklin 2004). Also, the neuronal activity can induce cell cycle exit and OPCs maturation to allow the so-called adaptive myelination, myelination of a specific active neural circuit (Amaral et al. 2016). This happens through electrical activity which causes an initially increase of OPC proliferation, followed by alteration of the chromatin state, which tends to become more "closed", a sign of differentiation. Upon this change, OPCs start to express myelin genes, as Myelin Basic Protein (MBP) and myelinate (Gibson et al. 2014). This relation between axons and OPCs is possible through expression of ionotropic glutamate receptors on their surface, especially AMPA, even though not through an all-or-nothing mechanism, but maturation requires other stimuli to be induced (Nishiyama et al. 2021).

2.4.2 Internal stimuli

Among the internal stimuli that control the correct timing for proliferation and differentiation of OPCs, we can identify different categories of main players. The most known and important are the transcription factors (TFs). The first acting on brain progenitors to induce oligodendroglial commitment, is Olig2 (Emery 2010). This basic helix-loop-helix transcription factor is present throughout the entire oligodendroglial lineage and is essential to induce expression of many downstream OLs markers, as Olig1, Nkx2.2, Sox10, Ascl1, YY1, and Tcf4 (El Waly et al. 2014). Specifically, Olig2 and Nkx2.2 concomitant expression is pivotal for differentiation (Fig. 2.8; Elbaz and Popko 2019). The homeobox and Sox family members TFs as Nkx2.2 and Sox8, 9 and 10 are all expressed during oligodendrogenesis, even though the specification of OLs lineage is a responsibility restricted only to Olig2 and just in some cases, as in *Olig2*-null mice, compensated by Olig1 (El Waly et al. 2014).

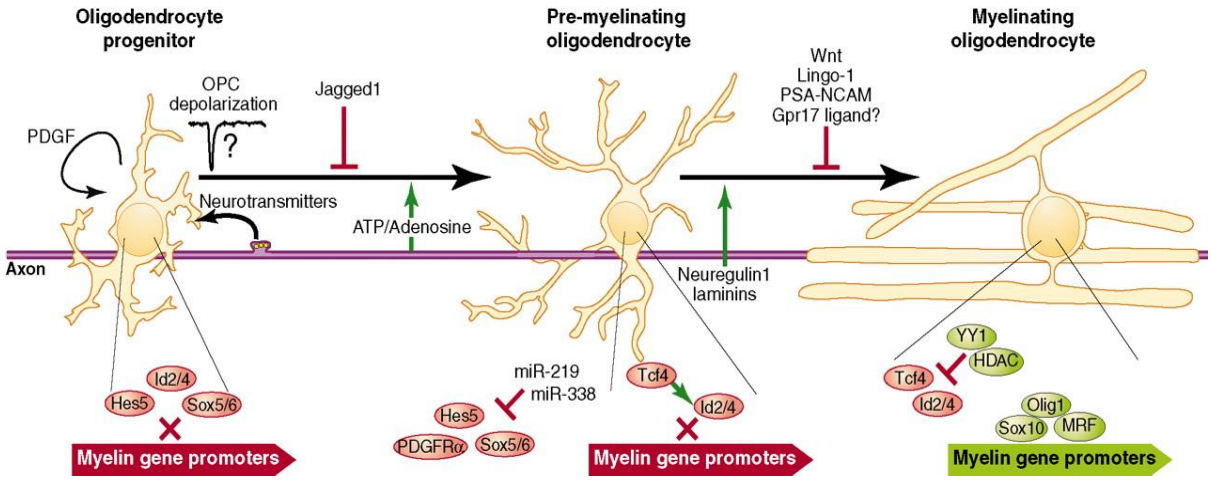

Fig. 2.8 Maturation of OPCs to myelinating oligodendrocytes. This process is tightly regulated by many transcription factors that works synergistically (Emery 2010).

Also, micro-RNAs are involved in OPCs maturation, mainly speeding up the differentiation of OPCs, by inhibiting PDGFα and Sox6. Zhao et al. (2010) indeed proved that in *in vitro* and in *Dicer*-deficient

mice, mir-219 and mir-338 allowed OPCs differentiation, rescuing the myelination defects. In contrast, mir-7a was discovered in oligodendrocyte precursors and its ablation could impair their specification, with a reduction in their pool from NSCs, during brain development (Zhao et al. 2012).

2.4.2.1 Epigenetic regulation of OPCs proliferation and differentiation

Among internal stimuli that control OPCs fate decision and maturation, epigenetic modifications hold a central role. They are persistent DNA changes, which modify genes expression without affecting the nucleotides sequence. Together with microRNAs, they include chromatin remodelers, DNA methylation and histones modifications. Since their plasticity, they allow to NSCs and OPCs to maturate and differentiate depending on environmental clues (Berry, Wang, and Lu 2020). Indeed, previous studies and from literature, epigenetic modifications take part in OPC/OL development, especially controlling the timing of specific genes expression (Tiane et al., 2019). Notably, different proteins are responsible of these modifications: HATs, histone acetyltransferase, which, adding acetyl groups to histone tails, induce relaxation in the chromatin structure, forming the euchromatin. CBP/p300, GNAT and MYST are the three major classes of HATs. Instead, HDACs, histone deacetylases, remove these chemical groups, creating a more closed structure of chromatin, called heterochromatin (Kouzarides 2007). Among them, we find class I (1-3), class II (4-7, 9 and 10) and IV (11). Different stages of differentiation in OPCs and OLs are characterized by specific chromatin structure, given their distinct needs. In details, OPCs, which are proliferative cells with a high levels of RNA transcription, require a more open chromatin, to allows gene accessibility, recruiting especially HATs proteins on cell cycle genes, but also on a group of transcriptional inhibitors (as Id2/4, Hes1/5). In this way, these latter can block the transcription of differentiation-associated genes with three different mechanisms: recruiting repressive complex constituted by HDACs on promoter of myelin genes, or to promoter of activators of myelin gene transcription, or in addition, through protein-protein interaction, they can sequestrate these transcriptional activators. The result is the inhibition of differentiation process and a high level of proliferation (Fig. 2.9 a; Berry, Wang, and Lu 2020; Hernandez and Casaccia 2015a). During differentiation, an opposite trend occurs, with formation of heterochromatin, due to higher activity of HDACs, especially on promoters of transcriptional inhibitors, that thus are repressed. In contrast, HATs recruitment on myelin genes allows expression of main proteins and enzymes involved in myelination. Together with inhibition of cell cycle genes, these orchestrated events grant OPCs differentiation (Fig. 2.9 b; Hernandez and Casaccia 2015a).

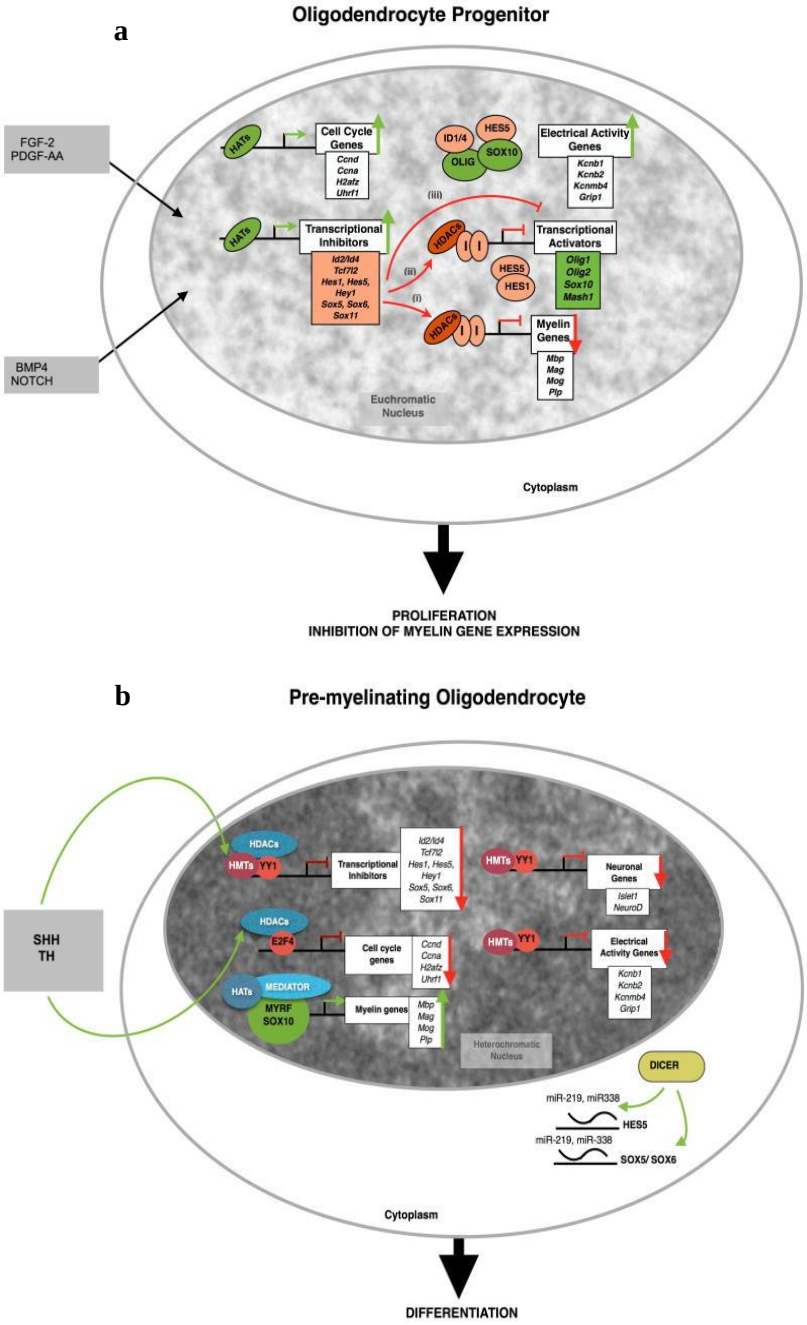

Fig. 2.9 Roles of HATs and HDACs in genes regulation during OPCs maintenance (a) and differentiation (b; Hernandez and Casaccia 2015)

This temporal controlled window is essential to ensure the correct timing of OPC proliferation and maturation and testify the crucial role of HDCAs in this process. Indeed, HDCA inhibition through tricostatin A prevents suppression of transcriptional inhibitors, affecting the OL maturation process (Conway et al. 2012). Similarly, in Neural Progenitors Cells, a premature repression of these deacetylases can induce myelin gene expression, upon thyroid hormone treatment (Castelo-Branco et al. 2014). Crucial role of HDAC on OPC differentiation could also be exerted through non-histone-dependent activity, as protein deacetylation involving transcription factors (Tiane et al., 2019). A clear example is OLIG1 (found by Dai et al. 2015) which, upon HDAC-mediated deacetylation, can't

interact with ID2. Consequently, it enters in the nucleus and promotes OPC differentiation. In parallel, HDAC1 and 2 can also create a repressive complex which, acting on Id2/4 and Hes5 promoters, blocks their expression and allows myelin gene expression (Liu and Casaccia 2010).

Similarly, histone methylation takes part in OPC maturation. This modification can exert a positive or negative effects on gene expression, given that H3K4me3 is generally associated with gene transcription, whereas H3K9me3 is mainly repressive (Berry, Wang, and Lu 2020). Enzymes responsible for this modification are the histone methyltransferases, whose pharmacological inhibition suggested a possible role of these proteins in OL commitment. Indeed, it was found by Liu et al., that a timely regulation of histone methylation is essential for transition from NSCs to OLs, through OPC stage. Particularly, H3K27me3 acts early on neural stem cells to silence gene for neuronal lineage, allowing oligodendroglial commitment; subsequently, H3K9me3 represses genes encoding ion channels and neurotransmitters signals, for the complete maturation of OPC to oligodendrocytes (Liu et al. 2015).

Another class of HDACs are sirtuins. They are NAD-dependent deacetylase which have a plethora of functional roles, from DNA stress repair, cell metabolism and cell cycle progression. There were identified 7 distinct types of sirtuins, which differ for their N and C-terminal, essential for activators/inhibitors binding but also for their subcellular localization. Indeed, sirtuins 3, 4 and 5 reside in the mitochondria; sirtuins 1, 6 and 7 are nuclear; whereas the 2 is cytoplasmatic (Carafa et al. 2016). Especially for those subtypes localized in the nucleus, sirtuins can exert effects also on histone modifications, acting on OPC/OL maturation. Yan et al., suggested that SIRT1 is crucial for oligodendrocyte differentiation (Yan et al. 2022) but its inhibition can allow OPCs pool expansion, without detrimental effects on their differentiation (Prozorovski et al. 2019; Rafalski et al. 2013a). Instead, SIRT2 can support OPC differentiation, by repressing the PDGFα receptor in oligodendroglial cell line (Yan et al. 2022). This result was confirmed also by Hisahara et al. (2021), which prove the negative effects of SIRT1 and 2 over differentiation, upon their knock-down in a mouse model. Here, oligodendrocytes presented more branched and numerous processes , with an upregulation of Myelin Basic Protein.
Overall, all these data suggest a central role of epigenetic modifications in cell cycle progression but a lot is to be known about their regulation in OPC/OL maturation process.

2.5 Oligodendrocytes myelination and metabolism

Once become mature, oligodendrocytes start wrapping around axons and creates myelin (Mitew et al., 2014). This is a highly organized multi-lamellar structure, constituted by cytoplasmatic extensions of OLs that are organized in segments, interspersed with nodes of Ranvier. These gaps in myelin

sheath allow the saltatory conduction of the action potentials, by concentrating the voltage-gated Na^+ channels (López-Muguruza and Matute 2023; Montani 2021). Myelin structure is similar to membrane composition but with some peculiarities. Indeed, it's constituted mainly by water and lipids, with a high percentage of cholesterol, phospholipid (ethanolamine phosphatide and phosphatidylcholine) and glycolipids (galactosyl ceramide and sulfatide). The acyl tails of the latter allow the formation of a compact structure; while cholesterol and phospholipids are arranged at high concentrations regions called lipid rafts, crucial for myelin fluidity, but also to guide proteins at their specific locations (Poitelon, Kopec, and Belin 2020; Montani 2021). Indeed, another key compound forming myelin sheath are the proteins, which have structural and functional roles. Proteomic analysis reveals a plethora of different proteins, but half of them comprises: MBP (Myelin Basic Protein) and PLP (Proteolipid protein; Soldán and Pirko 2012). The first one is a protein with highly disordered structure, with a key role in formation of compact myelin. Indeed, it's localized on surface of OLs, where it binds negatively charged lipids, through electrostatic interactions, and allows adhesion of the multi layers of myelin, creating a solid and compact sheath. Notably, rodents lacking for MBP gene are characterized by loss of compact myelin, with reduction of myelin sheath thickness, also in Peripheral Nervous System (Boggs 2006). PLP instead is a highly hydrophobic transmembrane protein which, upon translation in endoplasmic reticulum, it's sent to Golgi Apparatus where it's conjugated with myelin lipids, to constitute lipids rafts. Thus, it has structural role, compacting the myelin layers, but it's also involved in other cell functions. The most important is OLs proliferation and development, considering that duplications/deletions of *PLP* gene in animal models bring to loss of oligodendrocytes via apoptosis (Greer and Lees 2002). Other key proteins of myelin layers are CNPase (2',3'-Cyclic Nucleotide 3'-Phosphodiesterase) localized on myelin cytoplasmatic side, MAG (Myelin Associated Glycoprotein), which allows the identification of myelinated/unmyelinated axons by oligodendrocytes processes and, lastly, MOG (Myelin Oligodendrocyte Glycoprotein), essential for the structural integrity of myelin (Fig. 2.10; Laule et al. 2007).

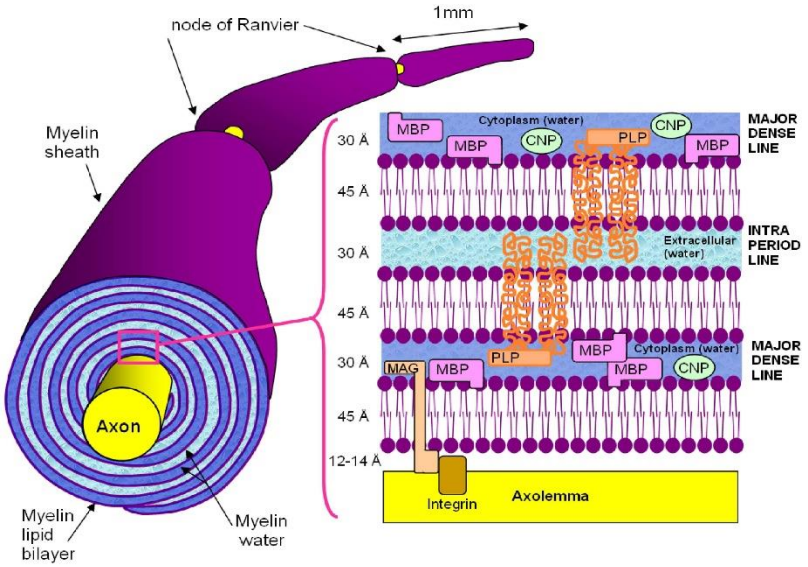

Fig. 2.10 Structure of myelin sheath around axon, and its internal composition constituted mainly by different proteins dipped into the multi lipidic layers (Laule et al. 2007)

To achieve complete OLs differentiation and myelination, a variety of morphological and structural changes are essential. However, these are highly energy demanding modifications, which require tightly controlled metabolism. Indeed, any alterations regarding lipids and proteins metabolism can affect the correct myelin formation, causing hypomyelination and leukodystrophies (abnormalities of white matter in CNS; Montani 2021). Since the great cost that myelination and myelin turnover require, OLs were found to have a high energy demand and this makes them more susceptible to energy deprivation (Rosko et al. 2019). Notably, brain bioenergetics was only recently found to be crucial in neurodegenerative disorders pathophysiology and a lot is still unknown about non-neuronal cells metabolism.

Brain is the most energy-demanding organ of our body, and glucose is its major carbon source. It's generally catabolized through oxidative glycolysis, which converts it into glucose-6-phosphate. This then can follow different destinations: the glycolytic pathway, the pentose phosphate pathway (PPP) or stored as glycogen. Just with the first two metabolic routes, glucose can be converted to acetyl-CoA, via pyruvate formation. From the cytoplasm, in presence of oxygen, acetyl-CoA enters the TCA cycle in mitochondria, where, through NADH and $FADH_2$ generation, can feed the electron transport chain and creates ATP. This is the oxidative phosphorylation pathway (OXPHOS), a more efficient way to produce energy in the cell than glycolysis, which instead is mainly used in anaerobic conditions. An exception are tumour cells, which preferentially use glycolysis, even in presence of oxygen (Warburg Effect; Fig. 2.11; Narine and Colognato 2022).

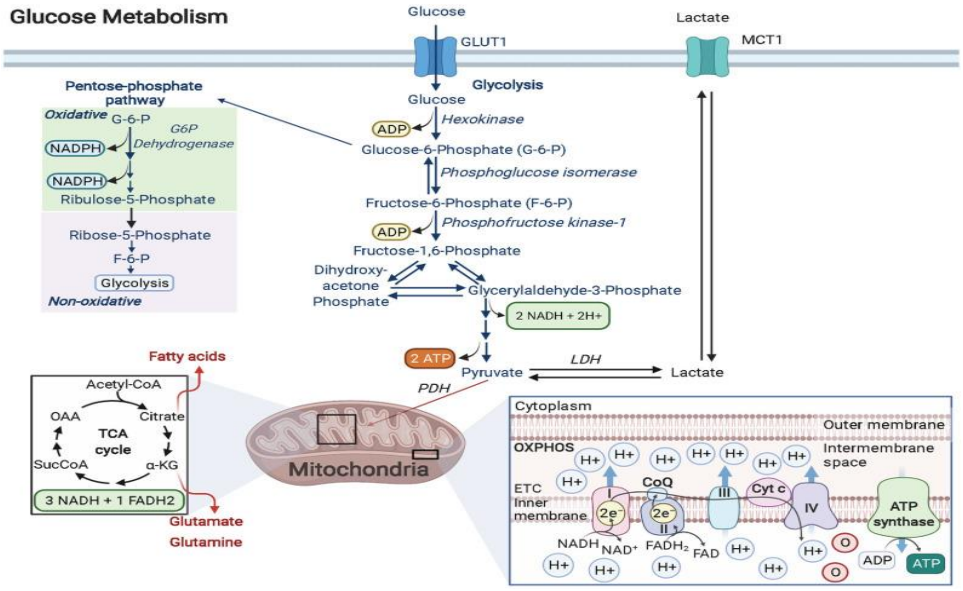

Fig. 2.11 OPCs/OLs glucose metabolism can follow different destinations, from PPP to glycolysis, necessary for energy but also macromolecules production, as proteins and lipids (Narine and Colognato 2022)

Preferences for one of these metabolic pathways depends on different parameters, first, the differentiation stage of OLs. Indeed, it was noted that treatment with rotenone (inhibitor of complex I of electron transport chain) which interferes with OXPHOS, reduced the viability of differentiating oligodendrocytes, while mature OLs seemed not affected. It was clear that OPCs and pre-myelinating OLs use oxidative phosphorylation for ATP production, whereas OLs or oligodendrocytes derived from adult tissues prefer glycolysis (Tepavčević 2021). Thus, metabolic shift is essential and affects the differentiation of OPCs. Indeed, during hypoglycaemic conditions, OLs just reduce their energy state, using glycolysis and blocking the myelin formation to favour survival, until nutrients level increases. Instead, OPCs require more ATP to sustain their physiological functions, thus, under nutrients deprivation, they can't reach a low metabolic state, and generally differentiate or die (Narine and Colognato 2022; Rosko et al. 2019). The ability of mature OLs to achieve their energy demand just through glycolysis relies on usage of alternative source of energy, as lactate. This can be produced from NADH and pyruvate, through reaction catalysed by Lactate Dehydrogenase (LDH) and used for acetyl-CoA and ATP production. In parallel, lactate could be also exported through Monocarboxylate Transporters (MCTs) to axons, where it acts as trophic support for neurons (Meyer and Rinholm 2021). This metabolite is not only vital for myelin formation, supporting remyelination upon Cuprizone-induced demyelinating lesions, but it can also help OPCs differentiation and cell cycle (Ichihara et al., 2017).

From glycolytic reactions, glucose can also be directed to Pentose Phosphate Pathway, a biosynthetic pathway which doesn't produce ATP. About 10-15% of glucose entering OLs is conveyed towards this pathway, with the production of glutathione (protects myelin from reactive oxygen species),

pyruvate for acetyl-CoA production but also NADPH for nucleotides and lipids synthesis. For this reason, altered PPP enzymes' expression were detected in diseases involving oligodendrocytes defects, as Multiple Sclerosis (Amaral et al. 2016).

Another metabolic process branching from glycolysis is the Hexosamine Pathway. Through this route, fructose-6-phosphate is converted into uridine diphosphate N-acetylglucosamine, a key molecule to produce glycoproteins, glycolipids and proteoglycans. For this reason, alterations of its enzymes can affect myelin composition, in which glycosylated molecules are abundant and crucial for its composition (Tepavčević 2021).

2.5.1 Fatty acids synthesis pathway

Among all metabolic routes, the fatty acid (FA) and myelin lipids synthesis pathway plays a vital role in OLs, since it sustains the myelination and remyelination processes. Alterations of lipid metabolism can affect especially myelin structure and composition (López-Muguruza and Matute 2023).

Fatty acids synthesis is an anabolic pathway, occurring in the cytoplasm, which extends, through a series of decarboxylation reactions, an alkanoic chain. Indeed, in physiological conditions, ATP-Citrate Lyase (ACLY) converts citrate into acetyl-CoA, which is then carboxylate to malonyl-CoA by Acetyl-CoA Carboxylase (ACC). After this reaction, malonyl-CoA and acetyl-CoA are used to create palmitic acids, via the rate-limiting enzyme, FASN (Fatty Acids Synthase N), upon serial condensation reactions for the elongations of the acyl chain. This lipid is then subjected to other desaturations and condensations, to create complex lipids, as phospholipids, sphingolipids (Garcia Corrales et al. 2021).

This metabolic pathway is tightly regulated by SREBPs (Sterol Regulatory Binding Proteins) family proteins, which includes SREBP1, with two isoforms 1a (in spleen and intestine) and 1c (in liver, skeletal muscles and brain), and SREBP2 (Eberlé et al. 2004). They are basic helix-loop-helix/leucine zipper transcription factors which, upon maturation, enters within the nucleus where they can bind DNA through recognition of SRE (Sterol Regulatory Elements) sequences and allow transcription of their target genes. Above overlapping functions shared among all isoforms, a peculiar specificity was also identified for each of them. Mainly SREBP1 is responsible for transcription of genes involved in FA synthesis pathway, as FASN and ACC. Instead SREBP2 regulates expression of proteins, as HMG-CoA reductase (3-Hydroxy-3-MethylGlutaryl-CoA), essential for cholesterol production (Monnerie et al. 2017). As already said, to be functionally active, SREBPs need to be cleaved and released into the nucleus. Indeed, these proteins are attached to Endoplasmic Reticulum (ER), anchored through SCAP (SREBP Activating Protein) binding. This is a sensor of sterol levels which, upon depletion of sterols, transports SREBP to Golgi apparatus, where S1 and S2 proteases (Site 1/2

Proteases) induced two proteolytic cleavages. These release the N-terminal of the protein, which can translocate into the nucleus. In addition, also insulin concentration acts on SREBP activation, through the activity of InsIG protein (Insulin Induced Gene), partner of SCAP for SREBP retention in the ER (Fig. 2.12;Eberlé et al. 2004).

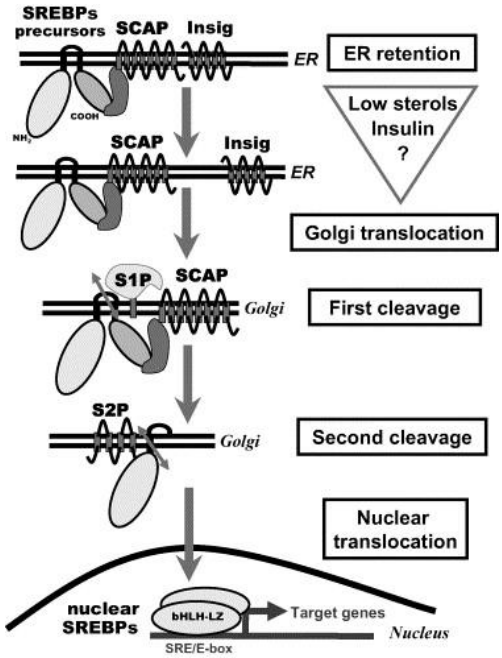

Fig. 2.12 Maturation and translocation of SREBP from ER to nucleus (Eberlé et al. 2004)

Many other proteins are involved in SREBP transcriptional regulation. Among others, there's mTORC1, which through its Raptor subunit, can help the cleavage of this TF, promoting SREBP activation (Dimas et al. 2019; Narine and Colognato 2022). On the contrary, Sirtuin 6, a NAD-dependent histone deacetylase, belonging to sirtuins family, exerts a negative action on SREBP. Specifically, this deacetylase can reduce its transcription but also act on AMPK, which, through phosphorylation, blocks SREBP maturation process (Elhanati et al. 2013).

Over its role in controlling lipids metabolism, SREBP is a crucial protein also for OLs maturation. Alterations of its proteolytic cleavage, upon use of S1P inhibitor, were found to affect growth processes, a peculiar element in OLs differentiation, together with myelin composition and SREBP targets, as ACC and FASN (Monnerie et al. 2017). Inhibition of SREBP targets however don't affect OLs maturation process. This is the case of FASN, the rate-limiting enzyme in palmitate production, whose role in *de novo* FA synthesis was analysed by Dimas et al. (2019). Upon induction of FASN depletion in a mouse model, they discovered no alterations on OLs proliferation and differentiation, but defects on myelin composition and stability of myelinated axons.

An alternative use of lipids is to fuel cells in case of carbohydrates deprivation, as energy storage, providing acetyl-CoA (López-Muguruza and Matute 2023). Indeed, upon their catabolism through FA β-oxidation, they are cleaved to reconstitute acetyl-CoA molecules, which, in the mitochondria

can feed the oxidative phosphorylation (Bogie et al., 2020). Cells can rely on substitute sources of acetyl-CoA, for energy production and replenishment of acetyl groups pool, for proteins acetylation and myelin lipids synthesis.

N-acetyl-aspartate can resemble an essential fount of acetyl-CoA and lipids for myelin production. Indeed, enzyme Aspartoacylase (ASPA) can convert it into aspartate and acetate. The amino acid is then directed to malate-aspartate/AGC1 shuttle, for the correct transport of reducing equivalents between cytosol and mitochondria, that ensures acetyl-CoA/ATP production, through OXPHOS (Rosko et al. 2019). The acetate instead can be converted directly into acetyl-CoA by Acetyl-CoA Synthetase (ACSS), with addition of coenzyme-A (Webster and Arsena, 1963). This enzyme is a SREBP-target protein, with two different isoforms, the first of which (ACSS1) mainly expressed in brain, with cytoplasmatic and nuclear localization. Especially during post-natal period, it allows acetylation of histones/proteins and myelin formations, using NAA-derived acetyl moieties (Ariyannur et al. 2010a; Moffett et al. 2007).

Acetyl-CoA and ATP can also be obtained from ketone bodies (KBs) and branched-chain amino acids (BCAAs). The first represent a crucial source of energy for brain, especially during development and for fatty acids synthesis required for myelin. Ketones are intermediate compounds of fatty acids β-oxidation occurring in liver, namely β-hydroxybutyrate (Bhb), acetoacetate (AcAc) and acetone, produced especially during prolonged fasting or exercises. Upon these conditions, their blood levels are quadruplicated, allowing a more efficient transport through MCTs (Mono Carboxylate Transporters) and entrance within the cells. Here, Bhb can be converted back to AcAc and, in turn into acetoacetyl-CoA and acetyl-CoA, through ketolysis, which replenishes the TCA cycle or acetate for myelin lipids synthesis (Tepavčević 2021; Jensen et al., 2020). Since 1984, Koper et al. (1984) shown the capacity of acetoacetate, as glucose, to sustain myelin lipids metabolism, especially in oligodendrocytes cultures. For their versatile roles in cell pathways, increasing KBs concentrations becomes a reliable therapeutic approach for many types of diseases, as neurodegenerative and demyelinating ones (Newman and Verdin 2017; Jensen et al., 2020). This can be achieved following ketogenic diet, with low carbohydrates levels, which was already seen to exert beneficial effects on myelination of mice model of Pelizaeus Merzbacher disease (leukodystrophy) and in AGC1 deficiency patients (Dahlin et al. 2015). In this latter case, KBs could compensate the lack of acetate groups derived from catabolism of N-acetyl-aspartate, which is reduced in AGC1 deficiency patients (Dahlin et al. 2015).

In parallel, KBs and acetyl-CoA can be obtained by BCAAs – leucine (Leu), isoleucine (Ile) and valine (Val). These amino acids catabolism starts in extra-hepatic tissues, with transamination reaction, especially in brain, where they can fuel the acetyl-CoA pool but also support glutamine

production, donating nitrogen groups (Sperringer, Addington, and Hutson 2017a). Just the first two reactions are in common in their degradative pathways: i) transamination via branched-chain aminotransferase isozymes (BCATs) and ii) oxidative decarboxylation by branched-chain α-keto acid dehydrogenase complex (BCKDC). After, that leucine can give rise to acetoacetate and acetyl-CoA, thus through ketogenic catabolism. Instead, valine, as glucogenic AA, can be converted just into succinyl-CoA; whereas isoleucine is both keto and glucogenic, since it can produce acetyl-CoA and succinyl-CoA (Fig. 2.13; Sperringer, Addington, and Hutson 2017a; Bixel and Hamprecht 1995). These metabolites can be directed towards TCA cycle, to supply OXPHOS, or used for myelin lipids synthesis.

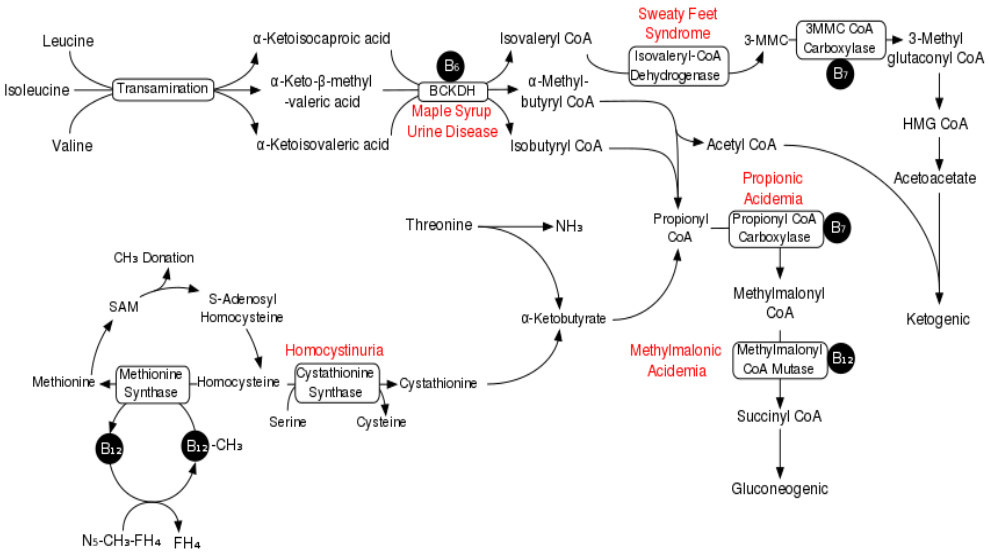

Fig. 2.13 Catabolism of leucine, isoleucine and valine. They are branched-chain amino acids, whose initial transamination reaction occurs in extra-hepatic tissues, especially brain, where they have different biological roles (Zachary P. Christensen, 2018)

2.6 Crosstalk between epigenetics and metabolism

Among others, Oligodendrocyte Precursor Cells and Oligodendrocytes are well-known environmental sensor cells. This mean that they can easily adapt their metabolic and transcriptional landscape to external clues, as neuronal activity, chemical and mechanical stimuli, time but particularly, to nutrients and metabolites availability (Dansu et al., 2021). These indeed have functional roles outside the most common energy production, as acting as signalling molecules to control epigenetic landscape for cell fate decision, metabolically driven differentiation and anti-inflammatory responses (Newman and Verdin 2017). Metaboloepigenetics studies this interplay between metabolism and epigenetic/gene expression regulation, which possesses a central role in all these cell pathways (Zijun Wang et al. 2018). Indeed, alterations upon nutrients/metabolites availability or production -thus, alteration at the metabolic routes- can affect gene transcription,

which, as we already saw in chapter 2.4.2.1, is crucial also for OPC/OLs maturation. This epigenetic alterations in turn could affect the metabolic asset, causing defects in OL functions, as myelin formation and trophic support to axons (Shen et al. 2008).

Metaboloepigenetics relies mostly on different types of metabolites, as ATP, S-adenyl methionine (SAM), flavin adenine dinucleotide (FAD), acetyl-CoA, nicotinamide adenine dinucleotide (NAD) and α-ketoglutarate (α-KG). These compounds work as cofactors/substrates of many epigenetic enzymes, regulating the chromatin architecture. SAM for example is source of methyl groups, which are essential for DNA/histone methylation, generally associate to silenced regions, and its deprivation could lead to hypomethylation, causing disturbances of pluripotency and differentiation (Liu and Casaccia 2010; Zijun Wang et al. 2018).

Another important metabolite is NAD, which is crucial for ATP production through OXPHOS, but also regulates the activity of many NAD-dependent proteins. Among them, we find DNA repair signalling protein Poly-ADP-ribose polymerases (PARPs), for DNA repair and metabolism control and sirtuins. The latter, as already discussed, are a class of deacetylases that can also target histones acetylation, as SIRT1 and 6. This reinforces NAD role in epigenetic modulation and induction towards pathological conditions in case of NADH/NAD^+ disbalance or altered sirtuins expression/activity. Indeed, abnormal levels of NAD or lack of sirtuins could induces aberrant glycolytic activation and tumorigenesis, with hyperacetylation of histones 4 (Zijun Wang et al. 2018; Chakrabarty and Chandel 2021; Russell et al. 2020). However, the most studied and known metabolite is acetyl-CoA. Beside fuelling the TCA cycle for ATP production (Narine and Colognato 2022) and replenishing acetyl groups pool for lipids synthesis (Garcia Corrales et al. 2021), it can regulate the levels of proteins and histone acetylation. There're two distinct pools of acetyl-CoA in the cells: one nuclear/cytoplasmatic and another mitochondrial, fed, as already discussed, through catabolism of many compounds (ketone bodies, citrate, acetate and some amino acids; Tepavčević 2021; Sperringer, Addington, and Hutson 2017a; Harris et al. 2005; Webster and Arsena, 1963). Their availability can regulate histone modifications, which could affect stem cell pluripotency, cell fate decision and maturation process (van der Knaap and Verrijzer 2016; Chakrabarty and Chandel 2021; Hernandez and Casaccia 2015b).

At the crossroad between metabolism/metabolites availability and epigenetic modifications/enzymes activity, there's a central organelle for cell, the mitochondrion. It's the well-known "powerhouse" of the cell, by hosting the electron transport chain and many enzymes involved in OXPHOS and ATP production (Chakrabarty and Chandel 2021). However, given its involvement in cellular metabolism, it was hypothesized an additional role of this organelle into regulation of nuclear epigenome. First evidence of mitochondrial-nuclear mutual influence was obtained by Delsite et al. (2002), which

identified aberrant DNA methylation upon mtDNA mutations, in cancer cells. These effects were counteracted by correcting these alterations in mitochondrial DNA, suggesting a crucial role of mitochondria in controlling epigenetic modifications. Nowadays, we clearly know that an anterograde regulation from nucleus, controls the biogenesis and activity of mitochondrial, accordingly to cell needs, whereas a retrograde response from mitochondria can modify the genes expression based on environmental factors. This complex process is called mitonuclear communication and its's the responsible for the link between metabolism and epigenetics (Matilainen, Quirós, and Auwerx 2017). Even though a lot is to be known about it, histone acetylation and DNA methylation regulation by mitochondrial were deeply discussed and analysed by different research groups. An example is the role of the one-C metabolism of mitochondria, which fuels the folate and methionine cycle in the cytoplasm, for SAM production and consequential DNA/histone methylation (Ormazabal et al. 2015). Also, acetyl-CoA levels are tightly regulated by this organelle. As already discussed, within mitochondria occurs most of the processes for acetyl-CoA production, thus, alterations of its levels could hamper the histone acetylation/deacetylation balance, which is extremely important, especially for cell maturation. This may occur when there's low energy condition, which reduces the acetyl-CoA concentration, repressing the gene transcription and protein synthesis (Menzies et al. 2016). Therefore, modulation of cell metabolism could alter acetyl-CoA production, as in the case of TIGAR depletion, an endogenous inhibitor of glycolysis, which during neural differentiation of NSCs can downregulate the ACLY enzymes, reducing acetyl-CoA formation. This in turn hamper acetylation on differentiation genes, as *GFAP*, affecting cells maturation (Fig. 2.14; Zhou et al. 2019).

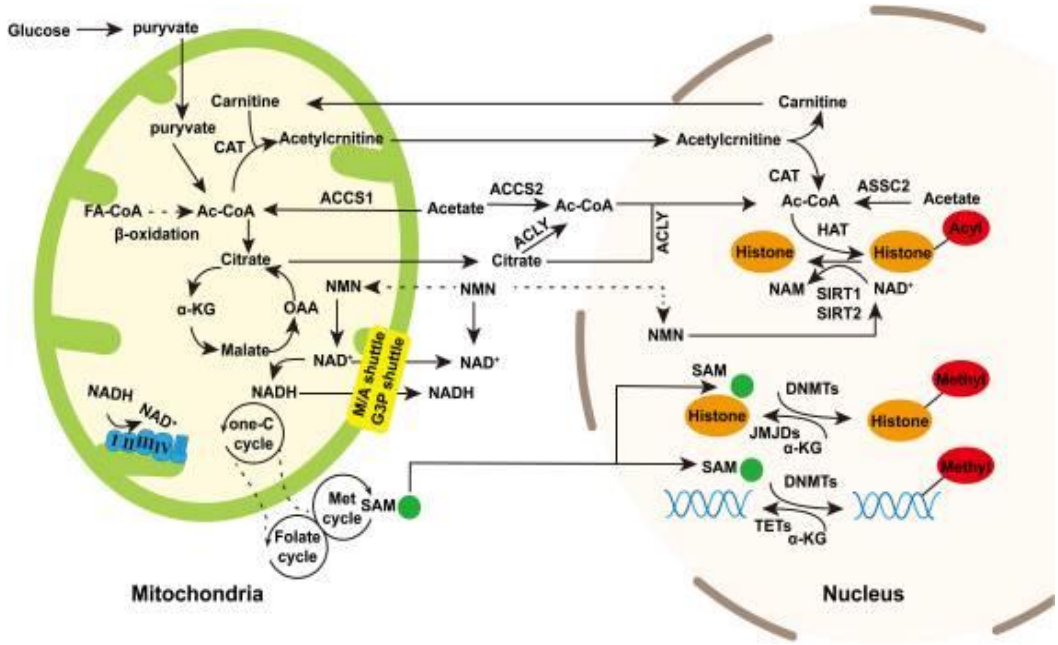

Fig. 2.14 crosstalk between mitochondrial metabolites production and their role in nuclear histone/DNA modifications (Xu et al. 2021)

Overall, these results suggest a role of mitochondria regulation on epigenome, with their involvement in the pathogenesis of many neurodegenerative, mitochondrial and demyelinating diseases (Qu et al. 2021; Xu et al. 2021; Bölsterli et al. 2022). Thus, possible approaches aiming to rebalance these metabolites alterations and mitochondrial dysfunctions are gaining more and more interest. Caloric restriction, fasting, fasting-mimicking diet and the ketogenic diet are the most known and applied methods (Taormina et al. 2019).

2.6.1 Ketogenic diet

Ketogenic diet (KD) is isocaloric regimen with low carbohydrates and high fat intakes, which induces changes from glycolytic metabolism to ketogenesis and β-oxidation usage (Bölsterli et al. 2022). Nowadays, it's a well-established treatment to therapy-refractory epilepsies (Murugan and Boison 2020; Dąbek et al. 2020). This approach aims to produce ketone bodies, avoid usage of glucose and favour OXPHOS and mitochondrial ATP production pathway (Qu et al. 2021). As mentioned before, the KBs comprise β-hydroxybutyrate and acetoacetate, which have been seen to exert effects on different biological pathways. Firstly, they can control and regulate voltage-dependent calcium channels of pyramidal cells, reducing the excitability of hippocampus. Bhb, particularly, has anti-seizure effect probably through reduction of the ATP production from glucose and resulting in hyperpolarisation of neurons (Augustin et al. 2018). Ketones could also act as antioxidant, counteracting cell death and reducing oxidative stress (Imdad et al. 2022; Qu et al. 2021). However, they mostly affect mitochondrial activity and dynamics. From literature, they were identified increase in bioenergetic pathways (TCA cycle, FA oxidation, ketolysis) and reduction of mitochondrial fission, with beneficial effects on mitochondrial elongation and clearance of morphological aberrations in mice brain and muscles, upon Bhb supplementations (Qu et al. 2021).

A late finding about KBs is their role as epigenetic modifiers. Indeed, they can produce and increase acetyl-CoA mitochondrial pool, through their catabolism, increasing the level of histone acetylation (Xie et al. 2016). Additionally, Bhb can also be used for specific lysine post-translational modification, called β-hydroxybutyrylation, which occur on histone3/4 (Kbhb) but also on proteins and enzymes, even though a little is known about this. Instead, it was studied that Bhb concentration guides the Kbhb (Ruan and Crawford 2018) and Bhb treatment can counteract the reduced levels of H3-Kbhb in depressive mice, ameliorating their behaviour, through antidepressant and neuroprotective effects (Chen, Miao, and Xu 2017). In parallel, an HDAC class I inhibitory activity was also testified for Bhb (Newman and Verdin 2017) with increase in histone acetylation of prefrontal cortex neuros in a mouse model of autism spectrum disorders, fed with KD (Fig. 2.15; Qin, Ma, and Yan 2022).

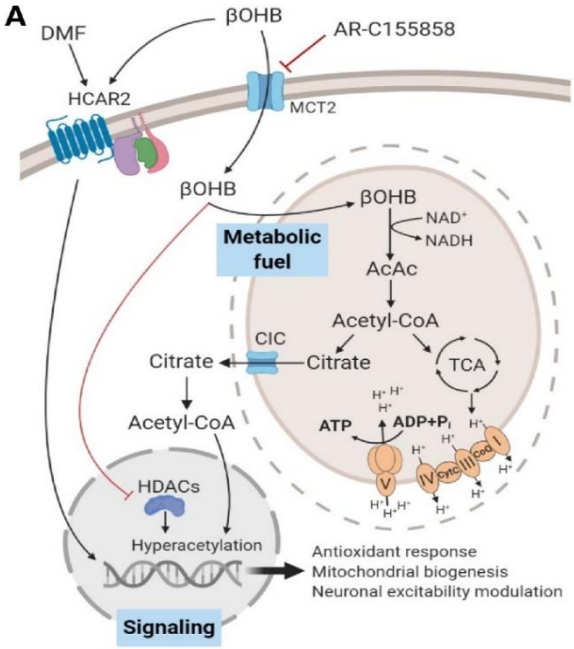

Fig. 2.15 Bhb and AcAc catabolism within the cell and their major role in biological pathway (Pérez-Liébana et al. 2020)

Given all these roles of ketone bodies and Bhb, KD was also proposed as a treatment for mitochondrial diseases, characterized by Malate-Aspartate Shuttle defects, as AGC1 Deficiency (Bölsterli et al. 2022). In 2015, Dahlin et al. (2015) administered KD to a 6-years old AGC1 deficiency patient, with a final composition of 4:1 (fat : carbohydrates and proteins) and they observed a clear improvement of motor skills (movements of legs, arms, stay sit and interact with external environment), twenty months after the start of the treatment, together with disappearance of seizures, within few days upon carbohydrates removal. In addition, MRI scan also confirmed an ameliorating of total myelination (Fig. 2.16).

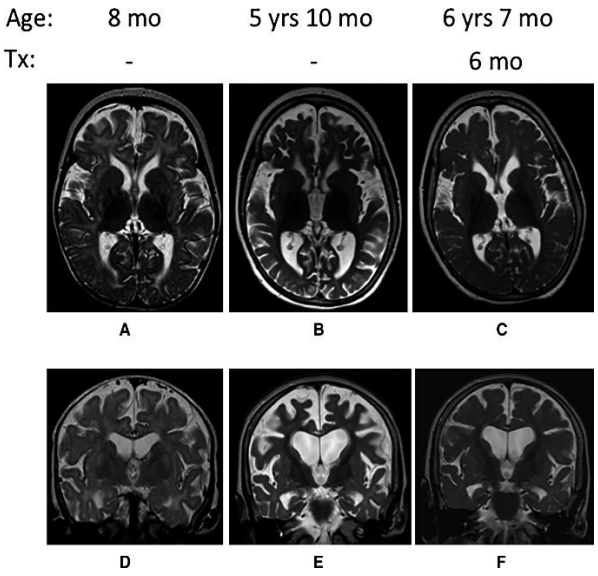

Fig. 2.16 Axial and coronal MRI scans of the patient's brain before and after six months of ketogenic diet, with diminution of white matter signal, as well as overall reduction of volume of the brain's ventricles (Dahlin et al. 2015)

Upon this case, the KD was followed by other patients affected (Bölsterli et al. 2022), even though it doesn't represent a definitive cure for the disease and its molecular mechanisms aren't still clear. Many hypotheses have however been proposed to explain the recovery of epileptogenic seizures and hypomyelination. Together with the KBs anti-inflammatory and antioxidant effects, the major change could be induced at metabolic level. Indeed, reduced glucose concentration, upon carbohydrate restriction, causes reduction of NADH production through glycolytic pathway. This will speed up NADH formation from FA oxidation and amino acids catabolism, but these processes are less efficient than glycolysis, provoking a decrease in $NADH/NAD^+$ ratio. This in turn, induces the NAD-dependent Malate Dehydrogenase (MDH) to oxidase malate to oxalacetate and this reaction allows the release of a molecule of NADH. More oxalacetate is present, more is converted to aspartate in the cytosol. This will compensate the reduced efflux of Asp from mitochondria, caused by AGC1 mutations, and it can be used for energy metabolism, N-acetyl-aspartate formation (for myelin lipids synthesis) and as nitrogen donors for the de novo glutamate production in astrocytes (Dahlin et al. 2015). These beneficial effects were also found for the solely administration of Bhb in AGC1 deficiency mouse model, in which neuronal metabolism and hypomyelination recovery were detected, even without depletion of glucose and carbohydrates (Pérez-Liébana et al. 2020). This clarifies some interesting molecular mechanisms that could take part to the ameliorative effect of KBs on AGC1 deficiency pathology, while others -as involvement of other cell types in KD- remain to be investigated.

3. AIM

The AGC1 deficiency is an ultra-rare demyelinating disorder, characterized by hypomyelination, psych-motor and growth defects, together with cerebral atrophy (Wibom et al. 2009; Falk et al. 2014). It's mainly caused by mutations in *SLC25A12* gene, which encodes for Aspartate-Glutamate Carrier 1, a mitochondrial carrier which enables the transport of the aspartate towards cytoplasm, for N-acetyl-aspartate production. This resembles the main source of acetate for oligodendrocyte myelin lipids synthesis and the reduced NAA concentration seen in AGC1 deficiency patients could explain the hypomyelination detected by MRI scans of their brain (Jalil et al. 2005; Sakurai et al. 2010).

Previous analysis from our group detected a proliferation and differentiation defects of two *in vitro* models of the pathology: Oli-Neu cells, immortalized murine OPCs in which AGC1 downregulation was induced upon shRNA-carrying plasmid, which leads to 30-40% reduction of the carrier activity. The second instead are neurospheres, 3D mixed pool of neural stem cells, deriving from sub-ventricular zone of mouse model of the disease, where gene trapping technique allows the deletion of one allele of *SLC25A12* gene (Petralla et al. 2019). This proliferation and differentiation defects were linked to alterations of the major signalling pathways involved, as PDGFR-α and TGF-β. In addition, following analysis on transcriptional and epigenetic landscape of these models highlighted an aberrant gene expression regulation, cause by altered epigenetic modifications and epigenetic enzymes levels and activities. These could probably affect the major transcription factors, whose expression was seen altered, as Olig2, c-Myc, REST, involved in proliferation and differentiation process, leading to the failure in myelin lipids synthesis and hypomyelination (Poeta et al. 2021).

Therefore, the aims of the present study are different. Firstly, we try to unravel, on a transcriptomic, epigenomic and metabolomic point of view, the consequences of AGC1 downregulation in our model of OPCs. For this purpose, RNA-seq, ATAC-seq and targeted metabolomic analysis were performed and *in vitro* validation through real-time PCR, Western Blot and Immunofluorescence analysis were done for all those proteins and enzymes of major interest. Secondly, given the potential therapeutic effects of ketogenic diet/ketone bodies on AGC1 deficiency pathophysiology (Dahlin et al. 2015; Pérez-Liébana et al. 2020), we performed supplementations with ketone bodies (β-hydroxybutyrate, acetoacetate) and branched-chain amino acids (leucine, isoleucine and valine), alone or in combinations on Oli-Neu and neurospheres models. From this analysis, we would understand if these compounds can revert the proliferation and differentiation defects detected previously, compensating the epigenetic/metabolic alterations. Indeed, through KBs and BCAAs catabolism, we try to counteract the lack of all those metabolites that we saw reduced during the metabolic analysis, and that are known to control epigenetic modifications and cell metabolism (primarily, acetyl-CoA and NAD; Wang et al. 2018). To assess this, proliferation analysis through Livecyte (for Oli-Neu) and

Incucyte (for neurospheres) imaging tools were performed and the most promising concentrations for each compound was screened. Subsequently, we tested the most effective compounds' concentration ability to also recover the differentiation defects of these *in vitro* models. This was done through immunofluorescence analysis, with specific lineage markers of differentiation, as CNPase, Olig2 (OL/OPC commitment), GFAP (astrocyte), Doublecortin (DCX, neuronal) and Nestin (stemness marker). At varying degrees, all compounds seemed to be effective at proliferative and differentiative point of view. Since the involvement of epigenetic modifications in regulation of proliferation and differentiation processes, we try to understand if the beneficial effects exerted by these supplementations can match with an ameliorating epigenetic landscape, analysing the major affected histone modifications; acetylation and methylation. This was done through Western Blot analysis, at two distinct time-points to see if the treatments -and the epigenetic improvements- are preceding or following the proliferation/differentiation recovery. At the end, preliminary analysis on proliferation was also conducted on Neural Progenitors, deriving from induced Pluripotent Stem Cells of AGC1 deficiency patients, to identify possible similar alterations in the human *in vitro* model of the disease.

4. MATERIALS and METHODS

4.1 Cell cultures

4.1.1 Oli-Neu

Oli-Neu cells are immortalized mouse Oligodendrocyte Precursor Cells (OPCs, kind gift from Dr. Jacqueline Trotter, University of Mainz, Germany), in which a partial silencing of AGC1 carrier was performed using a shRNA, to create a stable *in vitro* model of AGC1 deficiency. As previously described (Petralla et al. 2019), the cells were transfected using Lipofectamine 2000 reagent (Thermo Fisher) and a pLKO1-pure DNA plasmid (Sigma-Aldrich) with a scrambled control sequence or an AGC1 targeting sequence, against *SLC25A12* gene. The clone, which better resembles the patience's phenotype (AGC1 carrier reduction up to 40%), was selected through Western Blot analysis of AGC1 expression profile and used for following experiments.

The cells were maintained on poly-L-lysine (Sigma-Aldrich, St Louis, MO, USA) coated Petri dishes at 37ºC and 5% CO_2, in SATO medium constituted by DMEM High Glucose medium to which we added: 2 mM glutamine, 10 µg/ml insulin, 5.5 µg/ml transferrin, 38.72 nM sodium selenite (insulin-transferrin-sodium selenite 100X supplement Thermo Fisher Scientific, Waltham, Massachusetts, USA), 100 µM putrescine, 520 nM, L-thyroxine, 500 nM triiodo-L-thyronine (T3), 200 nM progesterone, 25 µg/ml gentamycin (all from Sigma-Aldrich), and 1% heat-inactivated Horse Serum (HS; Sigma-Aldrich). To select and maintain the stable clones, 1 µg/ml puromycin (Sigma-Aldrich) is added in culture medium (Trotter et al., 1989).

For the passage, cells were detached using 0.01% trypsin - 0.02% EDTA-HBSS (Sigma-Aldrich) for 3 minutes at 37ºC, then inactivated by an equal volume of DMEM High Glucose medium plus 10% Horse Serum. After collection, cells were centrifugated for 5' at 1000 rpm and the pellet was resuspended in complete medium, counted, and plated on dishes, for experiments.

4.1.2 Neurospheres

Neurospheres are tri-dimensional mixed pool of Neural Stem Cells (NSCs) deriving from Sub-Ventricular Zone (SVZ) of 8-months old male mice (*Mus musculus*), wild type ($AGC1^{+/+}$) and heterozygous ($AGC1^{+/-}$) for SLC25A12, generated through gene-trapping technique by the Texas A & M Institute for Genomic Medicine (Houston, Texas, USA). Specifically, a premature stop codon was inserted -through homologous recombination- between exon 2 and 3 of AGC1 mRNA, creating an inactive form of the protein. This model overcomes the lethality issues deriving of the homozygous mouse -whose pups generally die during embryonic age- and shows a reduction up to 50% of AGC1 carrier activity (Petralla et al. 2019). Mice health and physical state was periodically controlled by

veterinarians and technicians from the University of Bologna, and approval for all animal experiments was granted by a regional bioethical committee (under Protocol number 3/79/2014), in full compliance with both Italian and European Community legislation (Directive 2010/63/EU) about the utilization of research animals, and in accordance with the guidelines outlined in the ARRIVE Reporting Guidelines. Following this, measures were taken to stabilize the cell line, thus eliminating the need for additional experiments involving animals.

The animals were bred with *ad libitum* access to food and water, in 12/12-hour light-dark cycle at 20 °C ± 2 °C and set humidity; for their mental and physical well-being, appropriate environmental enrichments were placed in the cages, where no more than 4 mice were hosted together.

For neurospheres culture preparation, mice ($AGC1^{+/+}$ and $AGC1^{+/-}$) were anesthetized through intraperitoneal injection of 10 mg/kg xylazine followed by cervical dislocation. The brain collected in PBS, was then cut above optic chiasm and the lateral ventricles and their respective anterior periventricular regions was dissociated mechanically in Hank's Balanced Salt Solution (HBSS; 3.9 mg/ml HEPES, 0.5 mg/ml NaHCO3, 0.9 mg/ml glucose, 0.5% penicillin/streptomycin). Then tissue is transferred in a 15ml tube and centrifuge for 5' at 1000 rpm. To enzymatically releasing of stem cells, the pellet is resuspended in papain solution (0.2 mg/ml EDTA, 0.66mg/ml Papain, 0.2 mg/ml cysteine in HBSS) and placed at 37°C for 20 min taking care to shake every 5'. Tissue was further dissociated adding HBSS and let other 10' in the heat bath. DMEM F-12 (Gibco Life Technologies, Waltham, MA, USA) was used to inhibit the papain reaction, and samples were centrifuged at 1000 rpm for 5'. Tissue-released cells were then plate in DMEM-F12 supplemented with 2 mM glutamine, 10 µg/ml insulin, 20 ng/ml Epidermal Growth Factor (EGF; PeproTech EC, London, UK), 20 ng/ml Fibroblast Growth Factor-2 (FGF2; PeproTech), 1% N2 (ThermoFisher Scientific, Waltham, MA, USA), 1% B27 (ThermoFisher), 10 units/ml penicillin and 10 µg streptomycin.

After 5/7 days, the single cells become 3D spheres which can be passed, collecting them from Petri dish and centrifuge at 1000 rpm for 5'. Then a wash with PBS was performed. To dissociate into single cells, the spheres pellet was resuspended in Accutase (Aurogene Srl, Roma, Italy) for 5' at 37°C. The reaction was stopped adding DMEM-F12 and after centrifugation, cells were count and plate for experiments, in complete medium.

Otherwise, to plate intact spheres, we collected them after 5-7 days of growth, centrifugated at 1000 rpm for 5', washed with PBS and the pellet was then resuspended in complete medium to count them with Trypan Blue. Suitable number of spheres were plated on Matrigel-coated (STEMCELL Technologies) dishes, to allow complete adhesion and differentiation for 4/7 days.

4.2 Supplementations

On different *in vitro* models of AGC1 deficiency, we performed supplementations of Ketone bodies (KBs, β-hydroxybutyrate and Acetoacetate) and Branched-Chain Amino Acids (Leucine, Isoleucine and Valine, all from Sigma-Aldrich) to try to balance the metabolites alterations. Three concentrations were firstly tested on proliferation assays (mainly Livecyte PhaseFocus and Incucyte S3 Live-Cell Analysis System – Sartorius, AG); then, we chose the most promising concentrations, in term of pro-proliferative effects, and test them to assess differentiation and histone modifications analysis. Specifically:

Compound	Concentrations
β-hydroxybutyrate (Bhb)	2,5 mM 5 mM 10 mM
Acetoacetate (AcAc)	0,5 mM 1 mM 1,5 mM
β-hydroxybutyrate + Acetoacetate	Bhb 2,5 + AcAc 0,5 Bhb 5 +AcAc 1 Bhb 10 + AcAc 1,5
Leucine (Leu)	200 mg/l 400 mg/l 800 mg/l
Isoleucine (Ile)	200 mg/l 400 mg/l 800 mg/l
Valine (Val)	200 mg/l 400 mg/l 800 mg/l
Amino Acids (aa)	aa200: Leu 200 + Ile 200 + Val 200 aa400: Leu 400 + Ile 400 + Val 400 aa800: Leu 800 + Ile 800 + Val 800

Table. 1 Table of supplementations compounds and concentrations.

4.3 Livecyte proliferation analysis

To assess the effects of ketone bodies and branched-chain amino acids on proliferation of Oli-Neu cells and IPSC-derived NSCs, we used the Livecyte PhaseFocus (through collaboration with CRBA, Centro di Ricerca Biomedica Applicata, Bologna, Italy). This is a live-imaging instrument that allows to perform different cellular assay monitoring the cells without disrupting their viability, also for long time, since the lens is put within an incubator, where temperature and humidity are controlled. Its

high sensitivity depends on the camera which is able to detect phase and not optical images, thus improving the overall quality.

For the experiments, 2×10^3 Oli-Neu cells/well were plated in 96-multiwells coated with poly-L-lysine. After 24 hours from plating, they were treated using ketone bodies and/or branched-chain amino acids, at different concentrations (Table 1) and put within the instrument for recording. For our purpose, the analysis has been set to acquire one image per well every hour, for 72 hours, overall. To measure the cell proliferation differences among all experimental groups, we use as parameter, the cell counts of each condition, tested in quadrupled.

4.4 Incucyte proliferation analysis

The same proliferation analysis, with ketone bodies and/or amino acids supplementations, was performed also on neurospheres, but since the three dimensional and suspended nature of this cell culture, we use IncuCyte S3 Live-Cell Analysis System (Sartorius AG, through collaboration with CRBA, Centro di Ricerca Biomedica Applicata, Bologna, Italy). It's a live-cell analysis system that, as for LiveCyte, allows real-time monitoring of cell cultures, without need of fluorescent label or dyes. The entire instrument is set within an incubator, which controls temperature and humidity. The difference with the previous one, is that the multi-well with cells stands still, while the lens moves along the plate and take brightfield images of each well.

For these experiments, 5×10^3 single cells -after neurospheres dissociation- were plated in complete medium, adding specific compounds (Table. 1). The analysis has been set to last 7 days (time interval necessary for the complete formation of spheres) and the device takes an image every 24 hours of each condition, tested in quadrupled.

The physiological growth from single cells to intact spheres includes an initial phase in which single cells number increases, until it reaches a plateau. From this step, the spheres size changes, increasing their dimension. Since this complexity and to consider the spontaneous tendency of $AGC1^{+/-}$ neurospheres to differentiate, adhering at the bottom of the well and forming branches, to assess proliferative effects of supplementations, we chose three different parameters:

- Brightfield Object Count: number of objects per image;
- Brightfield Object Total Area: total area of object in the image;
- Brightfield Object Average Eccentricity: average eccentricity of the object in the image, ranges from 0 to 1 (0 means that the object can be considered as a perfect sphere, while 1 represented an elongated and branched shape).

The first two parameters were analysed in the first four days of growth, in which neurospheres have the major alterations in term of number and dimension, without the interference of branches

formation; whereas the third was accounted for the entire analysis time, to distinguish the variations in shape among all experimental groups.

4.5 Western Blot

For Western Blot analysis, all samples from Oli-neu or differentiated neurospheres were collected in lysis buffer (50 mM Tris pH 7.4, 1 mM EDTA, 1% SDS, 10 µl/ml protease and phosphatase inhibitors) and after 5' sonication with Branson 250 digital sonifier (3 pulses of 2 seconds each, with 5 seconds rest between each pulse) at 10 % power output, they were quantified through Lowry protein quantification method, and standard calibration curve made by bovine serum albumin (BSA, 1.5 mg/ml). All samples were quantified in duplicate as follow: 2µl of sample + double-distilled water (ddH2O) to a final volume of 200 µl. Then, to each samples we added 1 mL of solution I (98% solution A; 2% Na2CO3 in 0.1N NaOH; 1% solution B: 0.5% CuSO4; 1% solution C; 1% Na-K tartrate); after incubation 10' at RT, 100 µl of solution II (50% Folin reagent and 50% ddH2O; all reagents were from Sigma-Aldrich) were added, and samples were vortexed and incubated 30' at RT. Absorbance was read at 700 nm using a spectrophotometer.

Following the quantification, we load an equal amount of protein with 4X Loading buffer (1M Tris-HCl pH 6.8, 20% sodium dodecyl sulphate, 0.4µl/ml glycerol, 2g/l bromophenol blue and 2M dithiothreitol; all from Sigma-Aldrich) on SDS-PAGE (Sodium Dodecyl Sulphate - Polyacrylamide Gel Electrophoresis). Transfer onto a nitrocellulose membrane (GE Healthcare Life Sciences, Little Chalfont, UK) was performed keeping the equipment in ice. Subsequently, non-specific sites were blocked 1h at RT with PBS 0.1% Tween-20 (Sigma-Aldrich) and 5% non-fat dried milk (Bio-Rad). Membranes were then incubated with primary antibody overnight at 4°C. The next day, we washed three time the membranes with 0.1% Tween-20/PBS + 5% dried milk, membranes for 10, and then they were incubated with the specific HRP-secondary antibody (horseradish peroxidase conjugated) 90' at RT. Following 3 washes in 0.1% Tween-20/PBS, labelled proteins were visualized by using ClarityTM Western ECL Substrate (Enhanced Chemiluminescence; Bio-Rad) and detected through Bio-Rad Image Lab software with ChemiDoc™ MP imaging system (Version 6.0.0; RRID:SCR_014210).

Antibody	Company	Dilution
AGC1/Aralar1 mouse monoclonal IgG	**Santa Cruz Biotechnology;** Cat# sc-271056, RRID: AB_10608837	1/1000
Anti-acetyl-Histone H3 rabbit polyclonal antibody	**Millipore;** Cat# 06-599, RRID:AB_2115283	1/1000
CNPase rabbit monoclonal IgG	**Cell Signalling Technology**; Cat# 5664, RRID:AB_10705455	1/1000
GAPDH mouse monoclonal IgG	**Santa Cruz Biotechnology;** Cat# sc-32233, RRID:AB_627679	1/20000
GFAP rabbit IgG	**Dakopatts**; Cat# sc-33673, RRID:AB_627673	1/1000
Histone H3 rabbit polyclonal IgG	**Santa Cruz Biotechnology**; Cat# sc-10809, RRID:AB_2115276	1/1000
OLIG2 rabbit polyclonal IgG	**Santa Cruz Biotechnology**; Cat# sc-48817, RRID:AB_2157550	1/1000
Pan-Met-H3	**MBL International**; Cat# LS-A4069, RRID:AB_591306	1/1000
Anti-**NG2** rabbit polyclonal IgG	**Abcam;** Cat# ab83178, RRID:AB_10672215	1/500
PDGFRα (C-20) rabbit polyclonal IgG	**Santa Cruz Biotechnology**; Cat# sc-338, RRID:AB_631064	1/1000
ACSS1 rabbit polyclonal IgG	**Cell Signalling Technology**; Cat# 3658, RRID:AB_2222710	1/1000
FASN rabbit polyclonal IgG	**Proteintech**; Cat# 10624-2-AP, RRID:AB_2100801	1/1000
SREBP1 mouse monoclonal	**Novus**; Cat# NB600-582, RRID:AB_10001575	1/1000
Goat anti-Rabbit	**Jackson ImmunoResearch Labs**; Cat# 111-035-144, RRID:AB_230739	1/5000
Goat anti-Mouse	**Jackson ImmunoResearch Labs**; Cat# 115-035-146, RRID:AB_2307392	1/5000

Table. 2 Primary and secondary antibodies used for Western Blot analysis

4.6 Immunofluorescence and BrdU Analysis

For immunofluorescence analysis, Oli-Neu cells were plated on glass coverslips previously coated with poly-L-lysine, whereas intact spheres on glass with Matrigel coating. Firstly, samples were fixed with PFA 4% for 30' and washed with PBS. To permeabilize the cell membrane, three washes with PBST (PBS + 0.1% Triton) were done and then blocked 1h in Blocking Buffer (PBS-0.1% Triton + 5% normal goat serum), to reduce aspecific sites binding. The glasses were then incubated overnight

at 4°C with primary antibodies in PBST-0,1% + 2% normal goat serum. The following day, three washes with PBST allows to remove primary antibodies excess. Then, samples were incubated 2 hours at RT with secondary fluorescent antibodies, in the dark. After three steps of 10' in PBST, and one in PBS, Hoechst 33258 (2 µg/ml, Sigma-Aldrich) nuclei staining was done for 5 min. the coverslips were then mounted with Ultracruz Aqueous Mounting Medium with DAPI (Santa Cruz, cat. no. sc-24941) and stored at 4°C in dark. Fluorescence signals were then detected using the Nikon EZ-C1 confocal microscope. Images were acquired from multiple (at least 3) randomly selected fields of the slide and using the 60X oil-objective. For neurospheres, we use Z-stack at 512 steps / 1µm–thickness and the 3D image reconstruction was performed with FiJi ImageJ software, specifically the Z-project plugin (RRID:SCR_002285).

BrdU (5'-bromo-2'-deoxy-uridine) is a thymidine analog, used to quantify phase S of cell cycle, thus crucial to quantify cell proliferation. Indeed, during DNA replication, if BrdU is present in the medium, cells can incorporate this analog in the DNA sequence, rather than Thymidine. Then, an anti-BrdU antibody, specific for BrdU, allows the detection. Thus, we plated Oli-Neu cells on poly-L-lysine coated glass coverslips and left them growth for three days, adding on the first and third days the BrdU (10 µM) to the medium. The NPCs from iPS instead were plated on Matrigel-coated glass coverslips and BrdU added to the medium upon cells adhesion. In this case, the experiment lasts 24 hours. The samples were then fixed with PFA 4% and after a wash with PBS, they were incubated for 30 min at RT with HCl 2N. Following three washes with PBS of about 10 min each, we proceed with the same protocol of other immunofluorescence analysis. The same was done for intact spheres plated on Matrigel-coated glass coverslips and left to grow for 4 days, adding on first and third days the BrdU (10 µM) to the medium. For BrdU quantification, 4 random fields were chosen in the glass and total nuclei stained with DAPI and BrdU positive nuclei were counted. The measurement was expressed as ratio of BrdU positive/DAPI stained cells.

Antibody	Company	Dilution
CNPase rabbit monoclonal IgG	**Cell Signalling Technology**; Cat# 5664, RRID:AB_10705455	1/1000
Anti-**Doublecortin** rabbit polyclonal antibody	**Abcam**; Cat# ab18723, RRID:AB_732011	1/500
GFAP rabbit IgG	**Dakopatts**; Cat# sc-33673, RRID:AB_627673	1/500
Anti-**NG2** rabbit polyclonal IgG	**Abcam**; Cat# ab83178, RRID:AB_10672215	1/500
OLIG2 rabbit polyclonal IgG	**Santa Cruz Biotechnology**; Cat# sc-48817, RRID:AB_2157550	1/500
Nestin mouse monoclonal	**Abcam**; Cat# ab6142, RRID:AB_305313	1/500
SSEA4-4 mouse monoclonal	**Santa Cruz Biotechnology**; Cat# sc-21704, RRID:AB_628289	1/500
ACSS1 rabbit polyclonal IgG	**Cell Signalling Technology**; Cat# 3658, RRID:AB_2222710	1/500
FASN rabbit polyclonal IgG	**Proteintech**; Cat# 10624-2-AP, RRID:AB_2100801	1/500
SREBP1 mouse monoclonal	**Novus**; Cat# NB600-582, RRID:AB_10001575	1/500
Ki67 rabbit polyclonal	**Abcam;** Cat# ab16667, RRID:AB_302459	1/500
BrdU rat monoclonal	**Abcam**; Cat# ab6326, RRID:AB_ 305426	1/500
Goat anti-Rabbit Alexa 488	**Abcam**; Cat# ab150078, RRID:AB_ 2722519	1/1000
Goat anti-Rat Alexa 488	**Abcam;** Cat# ab150157, RRID:AB_ 2722511	1/1000
Goat anti-Mouse Alexa 488	**Abcam**; Cat# ab150113, RRID:AB_ 2576208	1/1000

Table. 3 Primary and secondary antibodies used for immunofluorescence analysis

4.7 DNA extraction and PCR

For genomic DNA extraction, we plate Oli-Neu cells on poly-L-lysine coated dishes and when they were confluent, we harvested them and washed the cell pellet twice with sterile PBS. Then, we resuspended the pellet in suitable volume of Lysis Buffer (Tris-HCl pH:8,00; NaCl 100 mM; EDTA 20 mM; SDS 0,5%; Sigma-Aldrich), and after 5' sonication with Branson 250 digital sonifier (3 pulses of 2 seconds each, with 5 seconds rest between each pulse) at 10 % power output, we added

proteinase K (0,2 mg/l, Zymo Research) and incubated overnight at 56 °C. The next day, we added Phenol-Chloroform-Isoamyl alcohol (PCI, 100 µl) and centrifuged at maximum speed for 10' at room temperature (RT). Then we saved the aqueous supernatant and added 100 µl of pure chloroform, mixed vigorously and centrifuged again for 10'. We repeated this step twice and at the end, we saved the supernatant in a tube with 1 µl of glycogen (20 mg/l, Sigma-Aldrich). Here, we added 1/10 of aqueous volume of sodium acetate (3 M, pH:5,2) and 2,5 times of ethanol 100% and vortex to allow complete precipitation. After 3 hours at -20 °C, we spin at full speed at 4°C for 30' and then washed the pellet with cold ethanol 75%. Following discard of supernatant, the pellet is left to dry and then resuspended in a suitable volume of milliQ water. For DNA quantification, we used NanoDrop 2000 (Thermo-Fisher Scientific). Values of ratios A260/A280, index of protein contamination respectively, was also evaluated. The purified DNA was stored at -20 °C for PCR.

For the reaction mix, 50 ng of DNA were used, with: forward and revers primer (10 µM, Invitrogen), 50 mM MgCl2, 10X PCR Buffer, minus Mg, 10 mM dNTPs mix and *Taq* DNA polymerase (5 U/µl). For the blanks, we added water instead of samples. We set the Biometra T3000 Thermocycler (Biometra, South San Francisco, CA, USA) at specific annealing temperature for each pair of primers that we would amplify.

Gene	**Primers (5'-3')**
ATPAF2	F: TATCCTGCTGAGAGTCCCATTC R: GGCTTTGAGATAAACCTGGACC
FASN	F: CCAGAGGGTGGTTGTTAGAAAG R: TCAACTCACTGGCAGAAGAGAA
GAPDH	F: AGGGTGGTGAAGCAGGCATC R: CGAACGTGGAAGAGTGGGAG
JMJD4	F: ATGGTAACCTGCCCTATGATGT R: GGGTAACTTCAGTATGTCCTCG
RAI1	F: CCAGAATCTTCACGCTTACCAG R: TTTGTGAGGTGATGGTCTTGGA
SNAP47	F: GAAGACCACATTTCGACTAGGC R: AGCGTGGCTTCTCATTTCTCTCT
SREBP1	F: TTGTTTGCGATGTCTCCAGAAG R: TGGCCAATGGACTACTAGTGTT
TRIM11	F: GCCATCTCTCATTCTACAGTGC R: GGATACTGATAGACGTCCGACT

Table. 4 Sequences of primers used for PCR

The termocycler programme was:

Step	*Temp*	*Time*	*Note*
1	95° C	30"	
2	95° C	10"	
3	58-60° C	30"	
4	65°C	1'	Go to 2, for 35 cycles
5	65°C	5'	
6	4°C	∞	

Table. 5 Amplification cycles

After amplification, PCR products and blanks were loaded on 2% agarose (Sigma-Aldrich) gel with Gel-red (EMD Millipore Corp) and after 30' at 80 V, we detected the bands using UV-transilluminator (Biorad Image Lab software with ChemiDoc™ MP imaging system).

4.8 RNA extraction and Real-Time PCR

To extract RNA, $1x10^6$ Oli-Neu cells were plated on 60 mm coated dish and let grown until confluence. Then, they were collected using 1 ml of TRI Reagent (TRI Reagent RNA Isolation Reagent; Sigma-Aldrich) and after adding 200 µl of Chloroform (Sigma-Aldrich), samples were incubated at room temperature (RT) for 10' and centrifugated (12000g 15' at 4 °C) to allow phases division. The upper aqueous phase containing RNA, was saved and RNA was precipitate adding 500 µl of isopropanol (Sigma-Aldrich). After incubation at RT for 20', another centrifugation step was done of 12000 g 10' at 4 °C. The pellet was then washed one time with ethanol 75%, and pellet was left to dry and then resuspended in milliQ water. We quantified the nucleic acids by NanoDrop 2000 (Thermo-Fisher Scientific). Values of ratios A260/A280 and A260/A230, indexes of protein and organic solvents contamination respectively, were also evaluated. The purified RNA was stored at -80 °C for RNAseq analysis and retro transcription/real-time PCR.

For neurospheres, we followed the same protocol for RNA extraction, using $1x10^6$ single cells, obtained after Accutase dissociation. Just an additional step with a Branson 250 digital sonifier (3 pulses of 2 seconds each, with 5 seconds rest between each pulse) at 10 % power output, was introduced to allow the complete release of nucleic acids, after TRI-Reagent mechanical dissociation of cells.

The RNA samples were then retro-transcribed. Firstly, 1 µg of Oli-Neu cells/neurospheres RNA, 10X Reaction Buffer with $MgCl_2$ and 1 U of DNase I RNAse-Free (1U/1µl) in a final volume of 10 µl in DEPC-treated water were used for DNase treatment (all from Thermo-Fisher Scientific). The reaction occurred in a Biometra T3000 Thermocycler for 30' at 37 °C; subsequently, a following incubation with 1µl of EDTA (to inhibit the reaction) at 65 °C for 10' was done. Thus, all genomic DNA contaminations were removed. After that, the Reverse Transcription mix (2X RT Reaction Mix, 2,5µl/1µgRNA RT Enzyme Mix; Thermo-Fisher Scientific) was prepared for each purified samples and they were incubated in the Thermocycler (25 °C x 10'→ 50 °C x 30' → 85 ° C x 5').

At the end, to remove all RNA contaminations from cDNA samples, 1µl per sample of E. coli RNase H was added and incubated at 37 °C x 20'.

For Real Time PCR, we used 40 ng of cDNA previously retro-transcribed, together with 0.8µM primer mix (drawn with Primer 3, Table 6) and 10µl Real-Time Mix containing SYBR-green (Bio-Rad). Blank sample had water instead of cDNA; GAPDH was used as endogenous control. All samples were loaded in a Multimode Plate Reader EnSpire (Perkin Elmer, Milan, Italy) and Real Time program was selected (95 °C x 90" → 40 cycles: 95 °C x 15", 60 °C x 60" → 95 ° C x 15" → 60 ° C x 60" → 94.5 ° C x 0,3").

Gene	Primers (5'-3')
ACSS1	F: AAGATTTCTGTGATGACGCTGG R: TCTGGGAAAGTGATGAGGAGAC
ATPAF2	F: TATCCTGCTGAGAGTCCCATTC R: GGCTTTGAGATAAACCTGGACC
CHODL	F: TTCCGAAACTGGTACACTGATG R: GGGATGGAAATGGTCACCTTAC
FASN	F: CCAGAGGGTGGTTGTTAGAAAG R: TCAACTCACTGGCAGAAGAGAA
GAPDH	F: AGGGTGGTGAAGCAGGCATC R: CGAACGTGGAAGAGTGGGAG
JMJD4	F: ATGGTAACCTGCCCTATGATGT R: GGGTAACTTCAGTATGTCCTCG
ME2	F: TCTGAGGAGGTGTCAGTGAAGA R: AGAGAGAGTGCATAGACCGGAA
NAT8L	F: TGCCATGCTGCACAACTACT R: AGATACTCAGTGACCCGAAGTC
RAI1	F: CCAGAATCTTCACGCTTACCAG R: TTTGTGAGGTGATGGTCTTGGA
SLC25A13	F: AGCTAGGTCGATTCCTGCATAG R: GAAGTGCAAGATTCTAGGCGAA
SNAP47	F: GAAGACCACATTTCGACTAGGC R: AGCGTGGCTTCTCATTTCTCTCT
SREBP1	F: TTGTTTGCGATGTCTCCAGAAG R: TGGCCAATGGACTACTAGTGTT
SREBP2	F: GGACAGTGATGTGGACTTGAAA R: GGGATAAGGTAACTGAGACTCG
TRIM11	F: GCCATCTCTCATTCTACAGTGC R: GGATACTGATAGACGTCCGACT

Table. 6 Sequences of primers used for Real-Time PCR

4.9 RNA-seq

For the sequencing analysis, we collected samples as described in the paragraph 4.8. Then, we sent to IGATech Technology Services Srl (Udine, UD Italy) for the data processing and analysis. The group of our collaborator, professor Federico M. Giorgi (University of Bologna, Italy), analysed the data obtained followed a specific RNA-seq pipeline, as described in Balboni, Babini et al., (2024). Briefly, three samples of control and siAGC1 Oli-Neu cells were processed and quantified for transcripts' expression through Salmon v0.12.0 in mapping-based mode (Patro et al. 2017), using *Mus musculus* transcriptome (cDNA from genome build GRCm39). The differential expression analysis was performed using DESeq2 (Love et al. 2020) and after Benjamini-Hochberg correction, *p-values* associated to *Log2FoldChange*s < 0.05 were considered significant. Moreover, through

Gene Ste Enrichment Analysis (GSEA), it was possible to analyse gene expression at the level of gene set, and no single gene.

4.10 ATAC-seq

ATAC-seq allows to identify the genomic regions that have open chromatin conformation or are bound to histones. For ATAC-seq analysis, four replicates for control and siAGC1 Oli-Neu living cells were directly sent to Genomix4Life Srl (Salerno, NA, Italy) for the data processing. The bioinformatic group of Professor Giorgi handled the data analysis following a specific protocol to identify regions (called peaks) of the genome with an enrichment of sequenced reads compared to the background, using MAC2. After the counting of the peaks, a matrix was created for DESeq2 to model differential chromatin accessibility between control and siAGC1 cells.

4.11 Quantitative metabolites concentrations

Through collaboration with the group of professor Laura Mercolini (University of Bologna, Italy), from cell media, it was possible to quantify through semi-automated microextraction by packed sorbent (MEPS) and liquid chromatography-tandem mass spectrometry (LC-MS/MS), the concentrations of specific polar metabolites: ADP, AMP, Citrate, Fumarate, GSSG, L-Asparagine, L-Malate, Lactate, NAA, alpha-ketoisocaproic acid, alpha-ketoisovaleric acid, CTP, GSH, GTP, Isoleucine, L-aspartate, L-glutamate, Leucine, 2-Oxyglutarate, L-alanine, Oxalacetate, Pyruvate, Succinate, Valine. The protocol was deeply discussed and described in (Protti et al. 2023). In summary, clean-up and pre-concentration was performed pre-treating samples. Then, LC-MS/MS analysis was carried out under multiple reaction monitoring (MRM) conditions and positive/negative electrospray ionization (ESI+, ESI-) polarity switching mode. The metabolite levels, reported as ng/mL in cell media, was calculated by group of Professor Giorgi, through the R *limma* package (Ritchie et al. 2015); resulting *p-values* corrected using the Benjamini-Hochberg method (Benjamini 2010).

Other set of metabolites, namely NADH/NAD^+, was instead measured on Oli-Neu cells pellet, from three distinct replicates in triplicate, at Metabolomics Core Technology Platform - Centre for Organismal Studies (University of Heidelberg, Germany). For these, cells were plated and after reaching confluency, they were harvested using trypsin reaction and, after two washes with PBS, cells were counted and pellet immediately frozen to preserve all those extremely labile metabolites.

4.12 iPSC-derived Neural Progenitor Cells

Human Induced Pluripotent Stem Cells (hiPSC) were obtained through reprogramming of human adult somatic cells, with four transcription factors: Oct4, Sox2, Klf4 and c-Myc (Takahashi and Yamanaka 2006). For this preliminary study, three lines of control healthy patients' fibroblast-deriving iPS (C MS, C ATCC, C TESSA) and two from affected patients were used. The first patient's line is coming from AGC1-deficient fibroblasts (from an Indian male patient affected by AGC1-deficiency, AGC1 M1-01). This line was kindly provided by Professor Stewart Anderson (Children's Hospital of Philadelphia, Upenn School of Medicine) and characterized by a *SLC25A12* mutation (c.1058G>A), with reduction of AGC1 protein activity of about 85% (Falk et al. 2014). The second instead is derived from a second German patient (AGC1 2MC), with a mutation in splicing site, causing production of truncated AGC1 protein and no AGC1 expression in fibroblasts. All the iPS lines were kindly donated by our collaborator, Dr. Massimo Lasorsa (IBIOM CNR Bari).
They were maintained in mTeSR1 (Basal Medium + 5X Supplement, STEMCELL Technologies, Cambridge, UK) with 10 μM Y-27632 dihydrochloride (RHO/ROCK pathway inhibitor, STEMCELL Technologies) and penicillin-streptomycin (10 units/ml penicillin and 10 μg streptomycin/ml Sigma-Aldrich) on Matrigel-coated dishes. Every day, half of medium volume was changed, but Y-27632 dihydrochloride was only added when cells are thawed or passed. For passage, the medium was removed, and 1 mL of Accutase (Aurogene Srl, Roma, Italy) was added and incubated for 3'/4' at 37 °C, until complete detachment of cells. The reaction was then inhibited adding equal volume of mTeSR1 and cells centrifugated for 5' at 1000 rpm. The pellet was then resuspended in mTeSR1 complete medium and plated on dishes, where previously Matrigel polymerized for at least 1 hour, at 37°C.

Since iPS can be reprogrammed into theoretically all types of cells, we differentiate all lines into Neural Progenitor Cells (NPCs), which better mimic the human pathophysiology. The protocol for differentiation (Choi et al. 2017) passed through the step of Embryoid Bodies (EB, spheres of undifferentiated cells that, morphologically, resemble a gastrula from suspended iPS cell aggregates). Here, the iPS are detached as previously described but plated on ultra-low adhesion (Corning) culture plates without Matrigel, for 3-4 days using N2-B27 medium: DMEM F-12 (StemCell) + Neurobasal (Invitrogen) in proportion 1:1; Fibroblast Growth Factor-2 (FGF2 10 ng/ml, PeproTech); Epidermal Growth Factor (EGF; 10 ng/ml, PeproTech); N2 supplement (1%, Thermo Fisher); B27 supplement (2%, Thermo Fisher); Penicillin-Streptomycin (1%, Sigma-Aldrich); L-Glutamine (2 mM, Sigma-Aldrich). Only for the first passage we added Y-27632 dihydrochloride (10 μM). After EB formation, we passed them as single cells and then plated on Matrigel-coated dishes, but using DMEM-F12

differentiation medium: DMEM F-12 (StemCell); Fibroblast Growth Factor-2 (FGF2 10 ng/ml, PeproTech); Epidermal Growth Factor (EGF; 10 ng/ml, PeproTech); N2 supplement (1%, Thermo Fisher); B27 supplement (1%, Thermo Fisher); Bovine serum albumin (BSA, 50 μg/ml, Sigma-Aldrich); Penicillin-Streptomycin (1%, Sigma-Aldrich); L-Glutamine (2 mM, Sigma-Aldrich). Only for the first passage we added Y-27632 dihydrochloride (10 μM).

4.13 Statistical Analysis

All results were analyzed by using Student's t-test or one/two-way ANOVA, followed by Bonferroni post-hoc comparison test, depending on the experiment. Statistical analysis was performed by using the GraphPad Prism 4 software (GraphPad Prism, San Diego, CA, USA; RRID:SCR_002798). *P*-values < 0.05 were considered statistically significant. For the Livecyte proliferation analysis, to analyze the differences among the growth curves, we used Kruskal-Wallis and Mann-Whitney test, followed by Bonferroni correction. This was a mandatory choice since the big dataset created by the instrument didn't allow the use of traditional statistical tools.

5. RESULTS

5.1 RNA-seq and *in vitro* analysis reveals alterations of fatty acids synthesis pathways in OPCs and neurospheres AGC1 deficiency models

From Petralla et al. (2019) and Poeta et al. (2021) works, we highlighted profound defects regarding the proliferation and differentiation processes of our *in vitro* models of AGC1 deficiency. However, no bioinformatic analysis were performed to unravel the molecular basis of these alterations. Transcriptome instead could give us clues to unravel the main affected genes/pathways in AGC1 deficiency, through RNA-seq analysis. Thus, we collected three control and three silenced samples of Oli-Neu cells, sent to IGATech Technology Services Srl (Udine, UD Italy) and the output was analysed by laboratory of Professor Giorgi (University of Bologna, Italy). Subsequently, to validate the results in our *in vitro* models, real-time PCR, Western Blot and Immunofluorescence analysis were done on a small and specific set of transcripts/proteins, among the more interesting and correlated with the pathology.

From RNA-seq differential expression analysis, it was detected a clear alteration of transcriptome in siAGC1 Oli-Neu cells, related to the different genotype, which causes downregulation of about 356 genes and upregulation of 413 (Fig. 5.1 a). This demonstrates the profound effect of AGC1 silencing. Some of these genes were then selected to verify their alterations also at transcript level, in the Oli-Neu model, using real-time PCR. This first result supports the validity of the transcriptomic analysis, confirming the RNA-seq data (Fig. 5.2 g).

Subsequently, as explained in Balboni, Babini et al. (2024), the laboratory of Professor Giorgi conducted a pathway enrichment analysis to identify the impaired cellular pathways, using the Molecular Signature Database (MSigDb). Among others, concerning cell adhesion, motility and neural differentiation, several genes involved in fatty acids and myelin lipids synthesis pathway were found to be altered (Fig. 5.1 b). This data is also in line with the hypomyelination seen in AGC1 deficiency patients (Wibom et al. 2009). Among all genes identified, we found *SREBP1* (Sterol Regulatory Binding Protein 1), a master regulator of fatty acids biosynthetic pathway. This transcription factor, upon increase in sterols levels, is activated by SCAP1 (SREBP Cleavage Activating Protein 1) protein, through a proteolytic cleavage and it enters the nucleus where it recognizes specific DNA sequences, called SRE and allows transcription of many proteins and enzymes responsible for fatty acids synthesis (Eberlé et al. 2004). This transcription factor was seen downregulated in siAGC1 Oli-Neu cells, suggesting a possible dysregulation of the entire pathway, confirmed also by the concomitantly downregulation of *FASN* (Fatty Acids Synthase N). This enzyme's responsible of the rate-limiting step in fatty acids biosynthetic pathway: the production of

palmitate from acetyl-CoA and malonyl-CoA (Dimas et al. 2019). From the literature, FASN and SREBP1 downregulation affects the myelination and remyelination processes, causing abnormal myelin formation and composition and interferes with late oligodendrocytes maturation (Dimas et al. 2019; Monnerie et al. 2017).

Similarly, *SREBP2* was seen downregulated. It's the second isoform of *SREBP1*, but whose functions are mainly involved in cholesterol synthesis, an essential component of membranes and myelin (Camargo, Smit, and Verheijen 2009). Thus, hypomyelination visible in AGC1 deficiency patients could originate from abnormal production of building blocks of membranes and myelin sheath, the fatty acids and lipids.

a

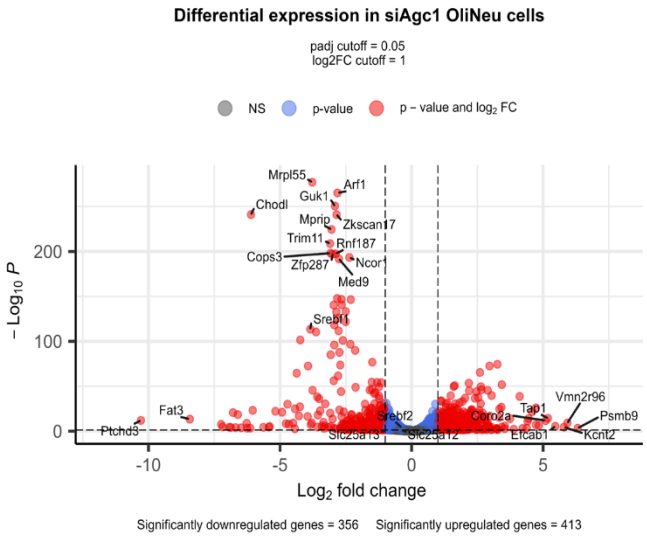

b

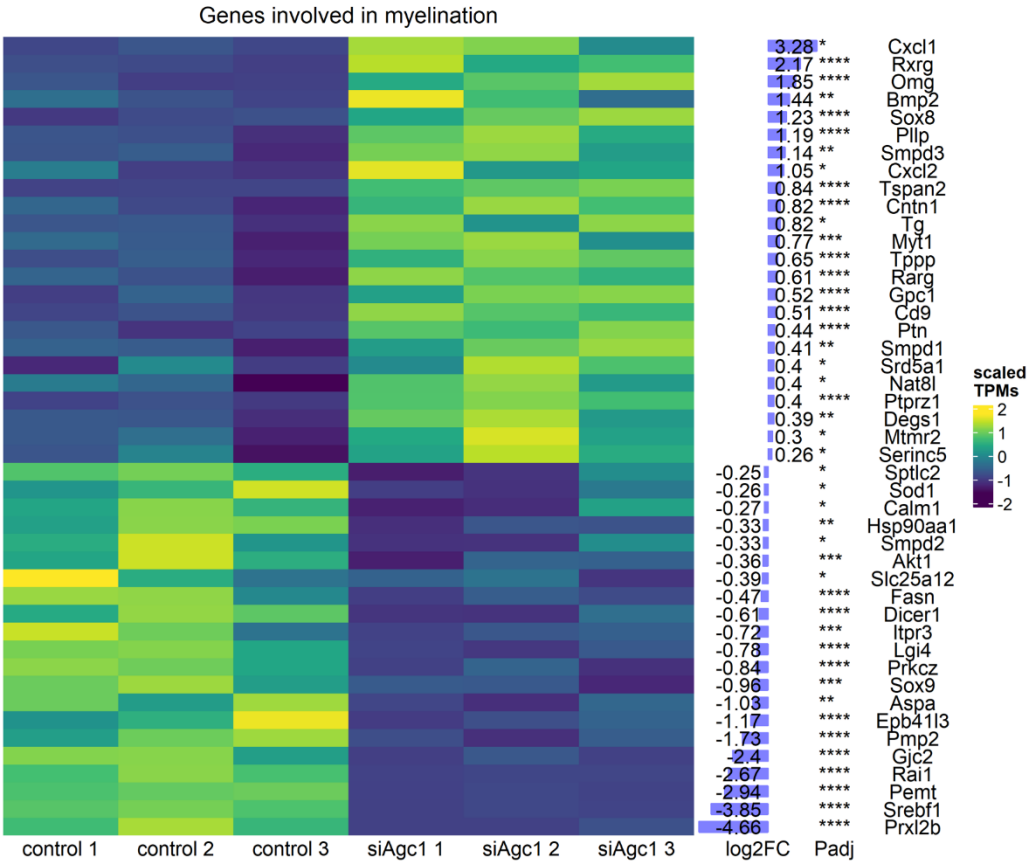

Fig. 5.1 Bioinformatic analysis on RNA-seq dataset. Volcano plot of siAGC1 vs control Oli-Neu (a), with major altered genes and Transcripts Per Million (TPMs) heatmap of mainly altered genes involved in myelination (b)

All these data were also tested in *in vitro* analysis. In Fig. 5.2.g, real time PCR of siAGC1 cells showed downregulation of *SREBP1* and *2* – data also confirmed at protein levels for SREBP1, through Western Blot (Fig.5.2 a, d and e) - respect to control one. In addition, FASN, which seems not altered at transcript level (Fig. 5.2 g), is less expressed in silenced cells respect to the control one

(Fig. 5.2 a and b). This confirms an overall alteration of fatty acids and cholesterol synthesis pathway, involving their main players.

Quite in contrast with these results, *ACSS1* (Acetyl-CoA Synthetase 1), responsible for acetyl-CoA production from acetate, was upregulated at transcript level in siAGC1 cells respect to control one, both in RNA-seq and real-time PCR data (Fig. 5.1 b, Fig. 5.2 g). It could be contradictory because this protein transcription is directly induced by SREBP1; however, recently Luong et al. (2000) highlighted just a partial control of the transcription factor over ACSS1. Nonetheless, at protein level (Fig. 5.2 a and c), siAGC1 cells didn't show any significant alterations of ACSS1 abundance. This result could be in line with a partial usage of this biosynthetic pathway by the cells, which in normal conditions, preferentially obtain acetyl-CoA from citrate, via ATP Citrate Lyase (ACLY; Wellen and Thompson 2012).

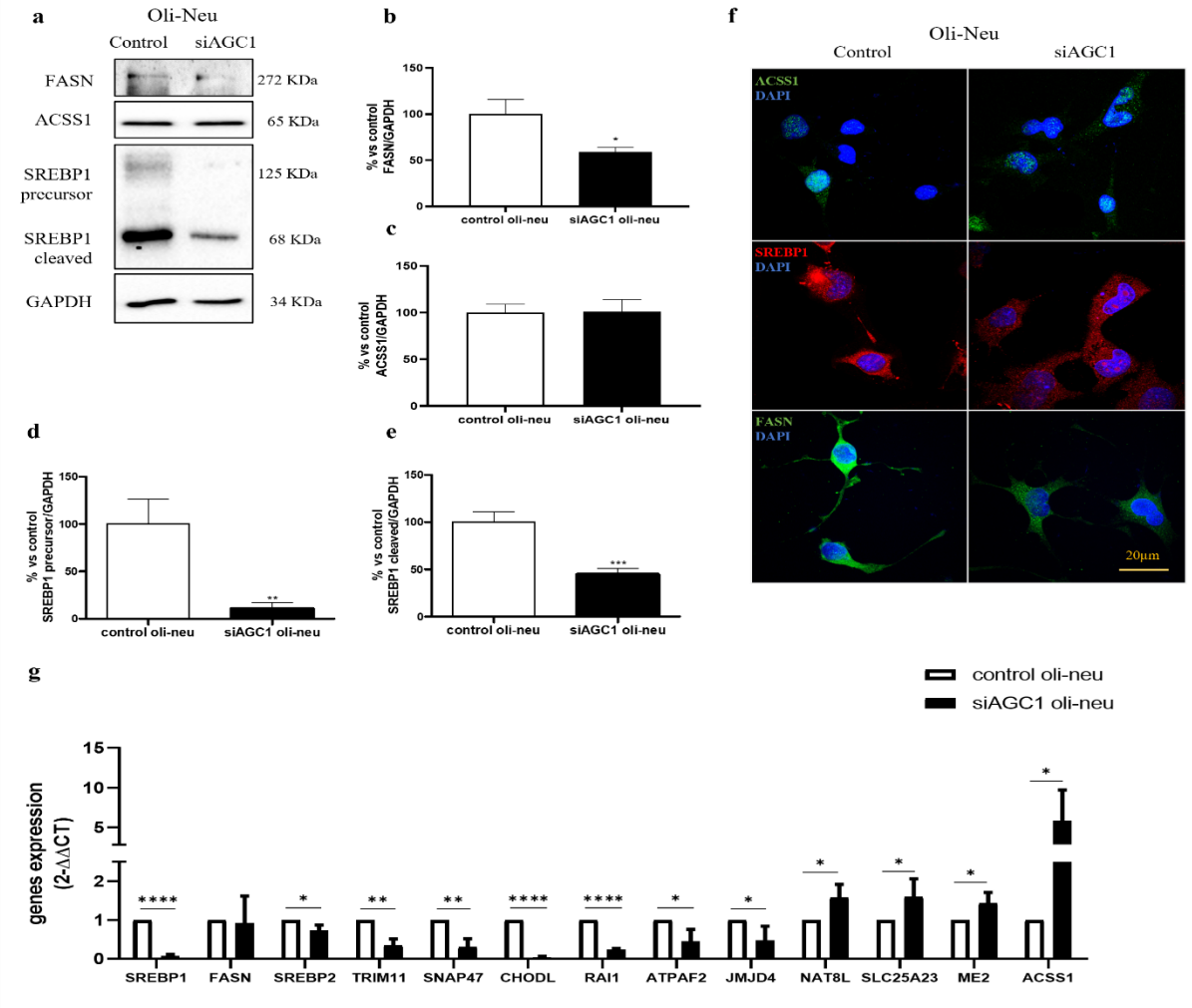

Fig. 5.2 Western blot and relative densitometries of FASN (a, b), ACSS1 (a, c), precursor and cleaved SREBP1 (a, d, e) expression in Oli-Neu cells; GAPDH was used for endogenous normalization. Confocal microscopy images (f) in Oli-Neu cells; nuclei were labelled with DAPI. Scale bar: 20 µm; 100x objective. RT-qPCR analysis (g). GAPDH were used as endogenous controls. Values are mean ± SD of at least 3 independent experiments; *** P <0.001, ** P <0.01, * P <0.05, compared to control Oli-neu; Student's t-test

To identify if similar alteration on fatty acids and myelin lipids synthesis were also present in neurospheres, deriving from AGC1 deficiency mouse model, we extended the *in vitro* analysis focused on these transcripts and proteins to the 3D AGC1 deficiency model (Fig.5.3). Neurospheres are a pool of neural stem cells which can potentially give rise to neuronal, astrocytic and oligodendroglial progenitors, mimicking better the pathophysiological environment of the disease. Thus, we performed real-time PCR, Western Blot and Immunofluorescence on the same subset of genes and proteins.

Concerning the transcript level, most of the data for real-time PCR in heterozygous spheres were consistent with the results of the RNA-seq and on Oli-Neu cells, confirming the presence of overlapping characteristics between these two models for the study of AGC1 deficiency (Fig. 5.3 g). The fact that neurospheres are a mixed pool of three neural precursors could explain the different results obtained for some genes, since potentially, each cell type could contribute differently to the enzymatic and protein set.

As for Oli-Neu cells, we performed Western Blot and Immunofluorescence analysis on major players of fatty acids and acetyl-CoA synthesis pathway: SREBP1, FASN and ACSS1 (Fig. 5.3 a, b, c, d and e). Regarding SREBP1 – similarly to the real-time PCR result – a reduction in the expression of $AGC1^{+/-}$ spheres was detected (Fig. 5.3 a, d and e), corroborating a possible dysregulated control of fatty acids synthesis. In parallel, its second isoform, *SREBP2*, was seen downregulated, at transcript level, highlighting cholesterol synthesis alteration, too (Eberlé et al. 2004; Fig. 5.3 g). However, FASN and ACSS1 showed an upregulation of about 50-90% in heterozygous neurospheres through Western Blot analysis, respect to wild-type ones. Similar results were also obtained at transcript level (Fig. 5.3 a, b, c and g). These data could be explained by the heterogenous pool of neurospheres and the cell-specific enzymes present in this model. In addition, upregulation of FASN could be explained by an increase in HDAC3 expression, seen in heterozygous spheres (Poeta et al. 2021). This deacetylase is indeed responsible for FASN protection, against its turnover (Lin et al. 2016).

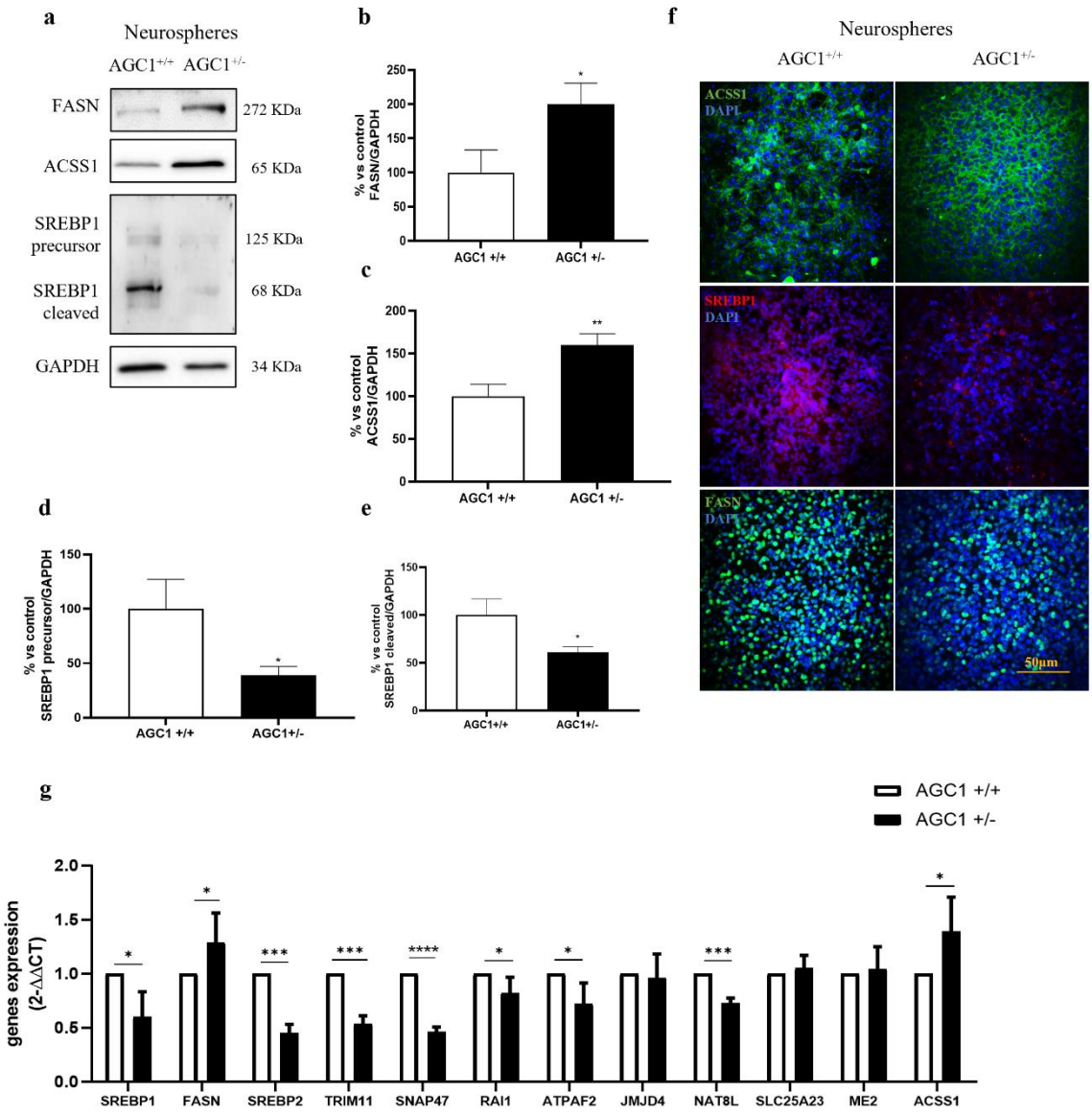

Fig. 5.3 Western blot and relative densitometries of FASN (a, b), ACSS1 (a, c), precursor and cleaved SREBP1 (a, d, e) expression in AGC1$^{+/-}$ and AGC1$^{+/+}$ neurospheres; GAPDH was used for endogenous normalization. Confocal microscopy images (f) in neurospheres; nuclei were labelled with DAPI. Scale bar: 50 µm; 60x objective. RT-qPCR analysis (g). GAPDH were used as endogenous controls. Values are mean ± SD of at least 3 independent experiments; *** p <0.001, ** p <0.01, * p <0.05, compared to AGC1$^{+/+}$ control neurospheres; Student's t-test

Overall, these results confirm that AGC1 silencing induces an overall transcriptome dysregulation. Of main interest was the alterations involving the fatty acids and acetyl-CoA synthesis pathways, in both AGC1 deficiency models. Lipids are essential for myelin formation but require acetyl groups, from acetyl-CoA, to be formed. Similarly, acetyl groups can be used for histone and proteins acetylation, which controls thousands of cell processes. Thus, availability of this metabolite can affect many biological functions, ranging from myelination to proliferation and differentiation regulation

of OPCs and NSCs, through epigenetic modifications (Chakrabarty and Chandel 2021; Zijun Wang et al. 2018).

5.2 ATAC-seq confirms the altered epigenetic landscape of siAGC1 Oli-Neu cells

From (Poeta et al. 2021), the presence of altered epigenetic regulation of proliferation and differentiation processes was well assessed in Oli-Neu model of AGC1 deficiency. Epigenetic modifications are extremely important for transcription factors and genes accessibility since the chromatin state regulates and influences transcription. For this reason, in collaboration with the laboratory of Professor Giorgi (University of Bologna), we decided to perform ATAC-seq on 4 replicates of control and siAGC1 Oli-Neu samples. This analysis enables to study the epigenetic landscape and chromatin remodelling, identifying the open and histone-bound regions, in terms of promoter accessibility (Grandi et al. 2022). This would help us to: i) identify if an overall altered epigenetic landscape is present, upon AGC1 silencing, in our model; ii) understand whether the up/downregulation of transcripts, detected through RNAseq, are induced by epigenetic mechanisms, especially for those genes involved in fatty acids and myelin lipids synthesis pathway.

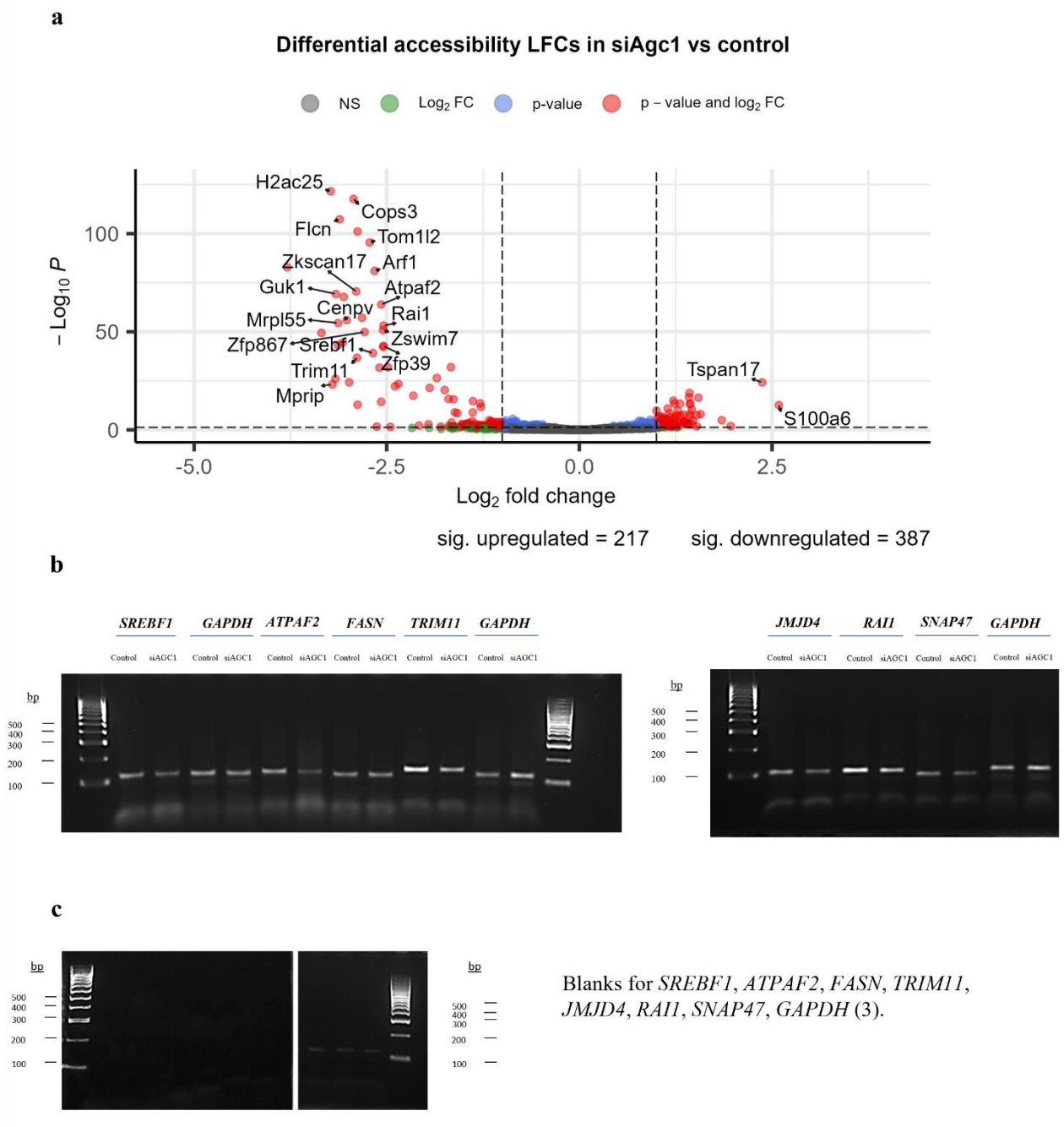

Fig. 5.4 Volcano plot of peaks counts deriving from ATAC-seq in siAGC1 vs control Oli-Neu cell samples (a) and PCR validation of target genes identified as downregulated in RNA-seq and within closed chromatin regions from ATAC-seq (b) and their blanks (c)

From the differential accessibility analysis (Fig. 5.4 a), Giorgi's laboratory discovered 217 peaks (where peak means regions of the genome where sequenced reads result enriched compared to the background) upregulated – thus, more open – and 387 downregulated – more closed – in siAGC1, respect to control samples. This firstly, confirms the presence of an altered epigenetic profile in silenced cell line. However, more interesting was the fact that some of the genes found statistically less accessible in ATAC-seq analysis, were also less expressed, in term of transcript, in the RNA-seq, as *Trim11*, *Atpaf2*, *Srebf1* and *Rai1*. To prove that these expression variations were correlated to an

altered epigenetic mechanism and not to a genome rearrangement, as a deletion caused by shRNA insertion, we performed a PCR, using specific primers for these genes that we also tested with real-time PCR previously (paragraph 5.1). Since no deletion was detected by the PCR on genomic DNA of control and siAGC1 cells (Fig. 5.4 b and c), we can stat that strong downregulation of these specifical transcripts is caused by an altered epigenetic mechanism, since their closed chromatin peaks overlap with the loci of downregulated genes.
In general, silencing of AGC1 seems to affect, in Oli-Neu cells, the epigenetic regulation of many different biological pathways, as proliferation, differentiation but also myelin synthesis.

5.3 Metabolic and epigenetic alterations in AGC1 deficiency models

AGC1 carrier is extremely important for cell bioenergetic, allowing – through the Malate Aspartate Shuttle – the correct passage, across mitochondrial membrane, of metabolites, which feed the TCA cycle and acetyl-CoA pool (Broeks et al. 2021). Since this involvement of AGC1 carrier in cell metabolism, we decided to verify the concentration of different metabolites in Oli-Neu cells, through a targeted approach. We chose among metabolites involved in many different anabolic and catabolic pathways, as TCA cycle intermediates, amino acids but also nucleosides and the metabolic species transported by AGC1 itself (aspartate, glutamate and NAA). For these quantification, three replicates of cell pellets and cell media (control and siAGC1) were collected and through collaboration with the laboratory of Professor Mercolini (University of Bologna, Italy), analysed via MEPS-LC-MS/MS approach (Protti et al. 2023). As expected, and in line with patients' data (Wibom et al. 2009; Dahlin et al. 2015; Falk et al. 2014), siAGC1 cells and media showed up reduced levels of aspartate and N-acetyl-aspartate. Also, a higher release of lactate in the media of siAGC1 Oli-Neu was detected, suggesting an increase in pyruvate conversion into this metabolite, rather than entering the TCA cycle for energy production. This is clear index of a more glycolytic phenotype of these cells (Narine and Colognato 2022). In addition, many amino acids (as L-asparagine, L-aspartate, L-glutamine and L-glutamate) seemed less abundant in silenced cells, respect to control ones (Fig. 5.5 a and b). These are essential amino acids which controls different biological reactions, as glutamatergic transmission and proliferation, for glutamine/glutamate (Xin et al. 2019; Bott et al. 2015). The latter is also involved in OPCs motility and induction of differentiation (Spitzer et al. 2016) and its synthesis starts from 2-oxoglutarate, which is indeed less concentrated in silenced cells, respect to control ones. In addition, we also detected a lack of branched chain amino acids as leucine and isoleucine, in siAGC1 Oli-Neu. These amino acids are essential, among others, for the replenishment of acetyl-CoA pool of cell (Sperringer, Addington, and Hutson 2017a), hampering many physiological functions, in which this signalling molecules is involved (Pietrocola et al. 2015). In addition, their alterations -as in the

case of Maple Syrup Urine Disease- can affect myelination, causing abnormalities in CNS patients' white matter (Schonberger et al. 2004). These metabolic abundances variations are tightly linked to the one of transcripts, obtained from RNA-seq, and this relationship is well-known in literature (Cavicchioli et al. 2022), testifying a strong link between transcriptome and metabolome.

For other types of metabolites, we sent three cell samples, in triplicates (control and siAGC1), to Metabolomics Core Technology Platform (Germany), that performed a similar technique, using LC/MS-MS approach. From this analysis (Fig. 5.5 c and d), Coenzyme-A (CoA) is significantly increased in siAGC1 Oli-Neu respect to control one, but not the acetyl-CoA, suggesting a possible lack of acetyl groups to support the complete synthesis or more generally a disrupting metabolism, affecting PHD (pyruvate dehydrogenase, which converts pyruvate into acetyl-CoA), hampering OXPHOS (Shurubor et al. 2020). Similarly, silenced cells exhibited an increase in NAD level -but not in NADH- as expected, since the role of AGC1 carrier in MAS, essential to keep balanced the reducing equivalents ratio, within cell compartments (Broeks et al. 2021).

Overall, these results suggest a clear dysregulated metabolic profile in silenced cells, respect to the control one, upon AGC1 silencing.

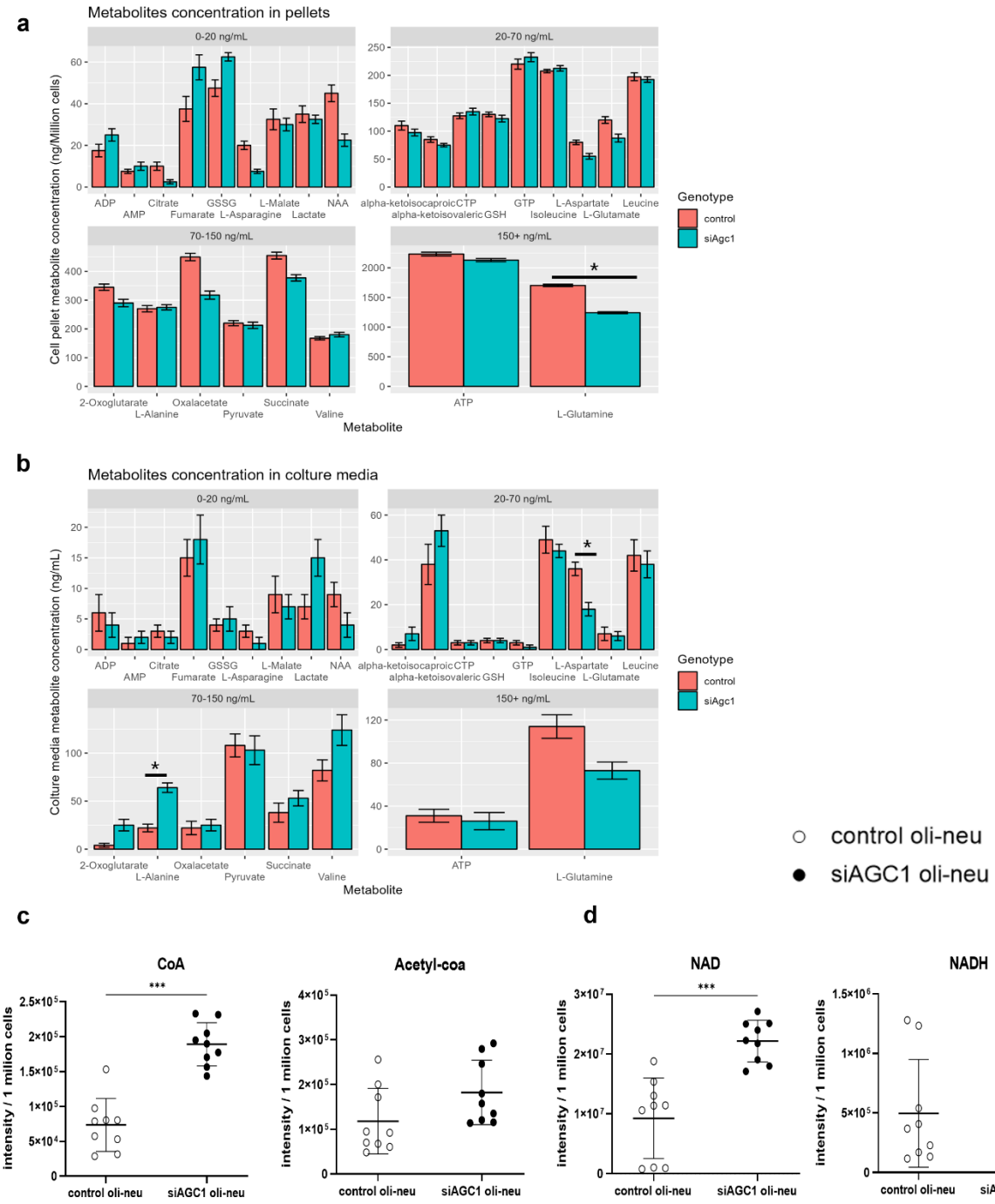

Fig. 5.5 Bar-graph showing concentrations (ng/mL) and relative error bars in siAGC1 and control samples, pellet (a) and culture media (b). Separated scatter of CoA, Acetyl-CoA (c), NAD and NADH (d) metabolites quantifications for 1 million of cells. Values are mean ± s.e.m. of at least 3 independent experiments; *** p <0.001, ** p <0.01, * p <0.05, compared to control Oli-Neu cells; Student's t-test

Following the discovery of NAD^+/NADH levels alteration, we decided to investigate a specific class of proteins/histones deacetylase, the sirtuins. This choice was made considered the central role of AGC1 in controlling NAD^+/NADH balance through Malate-Aspartate Shuttle, but also the NAD-dependent activity of sirtuins (Mei et al. 2016). Indeed, we hypothesized that AGC1 silencing could hamper the MAS function and, in general, the cell bioenergetics, leading to metabolites variations.

These metabolites contribute to the correct functioning of many enzymes and proteins, as sirtuins, histone acetyltransferase (HAT) and deacetylase (HDAC). For these last, previous analysis from our laboratory (Poeta et al. 2021) already detected variations in expression and activity, for both *in vitro* models of AGC1 deficiency, supporting the presence of an altered epigenetic profile, deriving from metabolic disturbances, which affects proliferation and differentiation mechanisms (Poeta et al. 2021). Thus, similarly, we moved to analyze the expression levels of sirtuins (specifically, sirtuin 1, phospho-sirtuin 1, sirtuin 2, 3, 5, 6 and 7) through Western Blot analysis. This would confirm the tight link between metabolites concentrations and epigenetic modifications, which, if affected, could induce harmful effects in transcription regulation of many biological pathways.

From Fig. 5.6, Oli-neu siAGC1 showed an upregulation of sirtuins 3 and 5, responsible for glucose metabolism, causing increase in aerobic glycolysis (Mei et al. 2016). In parallel, a slight but not statistical increase of SIRT1 phosphorylated form, respect to control ones, was present in silenced Oli-Neu cells. This would have effects on lipid metabolism, since this sirtuin directly controls the degradation of SREBP1 (Walker et al. 2010) but also the oligodendroglial commitment, due to its role in OPCs specification (Rafalski et al. 2013b). Sirtuin 2, surprisingly, is not expressed in this cell model, both in control and silenced cells.

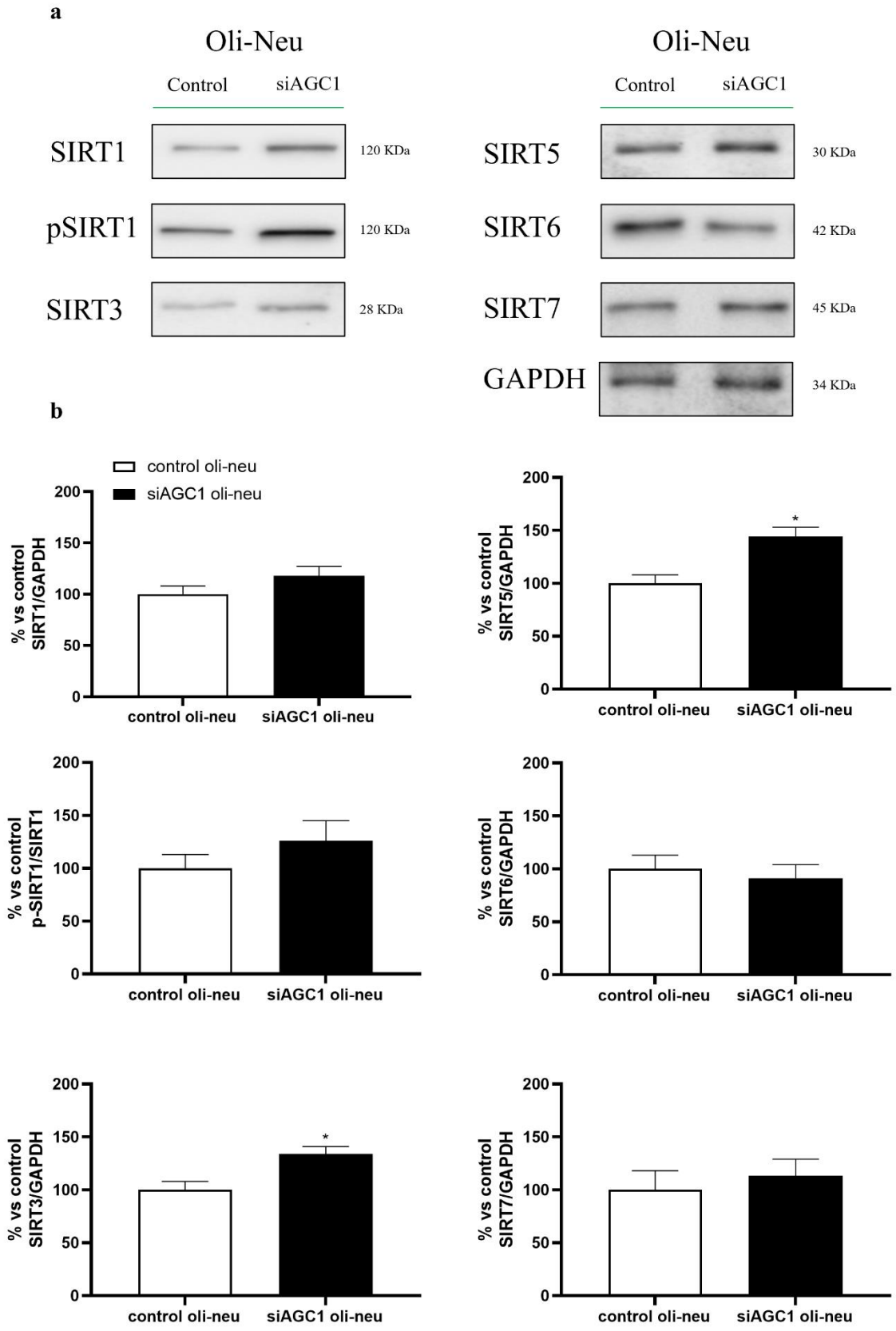

Fig. 5.6 Western blot and relative densitometries of sirtuin 1, phosphorylated-1, 3, 5, 6 e 7 (a, b) expression in in Oli-Neu cells; GAPDH was used for endogenous normalization. Values are mean ± s.e.m. of at least 3 independent experiments; *** P <0.001, ** P <0.01, * P <0.05, compared to control Oli-neu; Student's t-test

Comparably, Western Blot was performed on neurospheres lysate to assess sirtuins abundances. In this model (Fig. 5.7), heterozygous spheres showed upregulation of phosphorylated sirtuin 1. Instead, a reduction of about 50-60 % of all sirtuin 2 isoforms was detected. Two of these isoforms have histone deacetylase activity (Rack et al. 2014a), thus their downregulation could explain the altered epigenetic profile seen in the AGC1 heterozygous spheres. Meanwhile, sirtuin 6 was upregulated in heterozygous spheres. This sirtuin is responsible at three distinct levels of SREBP1 inhibition, thus, its upregulation widely correlated with the downregulation of SREBP1, described before (Elhanati et al. 2013).

Sirtuins represent a clear bridge between metabolism and epigenetic, as HATs and HDACs, since their dependence on metabolites concentrations and their role -among others- in epigenetic modifications; thus, alterations regarding these enzymes highlight a possible dysregulation of metabolome and epigenome, responsible for many defects that we already detected in these models.

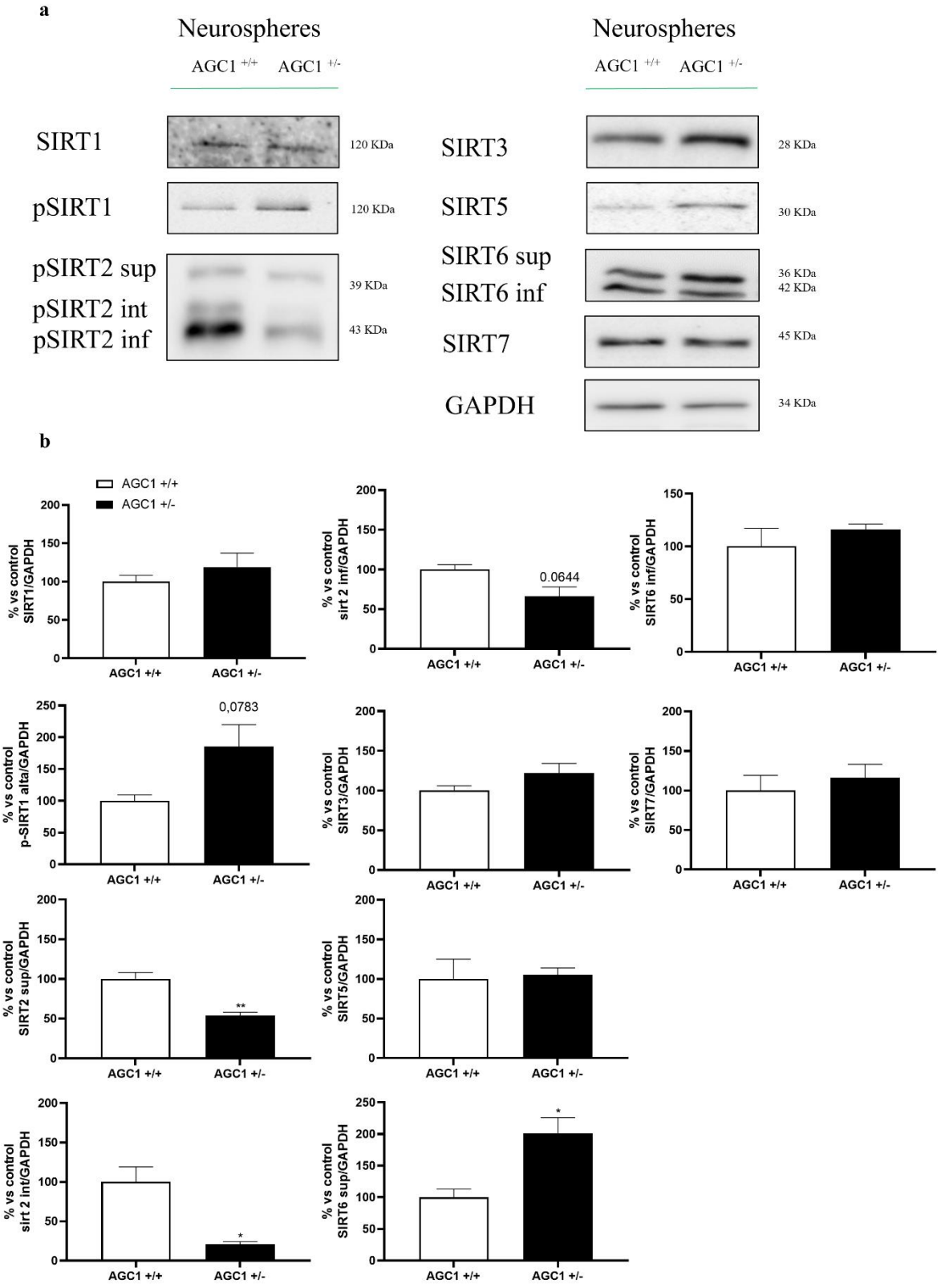

Fig. 5.7 Western blot and relative densitometries of sirtuin 1, phosphorylated-1, 3, 5, 6 e 7 (a, b) expression in AGC1$^{+/-}$ and AGC1$^{+/+}$ neurospheres; GAPDH was used for endogenous normalization. Values are mean ± s.e.m. of at least 3 independent experiments; *** P <0.001, ** P <0.01, * P <0.05, compared to AGC1$^{+/+}$ neurosphere; Student's t-test

5.4 BCAAs and KBs supplementations improve proliferation in AGC1 deficiency models

Since the defects on epigenetic modifications seems to be induced by abnormal metabolites concentrations, we try to compensate these deficits of both *in vitro* AGC1 models, performing supplementations with compounds that could replenish the cells with those metabolites they lack/exceed, as acetyl groups (for histone/protein acetylation) and NAD (for sirtuins activity). In this way, the final goal was to investigate if single or mixed compounds could recover the proliferative and differentiative defects of silenced Oli-Neu cells and heterozygous neurospheres (Petralla et al. 2019; Poeta et al. 2021), working on the metabolic/epigenetic alterations. These compounds mainly constitute the key macromolecules of the ketogenic diet, as ketone bodies (KBs) and branched-chain amino acids (BCAAs). Indeed, nowadays, this diet has brought some psychomotor and myelination improvement in AGC1 deficiency patients (Dahlin et al. 2015), even though a controlled regimen and lowered side effects aren't easy to reach. For this purpose, supplementations with KBs and BCAAs were done on Oli-Neu cells and neurospheres, to identify the most promising compounds.

For the pro-proliferative effects of supplementations on Oli-Neu cells, we use the LiveCyte PhaseFocus to monitor the cell growth, during time (72 hours). From the cell count, the instrument gives back growth curves of the single tested conditions, analysed through Kruskal-Wallis and Mann-Whytney test, followed by Bonferroni correction.

Upon a prolonged exercise or following a ketogenic diet, our body starts to produce ketone bodies (β-hydroxybutyrate and Acetoacetate) and their levels in blood stream increase. They are essential since they can be used, especially Bhb, as alternative glucose fuel by brain (Tepavčević 2021). Concerning their supplementations, three distinct concentrations were analysed on seeded Oli-Neu cells, for β-hydroxybutyrate (Bhb 2,5; 5 and 10 mM) and aceto-acetate (AcAc 0,5; 1; 1,5 mM). In addition, to better mimic the ketogenic diet effects, mix of the two compounds were also tested.

From Fig. 5.8, we firstly confirm the presence of lower proliferation rate of siAGC1 cells (red line) respect to the control one (black line), accordingly to data from Petralla et al. (2019) on proliferation. Interestingly, most of the concentrations has induced a recovery in this defect, increasing the proliferation of siAGC1, at least respect to the untreated silenced control. Specifically, for Bhb, the most promising concentrations was 10 mM, which enhanced the proliferation over the control Oli-Neu curve (Fig. 5.8 a). Whereas for AcAc (Fig. 5.8 b), the intermediate concentration seemed more effective. Regarding the combinations between two compounds, just the one with the lowest concentrations of both (Bhb: 5 mM + AcAc: 0,5 mM, Fig. 5.8 c) increased the proliferation. This effect could be explained by an increment of cell oxidative phosphorylation, which could accumulate reactive oxygen species, harmful for cells integrity (Andreyev, Kushnareva, and Starkov 2005).

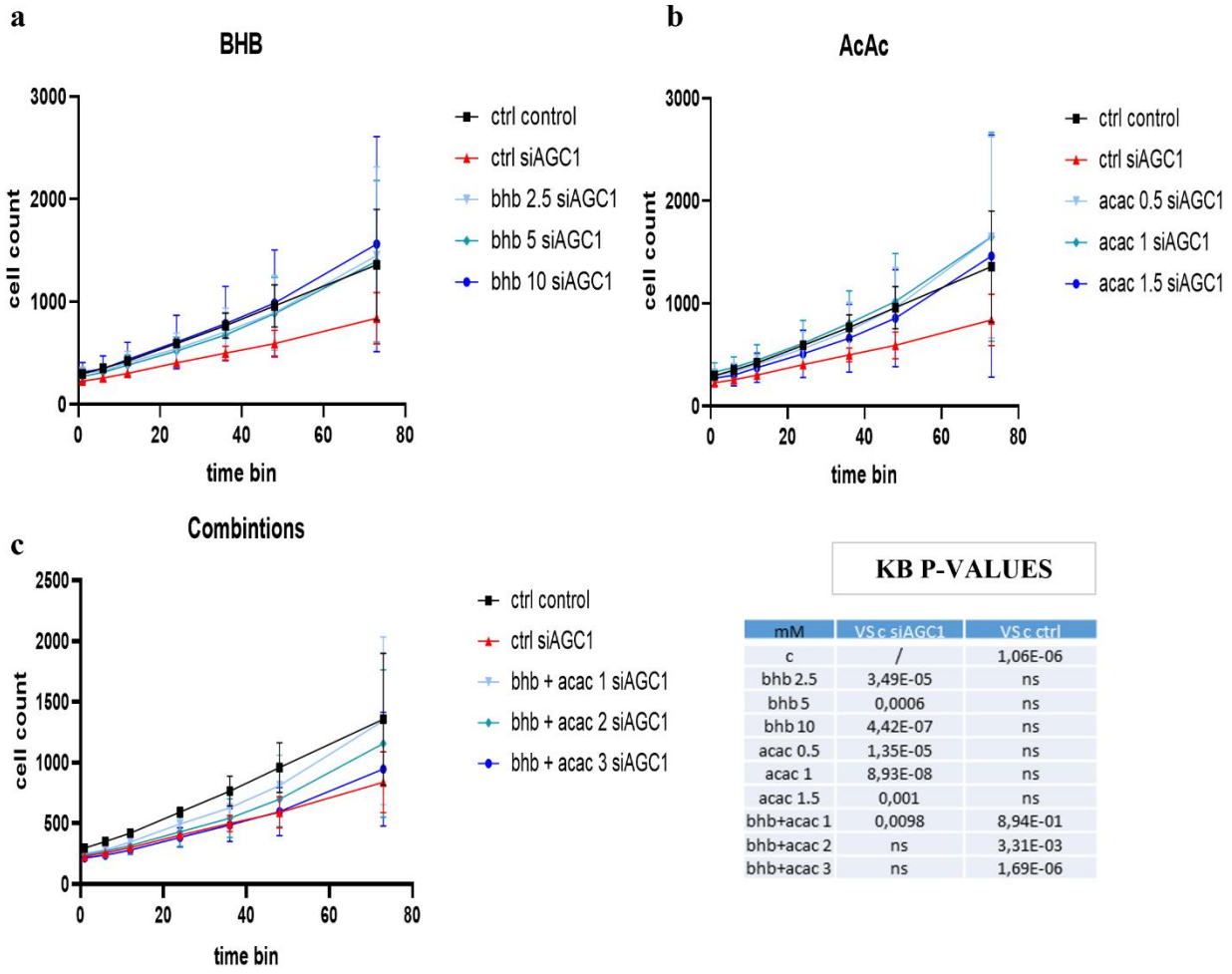

mM	VS c siAGC1	VS c ctrl
c	/	1,06E-06
bhb 2.5	3,49E-05	ns
bhb 5	0,0006	ns
bhb 10	4,42E-07	ns
acac 0.5	1,35E-05	ns
acac 1	8,93E-08	ns
acac 1.5	0,001	ns
bhb+acac 1	0,0098	8,94E-01
bhb+acac 2	ns	3,31E-03
bhb+acac 3	ns	1,69E-06

Fig. 5.8 Growth analysis of Oli-neu cells with Livecyte PhaseFocus and their relative p-values. We plate 2000 cells per well and let spontaneously growth for 3 days, with beta-hydroxybutyrate (Bhb 2,5 – 5 – 10 mM, a) acetoacetate (AcAc 0,5 – 1- 1,5 mM, b) or their combinations (Bhb 2,5 mM + AcAc 0,5 mM – Bhb 5 mM + AcAc 1 mM – Bhb 10 mM + AcAc 1,5 mM, c). Images were acquired every hour. N=3 ± s.e.m. Kruskal-Wallis test, Mann-Whitney test and Bonferroni correction were performed

Similarly, we tested on Oli-Neu cells three different concentrations (200; 400; 800 mg/l) of branched-chain amino acids (BCAAs): leucine, isoleucine and valine, alone and in combinations. These compounds were chosen since their essential role in brain metabolism (Sperringer, Addington, and Hutson 2017a). Indeed, BCAAs are essential amino acids, whose transamination reactions occurs in extra-hepatic tissues, such as CNS, supporting energy production and proliferation, through their catabolism, which allow to classify them into two categories: ketogenic and gluconeogenic. In the first class, there're leucine and isoleucine, since they could be converted into ketone bodies; in the second, valine but also isoleucine, which can give rise to different TCA cycle intermediates, as succinyl-CoA (Sperringer, Addington, and Hutson 2017a; Bixel and Hamprecht 1995).

LiveCyte analysis of BCAAs supplementations (Fig. 5.9) revealed a general increment of siAGC1 proliferation upon addition of 400 mg/l of leucine (a) and isoleucine (b). Valine supplementations instead resulted statistically significant respect to untreated siAGC1 cells (red line) already at 200

mg/l, probably due to the higher concentration of this amino acid in the siAGC1 media, as discovered through LC-MS/MS quantification (paragraph 5.2). For the combinations of the three different BCAAs (Fig. 5.9 d), only the one with lowest concentrations of all three had a modest effect on siAGC1 proliferation (p=0,005). Also in this case, we can hypothesize an increase of the acidaemia, induced by higher concentrations of BCAAs, as cause for the slower proliferative pace (Sperringer, Addington, and Hutson 2017b). Overall, the supplementations increased the proliferation rate, at least respect to untreated siAGC1 cells, especially for single compounds tested.

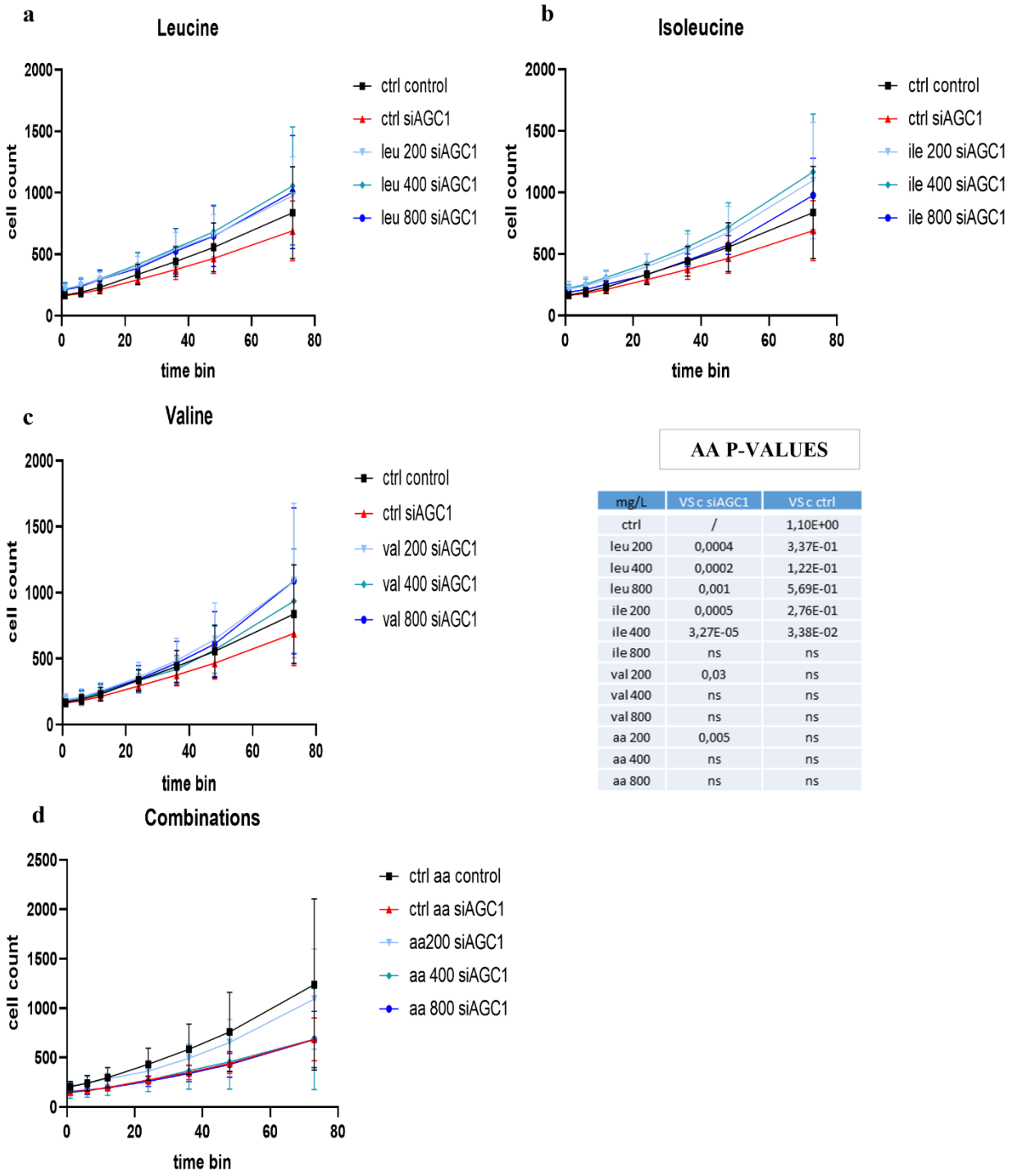

AA P-VALUES

mg/L	VS c siAGC1	VS c ctrl
ctrl	/	1,10E+00
leu 200	0,0004	3,37E-01
leu 400	0,0002	1,22E-01
leu 800	0,001	5,69E-01
ile 200	0,0005	2,76E-01
ile 400	3,27E-05	3,38E-02
ile 800	ns	ns
val 200	0,03	ns
val 400	ns	ns
val 800	ns	ns
aa 200	0,005	ns
aa 400	ns	ns
aa 800	ns	ns

Fig. 5.9 Growth analysis of Oli-neu cells with Livecyte PhaseFocus and their relative p-values. We plate 2000 cells per well and let spontaneously growth for 3 days, with Leucine (Leu 200 – 400 – 800 mg/l, a) Isoleucine (Ile 200 – 400- 800 mg/l, b), Valine (200 – 400 – 800 mg/l, c) or their combinations (aa200 Leu 200 + Ile 200 + Val 200 – aa400 Leu 400 + Ile 400 + Val 400 – aa800 Leu 800 + Ile 800 + Val 800, d). Images were acquired every hour. N=3 ± s.e.m. Kruskal-Wallis test, Mann-Whitney test and Bonferroni correction were performed

To determine whether KBs and BCAAs supplementations would have same pro-proliferative effects on heterozygous neurospheres, we used the Incucyte S3 system to monitor for 7 days the growth, from single cell to complete spheres. Indeed, as already demonstrated (Petralla et al. 2019),

heterozygous neurospheres showed a reduced proliferation, in favour of a premature differentiation. To counteract this tendency, we plated $5x10^3$ single cells per well, in suspension, and treated with ketone bodies or branched chain amino acids, following the same concentrations already used for Oli-Neu cells. For the analysis of this 3D model, three parameters were considered in distinct time phases: object count per image (count of the cells in each well); total area of objects in the image and the average eccentricity (how much the object could be considered as a sphere). Specifically, the first two parameters were analysed until the fourth day. In this time interval indeed, there's the major proliferation of spheres, which increase their number and their size. The eccentricity instead was calculated along the entire analysis interval (seven days). This parameter enables to know if the spheres maintain their roundness or instead, start to differentiate upon attaching to the well and forming branches and ramifications. This situation generally occurs for heterozygous spheres, which -after the fourth day- tend to adhere and spontaneously differentiate, creating a star-like shape, which increases the eccentricity parameter value. For this reason, the total area was set at 4^{th} day, otherwise the branched shape acquired from this day by $AGC1^{+/-}$ spheres would affect the analysis of this parameter.

In details, as shown in Fig. 5.10/5.13, untreated heterozygous spheres proliferate more slowly, with a peak in their number at 3/4 days. This doesn't occur for wild-type one, which instead reach the peak at the second day and then, start to increase their size (Fig. 5.11/5.14), becoming larger than $AGC1^{+/-}$, whereas their number slightly decreases. Concerning eccentricity (Fig. 5.12/5.15), heterozygous neurospheres showed values near to 1, especially after the 5^{th} day, when they start to acquire branched shape. Meanwhile, wild-type ones tend to have a more uniform round shape, with eccentricity values around 0,4 – 0,5.

Ketone bodies supplementations well counteracted this trend, speeding up the proliferation of spheres. Regarding the object count, we saw modest results from AcAc at 1mM and Bhb at 2,5 mM, and none from the combinations of both ketones (Fig. 5.10, a, b and c). More impressive data were instead obtained for the object area, with a complete recover respect to untreated AGC1+/- spheres for acetoacetate (1 mM) and β-hydroxybutyrate (2,5 mM), but also their combination (Bhb 2,5 mM+ AcAc 0,5 mM, Fig. 5.11). This increase in size is also accompanied by slight decrease in eccentricity, even though not statistically significant (Fig. 5.12).

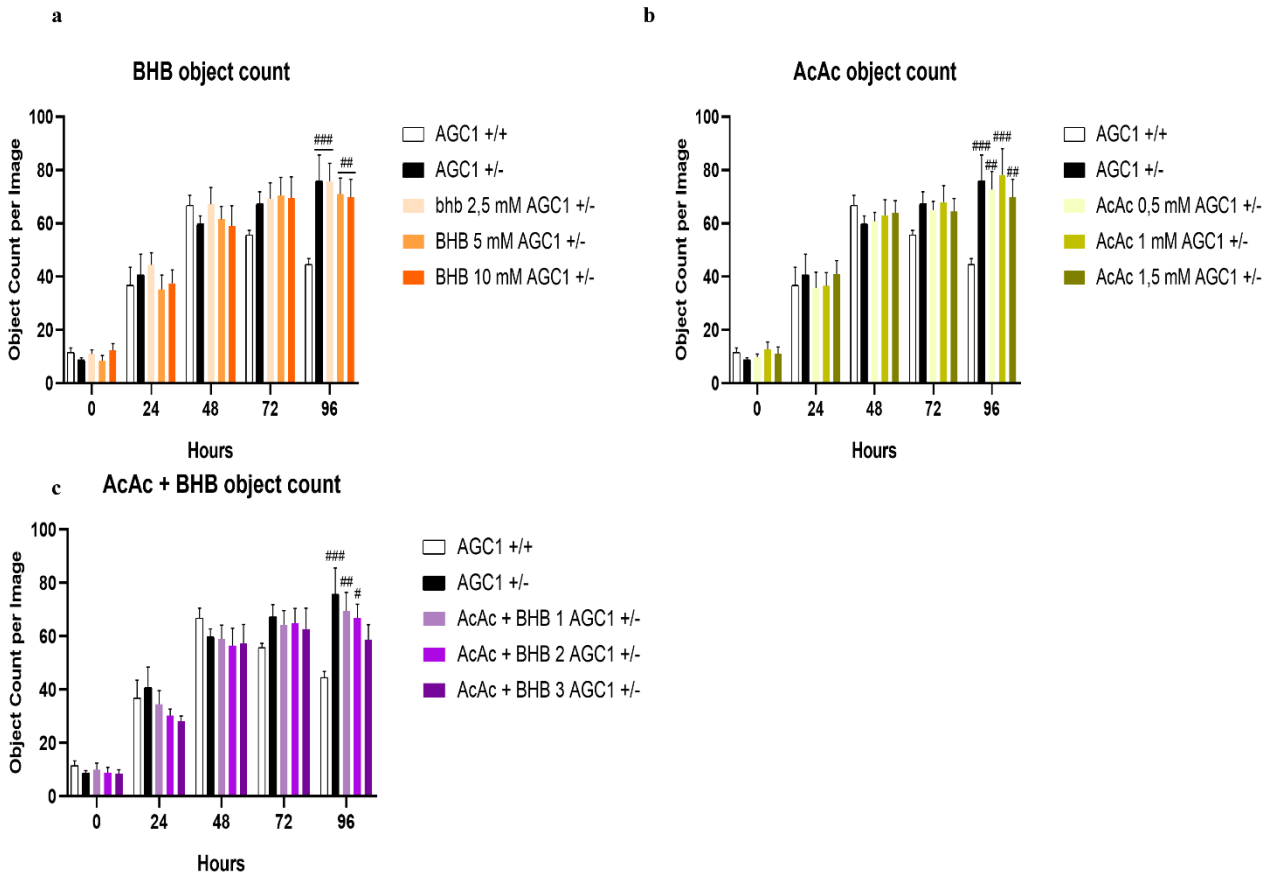

Fig. 5.10 Growth analysis of neurospheres through the analysis of the object count of the brightfield object in the image. Single neurospheres were plated (5000 per well) and let spontaneously growth for 7 days with beta-hydroxybutyrate (Bhb 2,5 – 5 – 10 mM, a) acetoacetate (AcAc 0,5 – 1- 1,5 mM, b) or their combinations (Bhb 2,5 mM + AcAc 0,5 mM – Bhb 5 mM + AcAc 1 mM – Bhb 10 mM + AcAc 1,5 mM, c). Images were acquired every 24h. N=3 ± s.e.m. # p-values <0,005 compared to $AGC1^{+/+}$ neurospheres; * p-values <0,005 compared to C $AGC1^{+/-}$ neurospheres, two-way ANOVA Dunnett's multiple comparison test (Bonferroni's post-hoc comparison test)

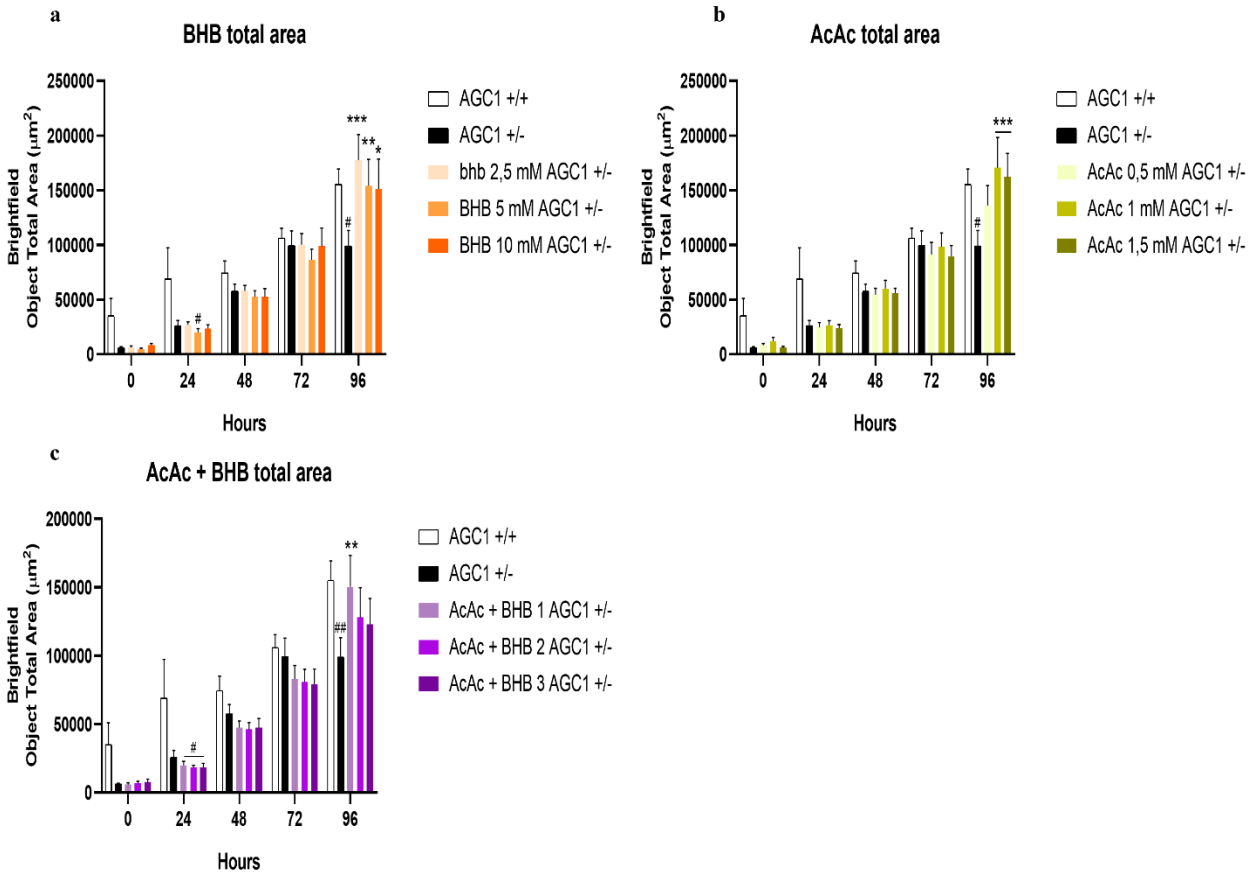

Fig. 5.11 Growth analysis of neurospheres through the analysis of total of the area of the brightfield object in the image (Area µm^2). Single neurosphere were plated (5000 per well) and let spontaneously growth for 7 days with beta-hydroxybutyrate (Bhb 2,5 – 5 – 10 mM, a) acetoacetate (AcAc 0,5 – 1- 1,5 mM, b) or their combinations (Bhb 2,5 mM + AcAc 0,5 mM – Bhb 5 mM + AcAc 1 mM – Bhb 10 mM + AcAc 1,5 mM, c). Images were acquired every 24h. N=3 ± s.e.m. # p-values <0,005 compared to AGC1$^{+/+}$ neurospheres; * p-values <0,005 compared to C AGC1$^{+/-}$ neurospheres, two-way ANOVA Dunnett's multiple comparison test (Bonferroni's post-hoc comparison test)

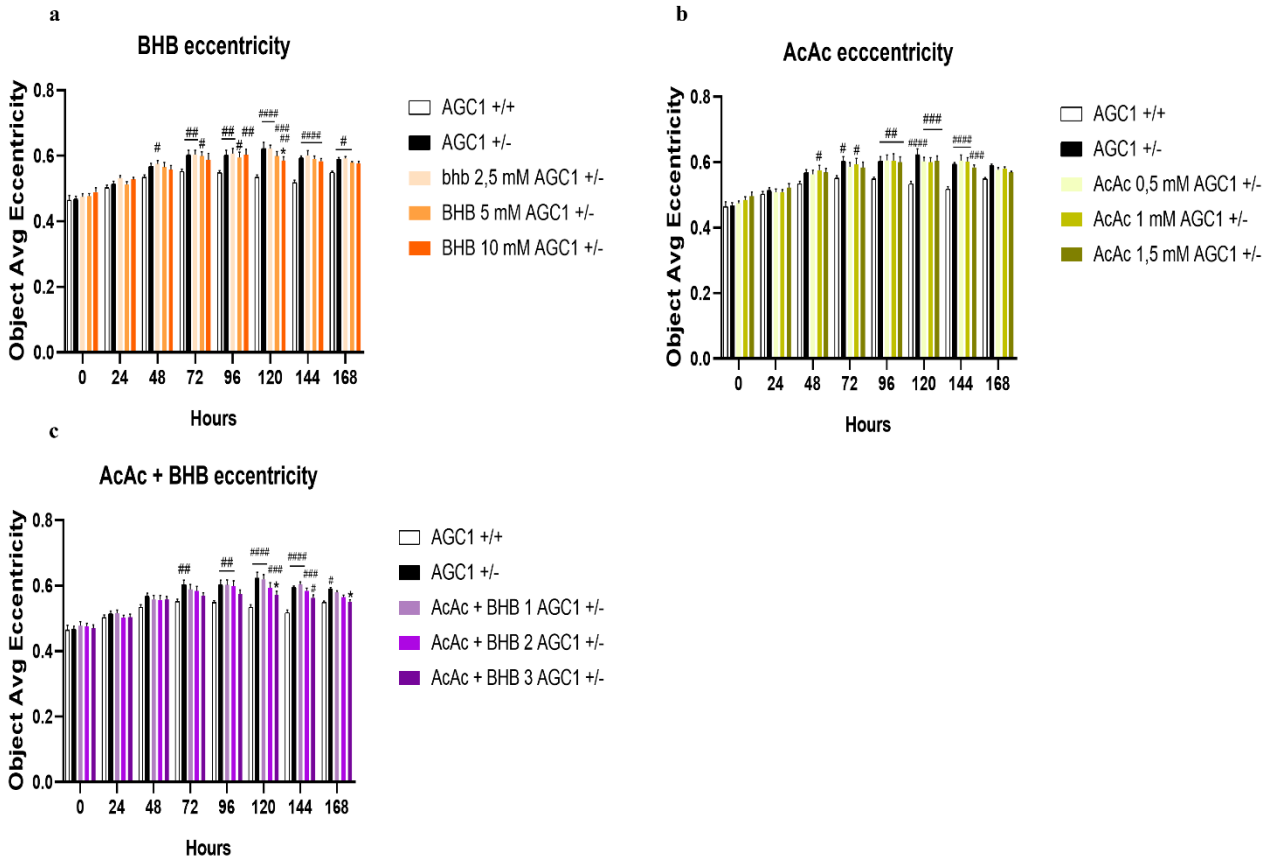

Fig. 5.12 Growth analysis of neurospheres through the analysis of the average of the eccentricity of the brightfield object in the image. Single neurosphere were plated (5000 per well) and let spontaneously growth for 7 days with beta-hydroxybutyrate (Bhb 2,5 – 5 – 10 mM, a) acetoacetate (AcAc 0,5 – 1- 1,5 mM, b) or their combinations (Bhb 2,5 mM + AcAc 0,5 mM – Bhb 5 mM + AcAc 1 mM – Bhb 10 mM + AcAc 1,5 mM, c). Images were acquired every 24h. N=3 ± s.e.m. # p-values <0,005 compared to AGC1$^{+/+}$ neurospheres; * p-values <0,005 compared to C AGC1$^{+/-}$ neurospheres, two-way ANOVA Dunnett's multiple comparison test (Bonferroni's post-hoc comparison test)

As reported by Fig. 5.13-5.14, also BCAAs have effect of neurospheres proliferation. Specifically, leucine and isoleucine at 800 mg/l increased the object number, with peak of proliferation before the 4th day. Valine instead allowed similar increment, but at lower concentration (200 mg/l, Fig. 5.13 c). More pronounced results were found for the total area. Indeed, same concentrations of BCAAs induced a complete recovery of this parameter, respect to untreated AGC1$^{+/-}$ but also wild-type spheres (Fig. 5.14 a, b and c). For the combinations, the one with all BCAAs at 200 mg/l had effects on total area, respect to untreated spheres (Fig. 5.14 d), whereas modest result was obtained on their number (Fig.5 13 d). This is probably due to the possible acidification of medium induced by presence of all amino acids at high concentrations. Respect to eccentricity, no significant alterations were detected upon amino acids supplementations, as shown by Fig. 5.15 (a, b, c and d), however more in-depth analysis would be conducted for differentiation analysis, in the following chapter.

Overall, these results suggest a positive effects of ketone bodies and branched-chain amino acids on proliferation of neurospheres, especially regarding their size and total area.

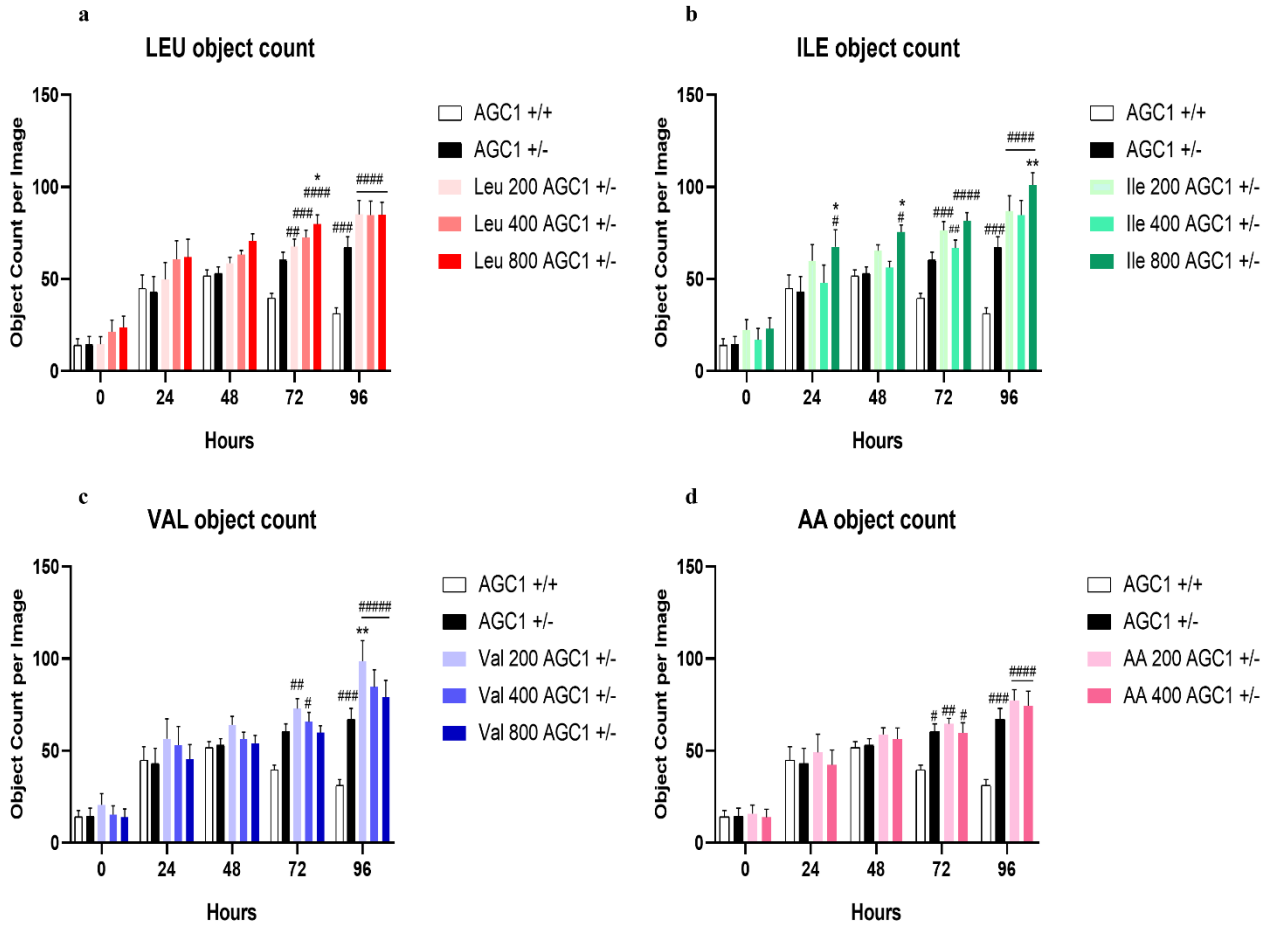

Fig. 5.13 Growth analysis of neurospheres through the analysis of the object count of the brightfield object in the image. Single neurospheres were plated (5000 per well) and let spontaneously growth for 7 days with Leucine (Leu 200 – 400 – 800 mg/l, a) Isoleucine (Ile 200 – 400- 800 mg/l, b), Valine (200 – 400 – 800 mg/l, c) or their combinations (aa200 Leu 200 + Ile 200 + Val 200 – aa400 leu 400 + Ile 400 + Val 400 – aa800 Leu 800 + Ile 800 + Val 800, d). Images were acquired every 24h. N=3 ± s.e.m. # p-values <0,005 compared to AGC1$^{+/+}$ neurospheres; * p-values <0,005 compared to C AGC1$^{+/-}$ neurospheres, two-way ANOVA Dunnett's multiple comparison test (Bonferroni's post-hoc comparison test)

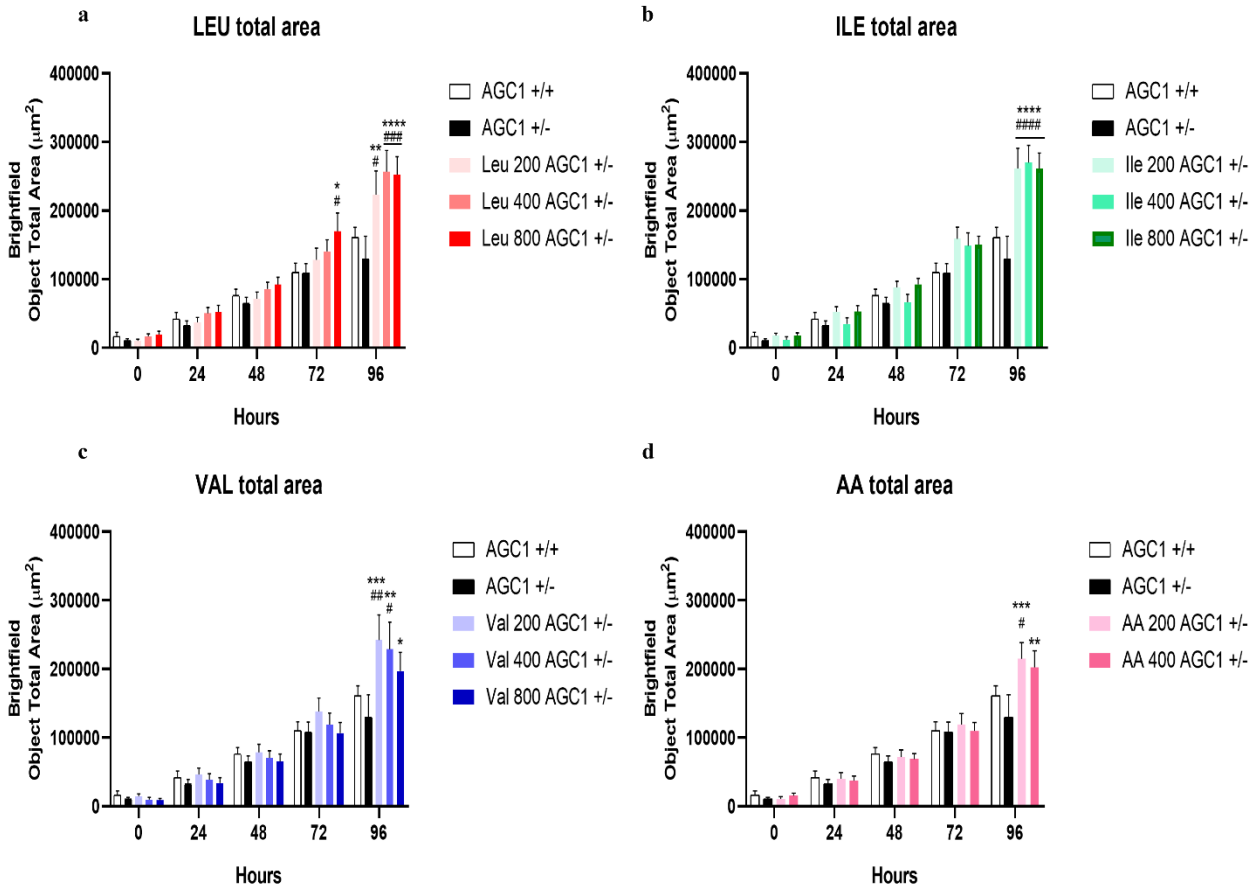

Fig. 5.14 Growth analysis of neurospheres through the analysis of total of the area of the brightfield object in the image (Area µm^2). Single neurosphere were plated (5000 per well) and let spontaneously growth for 7 days with Leucine (Leu 200 – 400 – 800 mg/l, a) Isoleucine (Ile 200 – 400- 800 mg/l, b), Valine (200 – 400 – 800 mg/l, c) or their combinations (aa200 Leu 200 + Ile 200 + Val 200 – aa400 Leu 400 + Ile 400 + Val 400 – aa800 Leu 800 + Ile 800 + Val 800, d). Images were acquired every 24h. N=3 ± s.e.m. # p-values <0,005 compared to AGC1$^{+/+}$ neurospheres; * p-values <0,005 compared to C AGC1$^{+/-}$ neurospheres, two-way ANOVA Dunnett's multiple comparison test (Bonferroni's post-hoc comparison test)

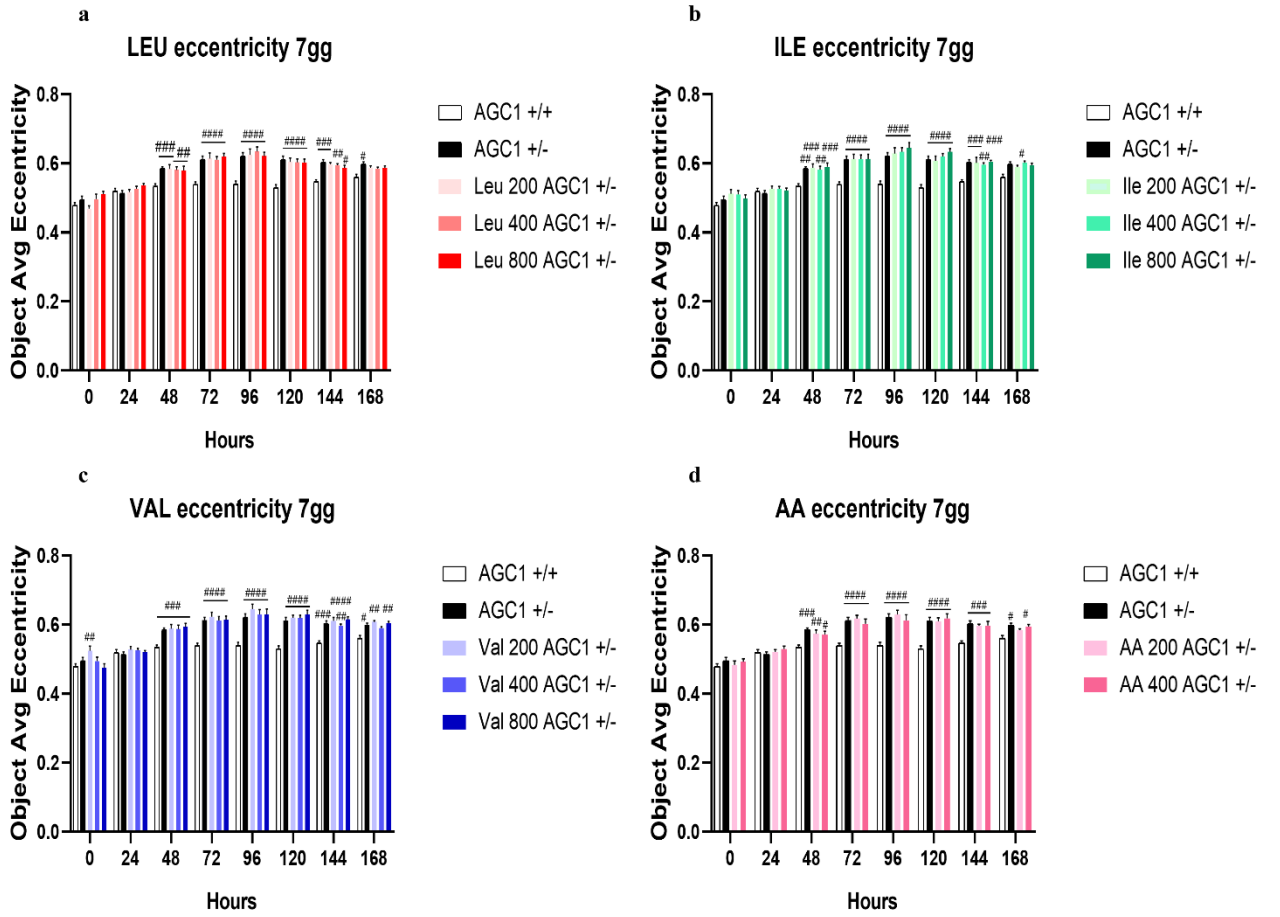

Fig. 5.15 Growth analysis of neurospheres through the analysis of the average of the eccentricity of the brightfield object in the image. Single neurosphere were plated (5000 per well) and let spontaneously growth for 7 days with Leucine (Leu 200 – 400 – 800 mg/l, a) Isoleucine (Ile 200 – 400- 800 mg/l, b), Valine (200 – 400 – 800 mg/l, c) or their combinations (aa200 Leu 200 + Ile 200 + Val 200 – aa400 Leu 400 + Ile 400 + Val 400 – aa800 Leu 800 + Ile 800 + Val 800, d). Images were acquired every 24h. N=3 ± s.e.m. # p-values <0,005 compared to AGC1$^{+/+}$ neurospheres; * p-values <0,005 compared to C AGC1$^{+/-}$ neurospheres, two-way ANOVA Dunnett's multiple comparison test (Bonferroni's post-hoc comparison test)

5.5 BCAAs and KBs supplementations restore the differentiation defects seen in Oli-Neu and neurospheres AGC1 deficiency models

As for proliferation, AGC1 deficiency models show differentiation defects, as demonstrated by Petralla et al. 2019). Specifically, Oli-Neu silenced cells have a more mature phenotype, with upregulation of CNPase, mature-specific oligodendrocyte marker (Barateiro and Fernandes 2014) and downregulation of NG2, marker of OPC, and Olig2, a TF essential for OPC specification, during early neurodevelopmental stages (Q. Zhou, Choi, and Anderson 2001). In summary, these alterations suggest a disrupted cell cycle progression and maturation in this *in vitro* model.

Similarly, heterozygous neurospheres display a strong premature differentiation, with a spontaneous tendency to differentiate, respect to wild-type ones. More in details, they present an increase in Doublecortin (DCX) and Glial Fibrillary Acidic Protein (GFAP), marker of neuronal and astrocytic lineage, respectively, whereas Nestin, marker of stemness, and Olig2, marker of OPCs, are

downregulated (Petralla et al. 2019; Poeta et al. 2021). Thus, a more mature phenotype with tendency to generate mainly neuronal and astrocytic cells affect this 3D model of AGC1 deficiency. Differentiation defects at levels of OPCs and NSCs could be harmful, hampering the physiological timing of cells expansion and maturation, which bring to formation of unfunctional network in developing brain. Thus, a well-balanced mechanism of proliferation and differentiation is essential. For these reasons, we would test if the pro-proliferative effects of ketone bodies and BCAAs supplementations induce a recovery also of the differentiation defects. To evaluate it, we performed immunofluorescence analysis, using specific markers of proliferation and differentiation. Only the most promising concentration in term of pro-proliferative effect were chosen for the differentiation analysis and tested.

For Oli-Neu cells, we verified if ketone bodies and branched-chain amino acids alter the expression of CNPase, NG2 and Olig2 but also BrdU incorporation, at 72 hours after the start of the treatment. The most impressive result upon supplementations was obtained for CNPase; indeed, both Bhb (10 mM) and AcAc (1mM) reduced the marker expression in silenced cells, respect to untreated ones (Fig. 5.16 a). Likewise amino acids did (leucine and isoleucine at 400 mg/l, valine at 200 mg/l; Fig. 5.16 c); just the combination of all BCAAs brought a smaller decrease, respect to silenced untreated cells. No significant alterations respect to C siAGC1 Oli-Neu were detected for NG2 (Fig 5.16 b and d) and Olig2 (Fig. 5.17 a and c), with all compounds, suggesting a possible recovery of mature phenotype but not the complete restoration of OPC status, as in control cells.

BrdU incorporation instead was done to confirm the Livecyte proliferation analysis. For all the compounds (Fig. 5.17 b and d), we saw an increase in BrdU signal, with statistical significance for β-hydroxybutyrate, leucine and combinations of all amino acids at 200 mg/l.

Taken together, these results demonstrate a strong influence of ketone bodies and branched-chain amino acids supplementation over OPCs differentiation, with effects on mature-specific oligodendrocyte marker.

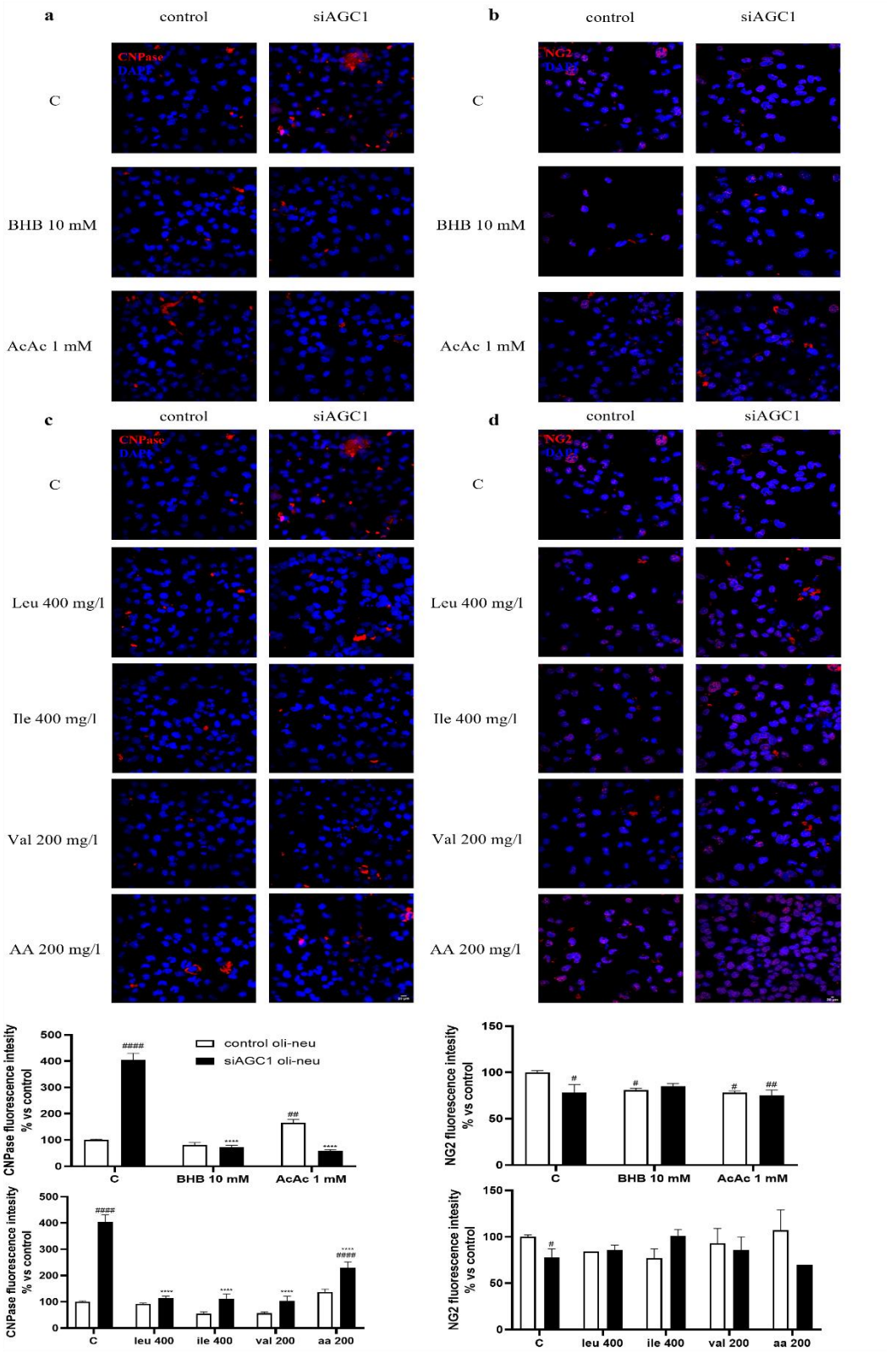

Fig. 5.16 Immunofluorescence analysis of Oli-Neu differentiation. Confocal microscopy images of Oli-Neu differentiation markers: CNPase (red, a and c) and NG2 (red, b and d), with ketone bodies and branched-chain amino acids supplementations, after 72 h from treatment. Nuclei were labelled with DAPI (blue). Scale bar: 20 µm; N=4. Images of the Oli-Neu were obtained with the Nikon EZ-C1 confocal microscope with the 60X objective, and 4 different fields were acquired and analyzed. Values are expressed as *ratio* of % fluorescence intensity of CNPase or NG2. # p-values <0,005 compared to C control Oli-Neu; * p-values <0,005 compared to C siAGC1 Oli-Neu, two-way ANOVA (Bonferroni's post-hoc comparison test)

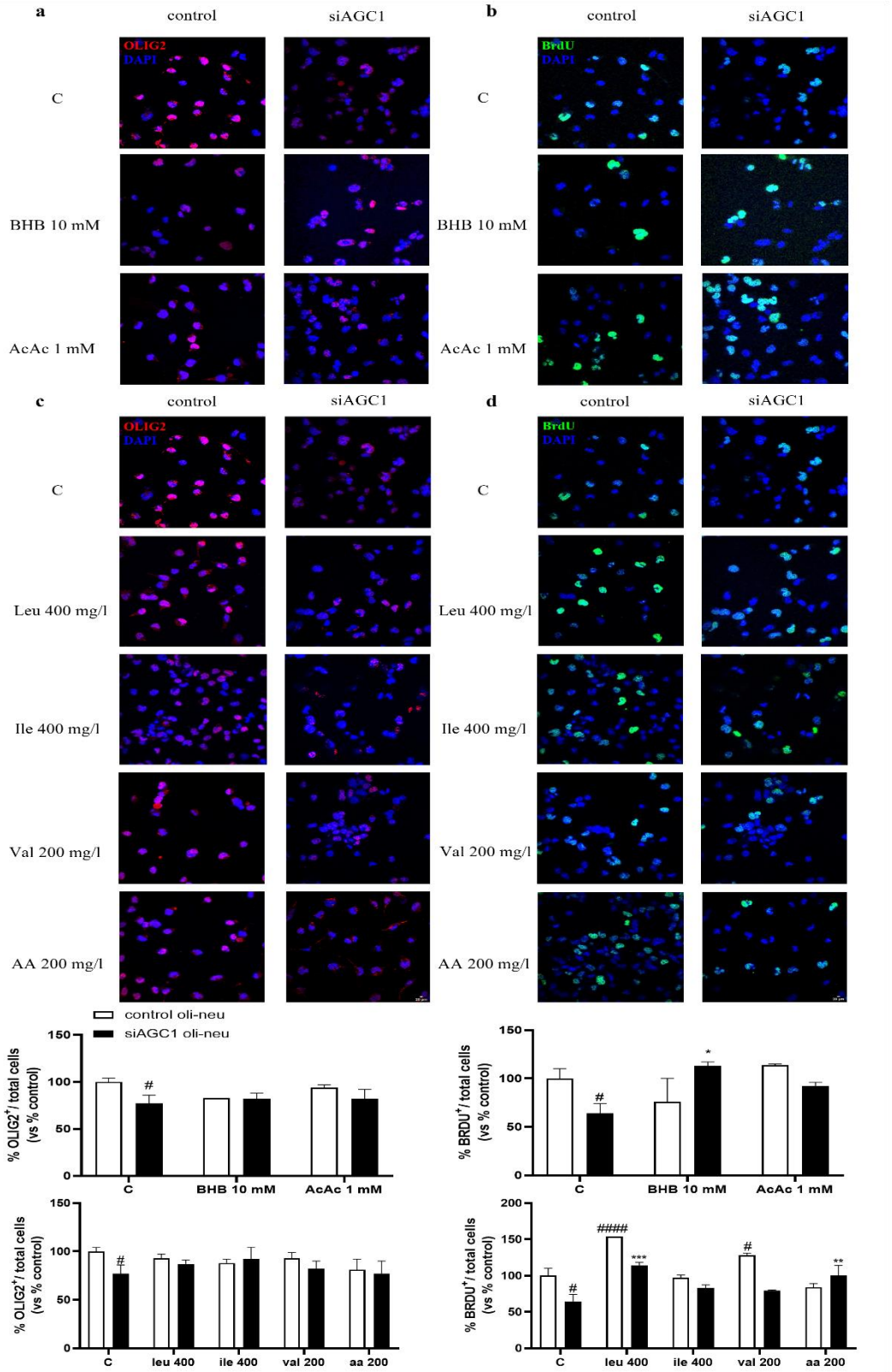

Fig. 5.17 Immunofluorescence analysis of Oli-Neu differentiation and proliferation. Confocal microscopy images and analysis of Oli-Neu differentiation and proliferation markers: OLIG2 (red, a and c) and BrdU (green, b and d) with ketone bodies and branched-chain amino acids supplementations, after 72 h from treatment. Nuclei were labelled with DAPI (blue). Scale bar: 20 µm; N=4. Images of the Oli-Neu were obtained with the Nikon EZ-C1 confocal microscope with the 60X objective, and 4 different fields were acquired and analyzed. Values are expressed as *ratio* of $OLIG2^+$ or $BrdU^+$ cells/total cells. # p-values <0,005 compared to C control Oli-Neu; * p-values <0,005 compared to C siAGC1 Oli-Neu, two-way ANOVA (Bonferroni's post-hoc comparison test)

Same analysis on differentiation state was performed on neurospheres, left differentiate in adhesion on Matrigel, for seven days. Since neural stem cells potentially can give rise to all neural lineage, different markers of specific commitments were analysed: DCX, GFAP and Olig2. In addition, Nestin was used as marker for stemness, to assess the undifferentiated state of the spheres; and BrdU, to confirm the Incucyte proliferation analysis.

As reported in Fig. 5.18, ketone bodies supplementations increased Nestin expression, with a peak for acetoacetate at 1 mM, whereas no statistical significance for combination of KBs, respect to untreated $AGC1^{+/-}$ spheres. Concomitantly, with increase in stemness, we detected a reduction in GFAP and DCX, especially for AcAc (Fig. 5.18 c and e). However, it seems that these compounds can't exert effects on oligodendroglial lineage, with no variations in Olig2 expression level (Fig. 5.18 d). We tried to analyse if a possible increment on Olig2 marker was induced at precocious stage of differentiation, plating the spheres only for four days, but also in this case no significant results were obtained, upon KBs supplementations (Fig. 5.19 a). For BrdU analysis instead, the spheres were plated and let differentiate for 4 days, to better mimic the result and analysis obtained by the Incucyte (paragraph 5.3). In general, BrdU incorporation confirmed the increment of proliferation of Bhb and AcAc in $AGC1^{+/-}$ spheres, respect to untreated heterozygous ones (Fig. 5.19 b).

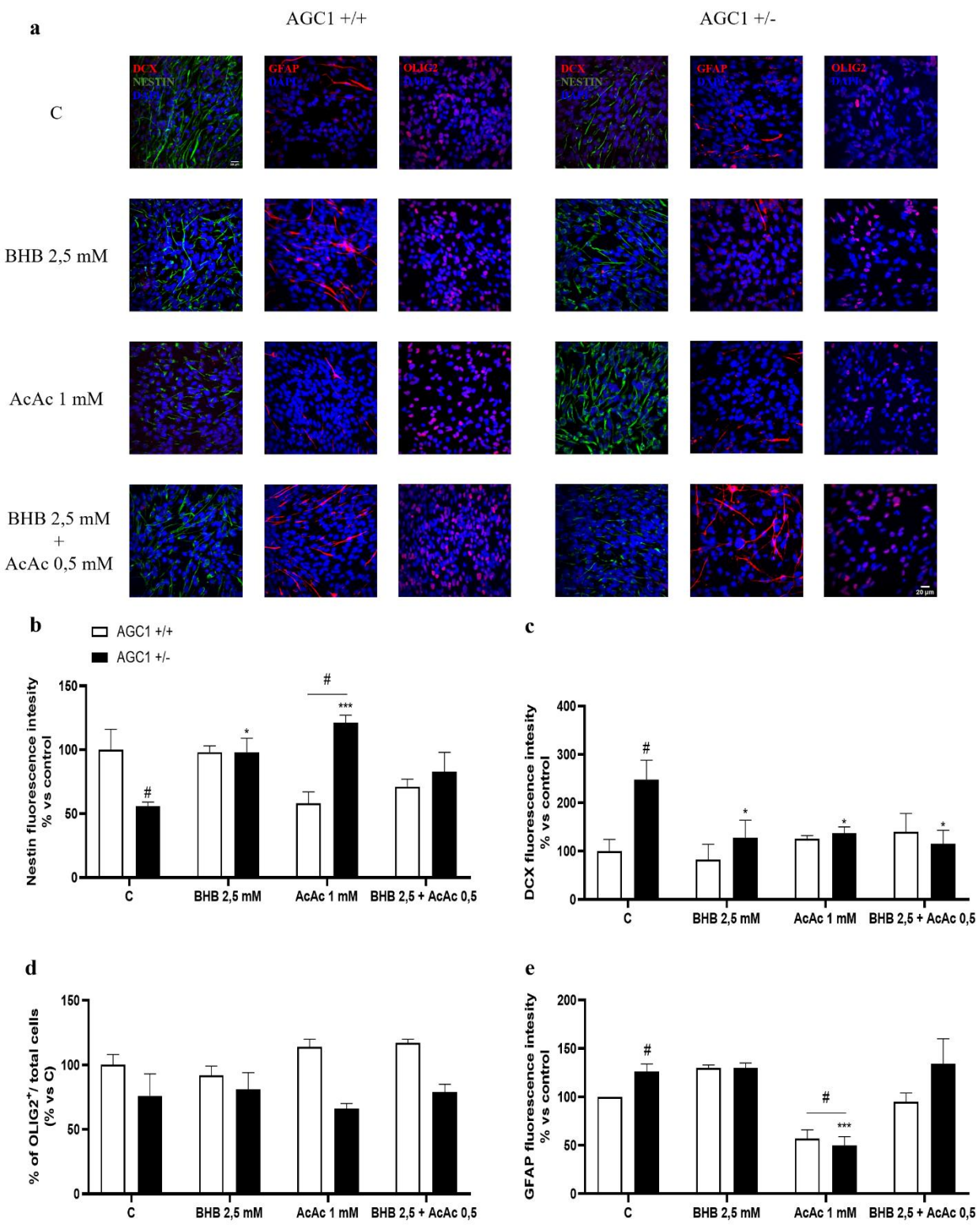

Fig. 5.18 Immunofluorescence analysis of neurospheres differentiation. Confocal microscopy images of neurospheres differentiation markers: Nestin (green, b), DCX (red, c), GFAP (red, e) and OLIG2 (red, d), with ketone bodies supplementations, after 7 days from treatment. Nuclei were labelled with DAPI (blue). Scale bar: 20 µm; N=4. Images of the neurospheres were obtained with the Nikon EZ-C1 confocal microscope with the 60X objective and 4 different fields were acquired and analyzed. Values are expressed as *ratio* of % fluorescence intensity of antibodies. # p-values <0,005 compared to C AGC1$^{+/+}$; * p-values <0,005 compared to C AGC1$^{+/-}$, two-way ANOVA (Bonferroni's post-hoc comparison test)

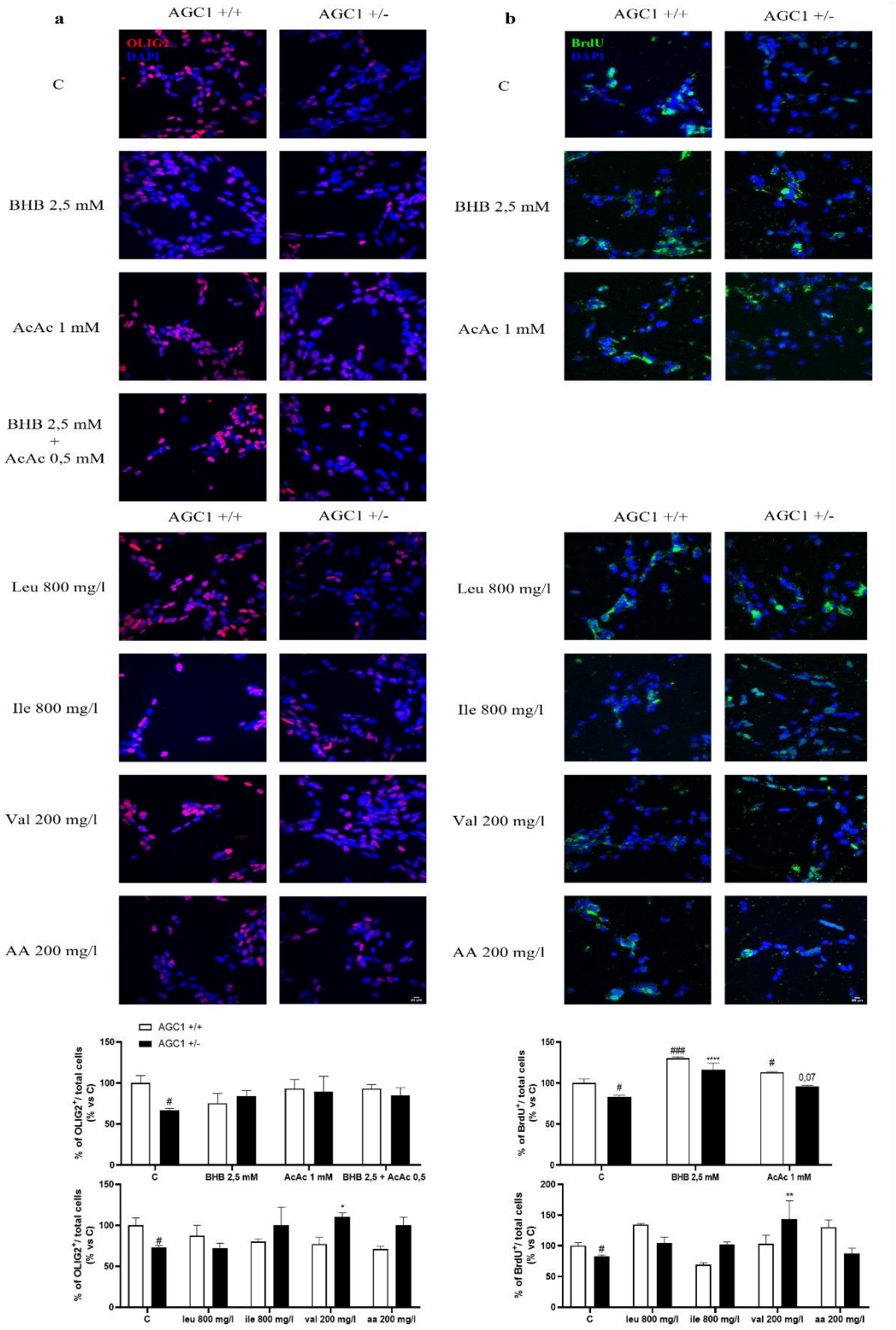

Fig. 5.19 Immunofluorescence analysis of neurospheres differentiation and proliferation. Confocal microscopy images of neurospheres differentiation/proliferation markers: OLIG2 (red, a) and BrdU (green, b), with ketone bodies and branched-chain amino acids supplementations, after 4 days from treatment. Nuclei were labelled with DAPI (blue). Scale bar: 20 µm; N=4. Images of the neurospheres were obtained with the Nikon EZ-C1 confocal microscope with the 60X objective and 4 different fields were acquired and analyzed. Values are expressed as *ratio* of $OLIG2^+$ or $BrdU^+$ cells/total cells. # p-values <0,005 compared to C $AGC1^{+/+}$; * p-values <0,005 compared to C $AGC1^{+/-}$, two-way ANOVA (Bonferroni's post-hoc comparison test)

Similar analysis was conducted to explore influences of branched-chain amino acids on NSCs differentiation. Firstly, we detected no statistical variations for neuronal and astrocytic lineage markers, except for the combinations of all amino acids, which increases the DCX expression (Fig. 5.20 c and e). Whereas isoleucine at 800 mg/l slightly decreases GFAP fluorescence intensity (Fig. 5.20 e). More pronounced gain in fluorescence was seen for Nestin, which appears statistically enhanced for all supplementations (Fig. 5.20 b). Also, Olig2 had similar trend, with the only exception of valine (Fig. 5.20 d), which however, seems to have a more precocious effect. Indeed, increase in this OPC marker was clearly detected on neurospheres at fourth day of differentiation, upon supplementation with this amino acid (Fig. 5.19 a). Concerning BrdU incorporation, after four days, all supplementations with BCAAs increase proliferation, respect to untreated heterozygous spheres, with statistically significant results, especially for valine (Fig. 5.19 b).

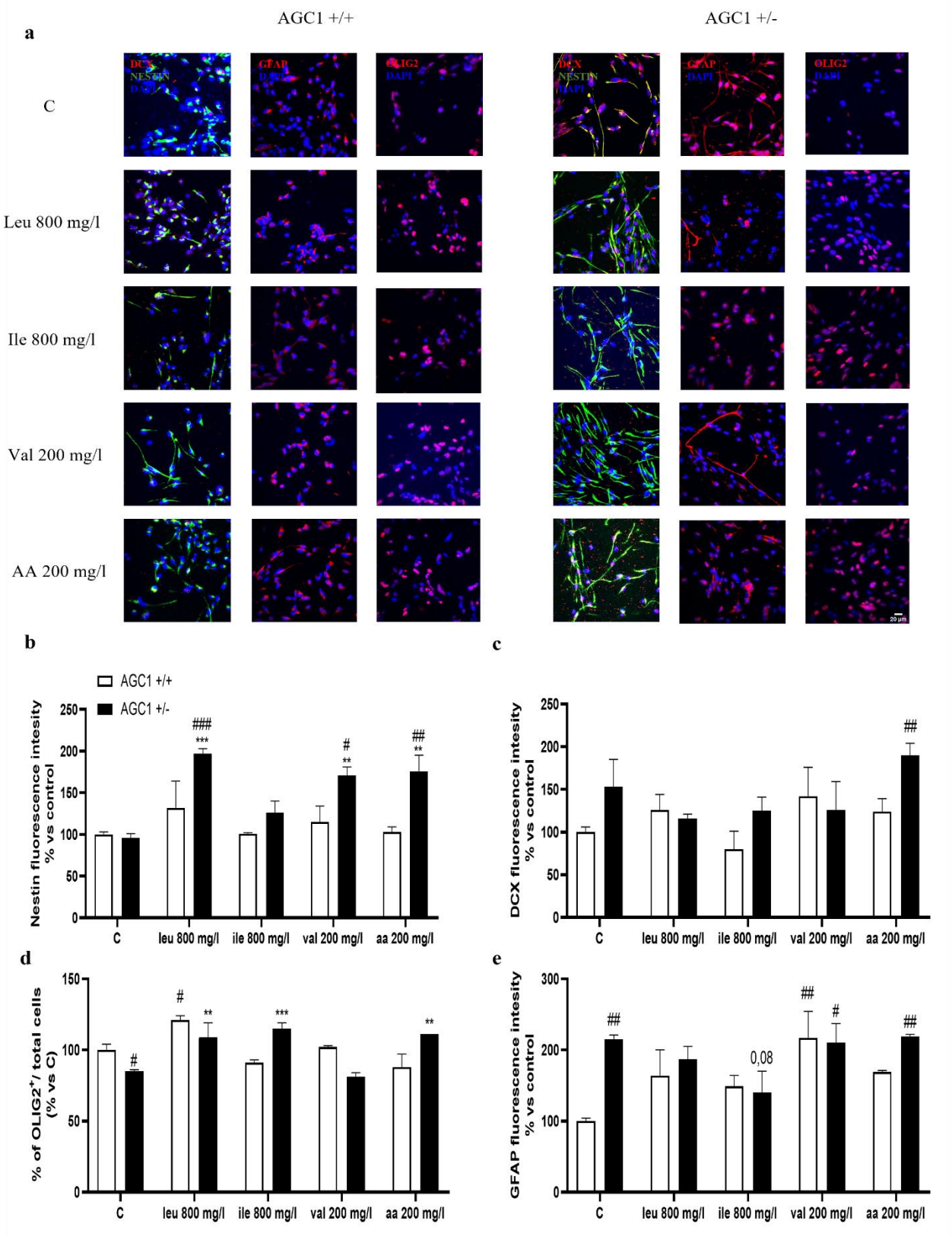

Fig. 5.20 Immunofluorescence analysis of neurospheres differentiation. Confocal microscopy images of neurospheres differentiation markers: Nestin (green, b), DCX (red, c), GFAP (red, e) and OLIG2 (red, d), with branched-chain amino acids supplementations, after 7 days from treatment. Nuclei were labelled with DAPI (blue). Scale bar: 20 µm; N=4. Images of the neurospheres were obtained with the Nikon EZ-C1 confocal microscope with the 60X objective and 4 different fields were acquired and analyzed. Values are expressed as *ratio* of % fluorescence intensity of antibodies. # p-values <0,005 compared to C AGC1$^{+/+}$; * p-values <0,005 compared to C AGC1$^{+/-}$, two-way ANOVA (Bonferroni's post-hoc comparison test)

In summary, we can stat that both KBs and BCAAs, despite marker-specific differences, exert an effect also on differentiation of Neural Stem Cells, with a particular focus on Nestin. The increase in stemness marker indeed, could explain the higher proliferation pace induced in this model, upon supplementation, and detected by Incucyte analysis.

5.6 Histone epigenetic modifications could explain the effects of KBs and BCAAs supplementations on OPCs model of AGC1 deficiency

From literature, it's well known and discussed the role of epigenetic regulation on proliferation and differentiation processes of OPCs and NSCs (Hernandez and Casaccia 2015b). Abnormal chromatin remodelling and histone modifications could lead to defects in these biological pathways, affecting the entire brain development. Previous analysis on both Oli-Neu and Neurospheres models highlighted altered epigenetic mechanisms, involving HATs/HDACs expression and activity. Also, histone modifications, especially histone 3 acetylation and methylation, were affected. Specifically, they are both less present in Oli-neu siAGC1 cells; while histones methylation increment was detected for heterozygous neurospheres, in parallel with decreased histone 3 acetylation level (Poeta et al. 2021). Worsening of the AGC1 deficiency models' phenotype was detected as well, upon use of HAT/HDAC inhibitors, suggesting a possible causative link between altered epigenetic modifications and proliferation and differentiation defects. This led us to investigate if instead the positive effects exerted by BCAAs and KBs supplementations on these biological processes were derived from the rebalancing of the epigenetic alterations. Indeed, supplementations with these compounds could feed the cells with all those metabolites they lack/exceed and that could use for histone acetylation/methylation.

To test this hypothesis, we performed preliminary untargeted analysis on histone 3 pan-acetylation and pan-methylation, through Western Blot, on Oli-Neu and neurospheres cell lysates, at two distinct time points: 24 and 72 hours, after start of treatment, for OPCs, at 4 and 7 days, for NSCs. This enables us to indicate whether possible epigenetic compensations occur before or after the proliferation/differentiation recovery.

Starting from Oli-Neu cells, ketone bodies supplementations were performed, with the following concentrations: Bhb 10 mM; AcAc 1 mM (Fig. 5.21). As shown in Fig. 5.21 c and d, neither 24 nor 72 hours supplementations induce significant increase in pan-acetylation levels, respect to untreated siAGC1 cell. Instead, concerning histone 3 methylation, we highlighted an initial increment at 24 hours after treatment, respect to untreated siAGC1 Oli-Neu cells, which became statistically significant at 72 (Fig. 5.21 a and b).

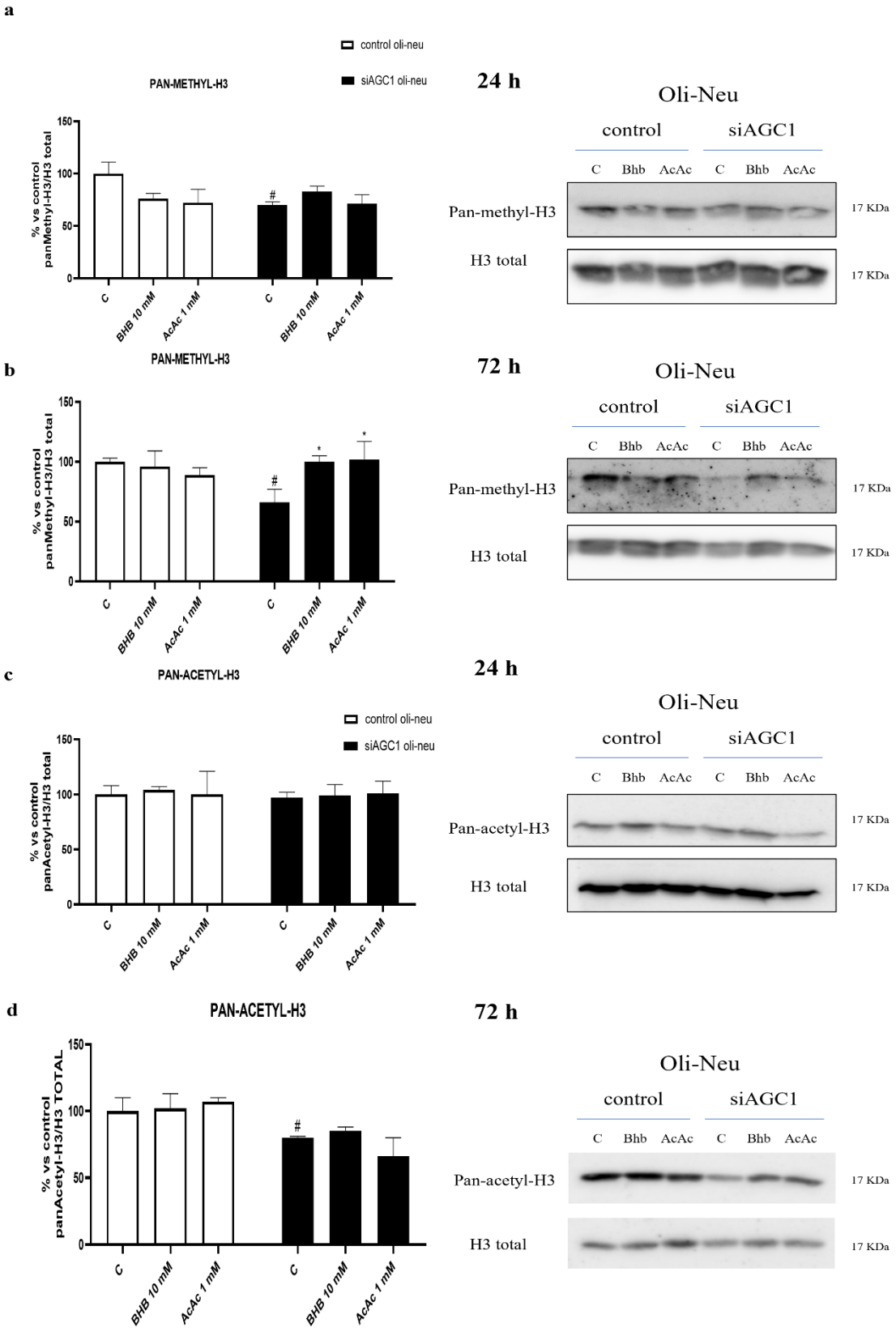

Fig. 5.21 Western blot and relative densitometries of histone 3 pan-methylation (a, b) and histone 3 pan-acetylation (c, d) expression in control and siAGC1 Oli-Neu at 24 and 72 hours, after ketone bodies supplementations; histone 3 total was used for endogenous normalization. Values are mean ± SD of at least 3 independent experiments; # P <0.05, compared to C control Oli-Neu; * P <0.05, compared to C siAGC1 Oli-Neu; Student's t-test

An opposite result was instead obtained for BCAAs supplementation. Indeed, despite a slight increase in histone methylation at 24 hours of silenced cells, but without any significant variation, histone acetylation was increased - for leucine specifically- at the same time-point (Fig. 5.22). This data suggests an overall effects of these compounds on histone modifications, but with different type and timing of action for KBs and BCAAs, that however requires more in-depth analysis to be unravel.

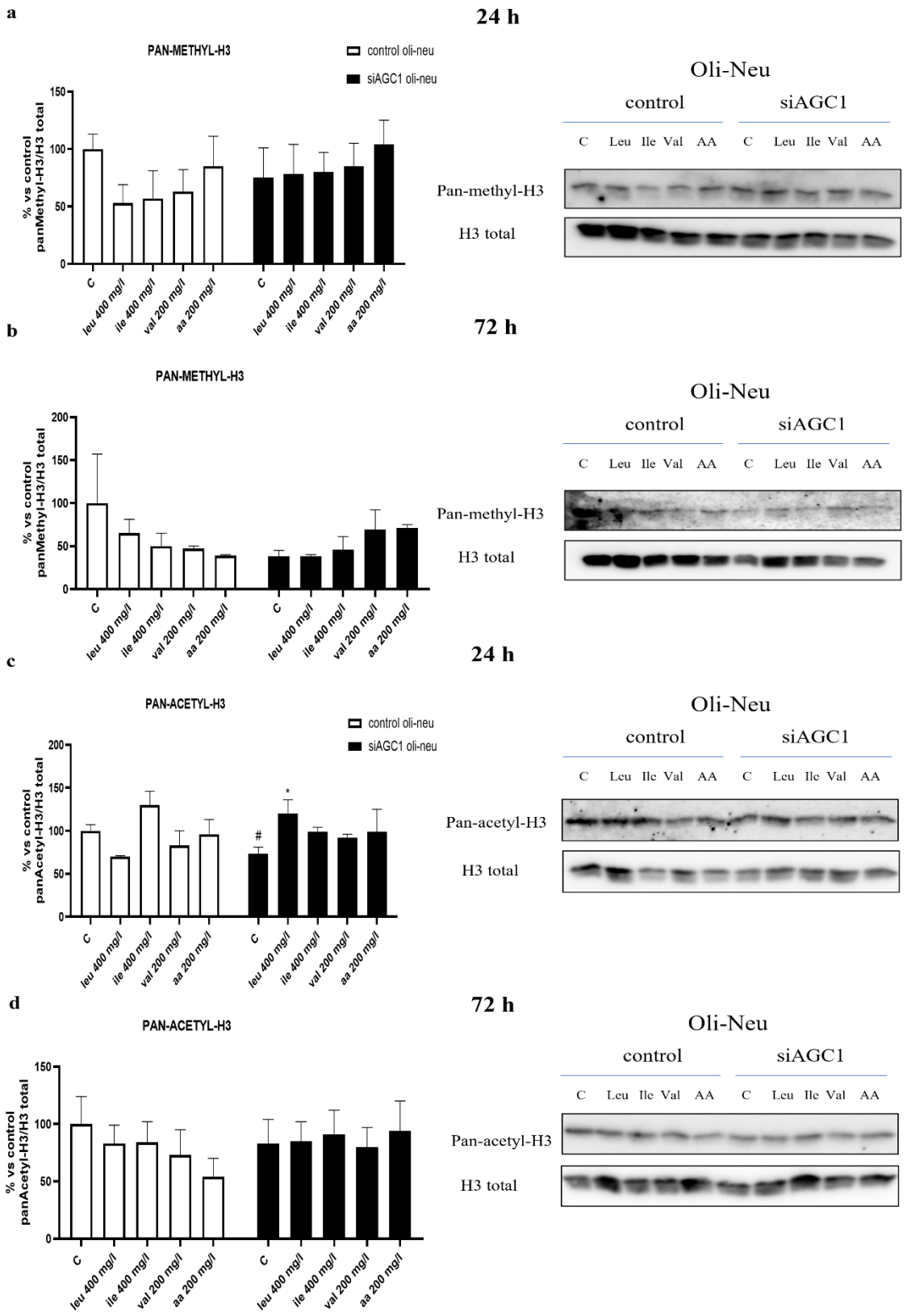

Fig. 5.22 Western blot and relative densitometries of histone 3 pan-methylation (a, b) and histone 3 pan-acetylation (c, d) expression in control and siAGC1 Oli-Neu at 24 and 72 hours, after branched-chain amino acids supplementations; histone 3 total was used for endogenous normalization. Values are mean ± SD of at least 3 independent experiments; # P <0.05, compared to C control Oli-Neu; * P <0.05, compared to C siAGC1 Oli-Neu; Student's t-test

Even though the intrinsic differences among OPCs and NSCs, we test if similar results can be achieved also on histone modifications of neurospheres, upon supplementations. From Fig. 5.23 a and b, no alteration was induced on histone methylation for all ketone bodies supplementations, at both time-points. Instead, a modest increment with Bhb at 2,5 mM on histone acetylation was detectable at seventh day of differentiation, respect to C heterozygous spheres, even though not statistically significant (Fig. 5.23 d).

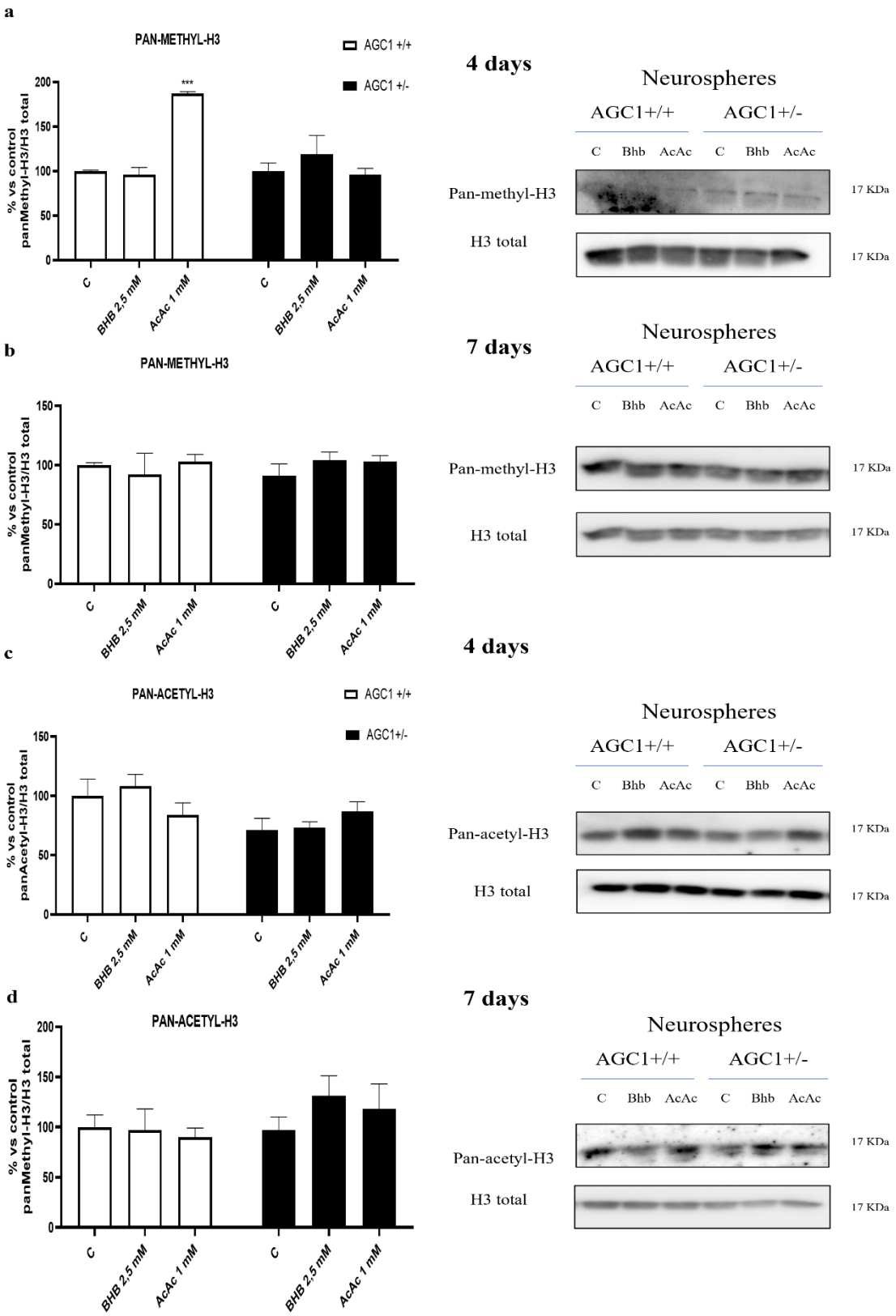

Fig. 5.23 Western blot and relative densitometries of histone 3 pan-methylation (a, b) and histone 3 pan-acetylation (c, d) expression in AGC1$^{+/-}$ and AGC1$^{+/+}$ neurospheres at 4 and 7 days of differentiation, after ketone bodies supplementations; histone 3 total was used for endogenous normalization. Values are mean ± SD of at least 3 independent experiments; # P <0.05, compared to C AGC1$^{+/+}$ neurosphere; * P <0.05, compared to C AGC1$^{+/-}$ neurosphere; Student's t-test

For BCAAs, the supplementations didn't vary the histone acetylation levels respect to the untreated AGC1 deficient neurospheres (Fig. 5.24 c and d). A slight decrease for histone 3 pan-methylation can be seen, especially for valine (200 mg/l; Fig. 5.24 b) at 7 days of differentiation, respect to C AGC1$^{+/-}$ neurospheres, but also in this case, it's not statistically relevant.

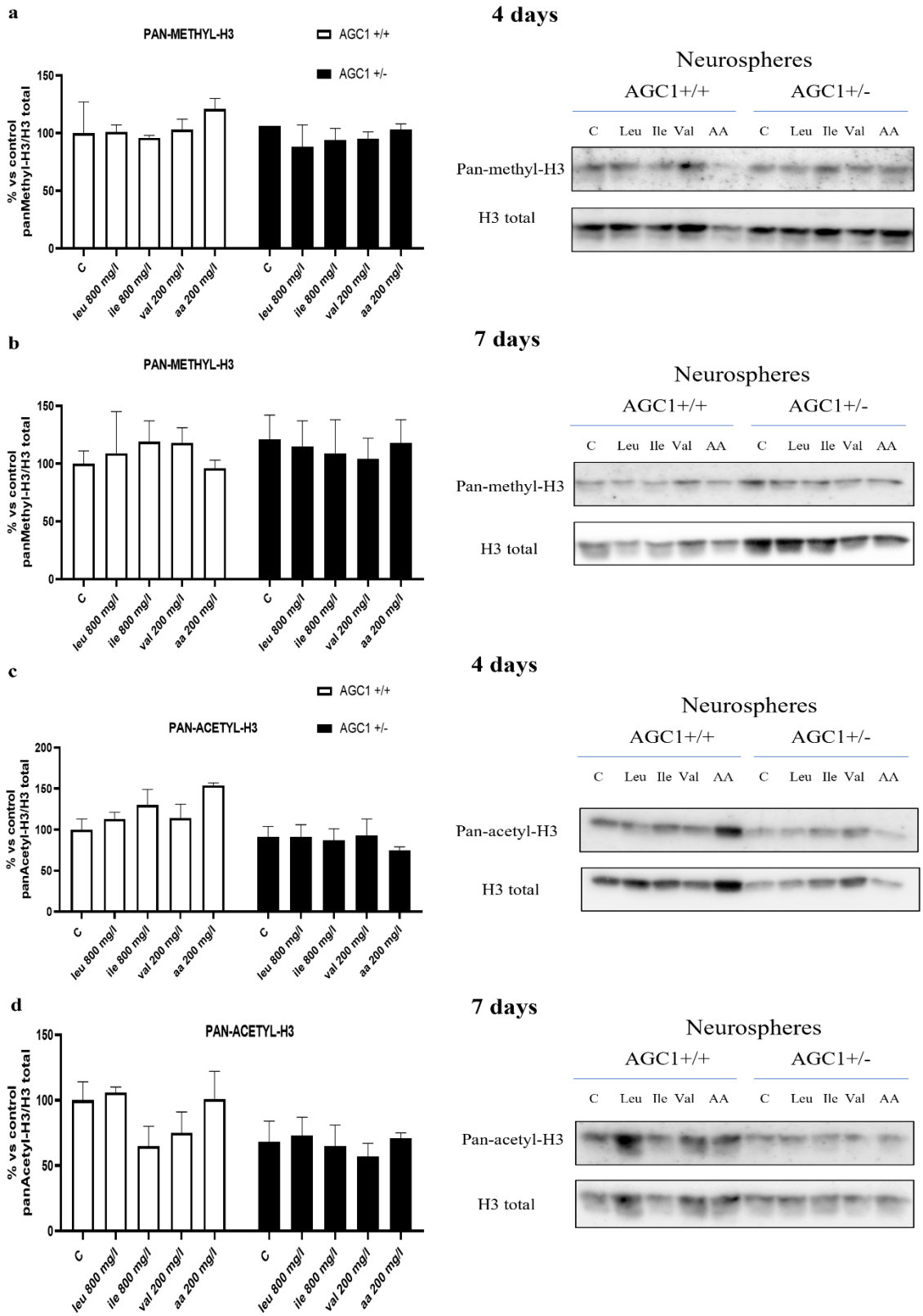

Fig. 5.24 Western blot and relative densitometries of histone 3 pan-methylation (a, b) and histone 3 pan-acetylation (c, d) expression in AGC1$^{+/-}$ and AGC1$^{+/+}$ neurospheres at 4 and 7 days of differentiation, after branched-chain amino acids supplementations; histone 3 total was used for endogenous normalization. Values are mean ± SD of at least 3 independent experiments; # P <0.05, compared to C AGC1$^{+/+}$ neurosphere; * P <0.05, compared to C AGC1$^{+/-}$ neurosphere; Student's t-test

Overall, we can stat that major variations, induced by KBs and BCAAs supplementations on histone modifications, are visible in the OPCs model of AGC1 deficiency, in which different compensation mechanisms between ketones and amino acids, with different timing and mode of action, could work to rebalance these alterations. The modest effects visible in the neurospheres could probably derive from their complexity as disease-model, constituted by a mixed pool of distinct Neural Precursors, which require more sophisticated and sensible assays to verify the possible effects of these compounds on histone modifications.

5.7 Preliminary experiments on iPSC-derived Neural Precursor Cells confirm presence of proliferation defects

To improve the reliability and translational validity of the results obtained in mice deriving AGC1 deficiency models and extend the analysis to human-deriving *in vitro* models of the disease, iPSC from patients' fibroblasts were differentiated into Neural Progenitors Cells, according to Choi protocol (Choi et al. 2017). Subsequently, we verified the presence of proliferation defects also in these cells. Firstly, we assessed the acquisition of the correct phenotype, through immunofluorescence analysis, upon differentiation protocol (Fig. 5.25 a). Indeed, these NPCs are DCX^+ cells but they don't express non-neuronal lineage markers: SSEA4 (marker of pluripotency), NG2, Olig2 (oligodendroglia) and GFAP (astrocytes), as expected. Then, to test the presence of proliferation defects, we plated NPCs on Matrigel coated glass coverslips and immunofluorescence analysis for ki67 and BrdU was performed. Ki67 marker is mainly expressed during G2 and mitosis, the active phases of cell cycle, while absent in the quiescent G0 phase (LI et al. 2015), thus - together with BrdU - it's a well-characterized marker for cell proliferation.

Quantification of ki67 positive cells (Fig. 5.25 c) confirmed the presence of reduced proliferation in all two lines of AGC1 deficient NPCs, respect to controls. BrdU incorporation suggested a similar result (Fig. 5.25 b), with statistically significant reduction of marker expression in patients' cell lines. These data confirm the presence of reduced proliferation rate also in iPS-derived NPCs, as that obtained for siAGC1 Oli-Neu cells and $AGC1^{+/-}$ neurospheres by Petralla et al. (2019). This common altered proliferative process among all AGC1 deficiency models reinforces the reliability of the results, laying the foundation for future experiments to check differentiation process in this latter cell lines, together with performing KBs and BCAAs supplementations, to evaluate their possible beneficial effects, also in patients-derived cells.

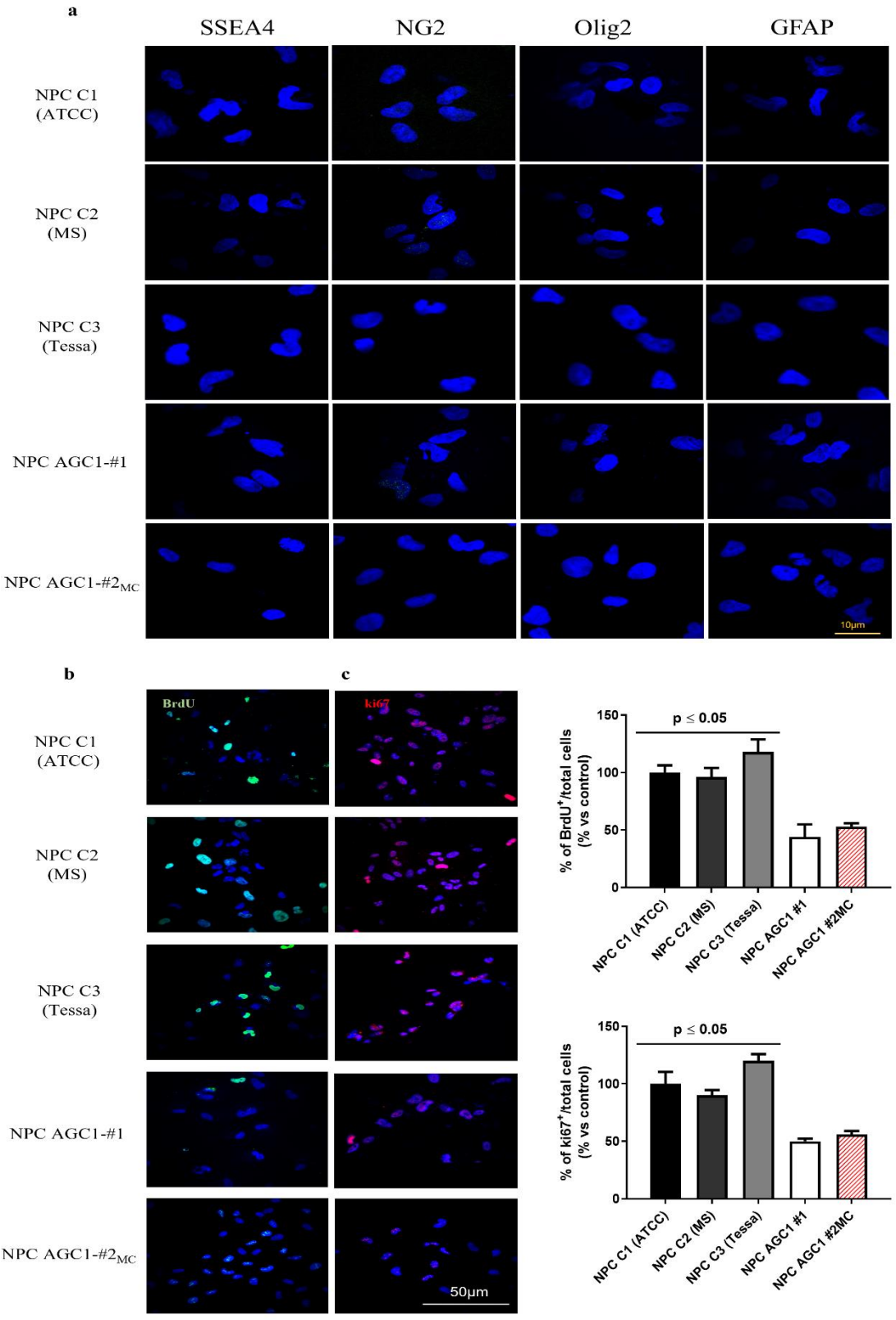

Fig. 5.25 Immunofluorescence analysis of iPS-derived NPC differentiation and proliferation. Confocal microscopy images and analysis of iPS-derived NPCs differentiation and proliferation markers: SSEA4, NG2, OLIG2 and GFAP (red, a) and BrdU (green, b) and ki67 (red, c). Nuclei were labelled with DAPI (blue). Scale bar: 50 µm; N=4. Images of the NPCs were obtained with the Nikon EZ-C1 confocal microscope with the 60X objective, and 4 different fields were acquired and analyzed. Values are expressed as *ratio* of $BrdU^+$ or $Ki67^+$ cells/total cells. # p-values <0,005 compared to C1/2/3; One-way ANOVA (Bonferroni's post-hoc comparison test)

6. DISCUSSION

AGC1 deficiency is an ultra-rare demyelinating disorder, caused by mutations in *SLC25A12* gene, which encodes for Aspartate-Glutamate Carrier 1 (AGC1). Its main pathological features include brain atrophy, developmental delay, with psych-motor defects and a secondary hypomyelination. In addition, AGC1 deficiency patients show reduced levels of N-acetyl-aspartate in blood, the main myelin lipids precursor. This alteration seems to be the responsible for the hypomyelination detected in patients' brain (Wibom et al. 2009; Falk et al. 2014). Indeed, AGC1 carrier belong to Malate-Aspartate Shuttle, where it allows the transport of aspartate, in exchange of glutamate and a proton, from mitochondrial matrix toward cytoplasm, where it's then converted to NAA, by aspartate-N-acetyltransferase. Subsequently, through trans-axonal transport, it's conveyed to oligodendrocytes, where it's degraded to aspartate and acetate. This latter resembles the main storage of acetyl moieties for myelin lipids synthesis in these cells (Wibom et al. 2009). From previous works, unlike murine neuroblastoma cell line, with AGC1 silencing, no alteration of this metabolite concentration was detected in oligodendrocyte precursor cells deriving from mouse model of AGC1 deficiency ($AGC1^{+/-}$). Despite this, OPCs showed altered myelin formation and differentiation. This reinforces the hypothesis that neuronal NAA production impairment, upon AGC1 downregulation, is strictly linked to defects regarding OPCs maturation (Profilo et al. 2017). Starting from these results, in our laboratory, two distinct models of AGC1 deficiency were established. The first is immortalized murine oligodendrocyte precursor cells (Oli-Neu), in which shRNA was transfected to induce AGC1 silencing, with a resulting reduction of about 30-40% of its activity. The second is a 3D model of neurospheres, Neural Stem Cells deriving from sub-ventricular zone of 8-months old mice heterozygous for AGC1 knock-out ($AGC1^{+/-}$ with C57BL6/N background), growing in suspension and forming spherical structures. Following analysis on these models highlighted defects on proliferation and differentiation, with reduced growth rate for both, accompanied by a more mature phenotype for siAGC1 Oli-Neu cells, and a switch in the NSC commitment, favouring differentiation into neuronal and astrocytic progenitors, rather than oligodendroglial ones (Petralla et al. 2019). These defects on proliferation and differentiation processes were then deeply analysed and the major transcription factors involved were seen to be down/upregulated in the models of AGC1 deficiency, as c-Myc, REST, Olig2 and CREB, revealing an altered transcriptional regulation of proliferation and OPCs/NSCs specification and differentiation (Poeta et al. 2021). Further experiments identified as the main responsible of this transcriptional dysregulation was an aberrant epigenetic landscape in Oli-Neu and neurospheres AGC1 deficiency models, with reduced epigenetic enzymes activity (namely HATs and HDACs) but also altered histone 3 modifications (acetylation and methylation). Indeed, chromatin remodelling strongly affects the temporal control of transcription factors activity and gene

accessibility (Ruijtenberg and van den Heuvel 2016; CHEN et al. 2014). Moreover, previous studies on OPCs/OLs confirmed the role of epigenetic modifications and chromatin architecture in their maturation processes (Emery 2010; Hernandez and Casaccia 2015b). Worsening of proliferation and differentiation defects was detected upon treatment of AGC1 deficiency models with HATs and HDACs inhibitors (curcumin and SAHA), reinforcing the hypothesis that the altered epigenetic landscape is responsible for the transcriptional dysregulation, which, in turn, hampers the proliferation and differentiation mechanisms. These defects in OPCs/OLs maturation ultimately could lead to aberrant myelin lipids synthesis and hypomyelination (Poeta et al. 2021).

Starting from this point, the first aim of this work was to unravel the biological pathways mainly affected and the resulting transcriptional profile, upon AGC1 silencing. Thus, RNA-seq analysis was performed in collaboration with the laboratory of Professor Federico M. Giorgi (University of Bologna). This analysis highlighted the presence of a plethora of genes up/downregulated in silenced Oli-Neu cells, respect to their control, which it's a clear index of an altered transcriptional profile. In addition, more in depth investigation of the affected biological pathways revealed impairment of fatty acids and myelin lipids synthesis. Notably, the main regulators of fatty acids and cholesterol synthesis, *SREBP1* and *SREBP2* (Sterol Regulatory Binding Protein) respectively, were seen to be downregulated in siAGC1 Oli-Neu cells. They are transcription factors activated upon decrease in sterols levels, which in turn induce transcription of genes involved in fatty acids and cholesterol synthesis (Eberlé et al. 2004). This alteration was also validated at transcripts level, through *in vitro* real-time PCR (and, for SREBP1, at protein level, through Western Blot) and confirmed by the consequential downregulation of one of the main SREBP1 target genes, *FASN*. This latter controls the formation of palmitate from acetyl-CoA and malonyl-CoA, the rate-limiting step in fatty acids synthesis (Dimas et al. 2019). Its downregulation was verified at protein levels in Oli-Neu silenced cells, reinforcing the hypothesis of altered lipids biosynthetic pathway, which in turn could affect the myelination process in these cells. Indeed, from literature, defects on these genes were seen to be responsible for aberrant myelination process but also impairment of OPCs/OLs maturation (Dimas et al. 2019; Monnerie et al. 2017). Quite in contrast with these results, *ACSS1* resulted to be upregulated in this AGC1 deficiency model. This gene encodes for Acetyl-CoA Synthetase 1, that controls the production of acetyl-CoA from acetate and CoA (Luong et al. 2000) but its upregulation was merely detected at transcript level, in Oli-Neu siAGC1 cells. The possible explanation for this discrepancy between protein and transcript expression could reside in the fact that cells, in physiological conditions, preferentially produce acetyl-CoA starting from citrate, rather than acetate, which indeed requires an already available pool of acetyl moieties to be used in this pathway (Wellen and Thompson 2012).

Similar alterations were also confirmed in the second AGC1 deficiency model, the neurospheres. Real time PCR on same subset of genes validated the results obtained with RNAseq on Oli-neu also in the cell line. In addition, SREBP1/2 downregulation at protein and transcripts levels in AGC1$^{+/-}$ neurospheres suggests a possible impairment of fatty acids and cholesterol synthesis pathway, thus hampering the myelin formation process. However, this model showed upregulation for both FASN and ACSS1 (mRNA and protein) that could derive by the heterogeneous nature of the neurospheres, in which each cell can give rise to neuronal, astrocytic o oligodendroglial precursors that contribute differently to the protein/enzyme pools. Poeta et al. (2021), indeed detected a tendency of heterozygous spheres to spontaneously differentiate into astrocyte and neuronal progenitors, rather than oligodendroglial ones. These types of cells could upregulate their lipogenic pathways (FASN and ACSS1) to counteract and compensated the defects derived from AGC1 knock-out in OPCs. Mixed cultures of OPCs and astrocytes indeed testify a crucial intervention of astrocytes to sustain myelination and lipids synthesis (Camargo et al. 2017). Thus, neuron/astrocyte-specific contribution to enzyme/protein set requires a more in-depth analysis in this AGC1 deficiency model. In parallel, upregulation of ACSS1 could derive by the metabolic distress conditions to which neurospheres, as a more complex model, could be subjected, upon AGC1 downregulation. Indeed, during nutrients-deprivation, as Traumatic Brain Injury (TBI), ACSS1 is upregulated, to furnish acetyl-CoA from acetate to the brain, sparing citrate for other uses (Rae et al. 2012). Moreover, ACSS1 -beyond its role in lipid synthesis- can also participate in nuclear protein acetylation by replenishing cells with acetyl groups for histone acetylation. Thus, the drop in acetyl-CoA availability, during TBI, could be compensated by ACSS1 activity, which enables to sustain the correct transcriptional control, through histone modifications (Ariyannur et al. 2010b; Moffett et al. 2013). A similar scenario could occur in AGC1 deficiency neurospheres, in which alterations of histone acetylation was indeed detected and proved by Poeta et al. (2021). Thus, neurospheres could try to compensate these defects by upregulating ACSS1. Altered acetylation levels can also explain the increase of FASN expression, in heterozygous spheres, since this protein turnover is controlled by acetylation/deacetylation process, through HDAC3 (Lin et al. 2016). This deacetylase is indeed upregulated in AGC1$^{+/-}$ neurospheres, where it reduces histone 3 acetylation but can also protects FASN from its turnover, upon deacetylation (Lin et al. 2016; Poeta et al. 2021). This doesn't occur in Oli-Neu silenced cells, since HDAC3 was downregulated, respect to control cells (Poeta et al. 2021).

The influence of acetyl groups availability on histone/protein modifications is well established in literature (Zijun Wang et al. 2018). For this reason, we would investigate the presence of an overall altered epigenome in silenced Oli-Neu cells, through ATAC-seq. Indeed, in collaboration with Giorgi's lab, we performed this analysis on three samples of control and silenced Oli-Neu cells, to

unravel the genes accessibility throughout the entire genome of this model. ATAC-seq allows to identify chromatin remodelling and the epigenetic landscape, differentiating between open and histone-bound regions of DNA, based on the promoter's accessibility (Grandi et al. 2022). Identification of 217 more open and 387 more closed regions in siAGC1 respect to control cells suggests a general altered epigenetic profile. Furthermore, localization of many of these less accessible genes matched with less expressed regions in RNAseq, one for all *SREBP1*. Given that no chromosomal deletion was detected through PCR for some of these genes, we suggested that the altered epigenetic regulation of their transcriptional accessibility could cause the down/upregulation of their transcripts and proteins seen with real-time PCR and Western Blot analysis. Overall, even though analysed only in Oli-Neu cells and other experimental validations are required, these data suggest a possible dysregulated fatty acids and myelin lipids synthesis pathways in both AGC1 deficiency models and that may be derived from an impairment of epigenetic regulation of the proteins/enzymes' transcription. Whether this effect on genes involved in myelin lipids metabolism is a concomitant or a consequential effect induced by the aberrant epigenetic regulation of proliferation ad differentiation pathways verified by Poeta et al. (2021), remains to be clarified.

Anyway, upstream of these alterations there would be the downregulation of AGC1. Indeed, its silencing affects the transport of aspartate for NAA synthesis but also brings to MAS failure, forcing the cells towards anaerobic metabolism, in which pyruvate is mainly converted into lactate, rather than entering TCA cycle, for acetyl-CoA production. This would hamper the total acetyl groups availability, necessary for epigenetic and proteins modifications but also for myelin lipid synthesis (Profilo et al. 2017; Poeta et al. 2021). Since this crucial role of AGC1 and MAS in controlling the cell bioenergetics (Broeks et al. 2021), and given the well-established link between metabolites concentrations and epigenetic modifications (Zijun Wang et al. 2018), a targeted metabolomic analysis of major metabolites involved in TCA cycle and glycolytic pathways was performed on Oli-Neu control and silenced cell, pellets and culture media, to unravel differences in these compounds which can give us clues on the energetic status of the affected cells. Through collaboration with laboratory of Professor Laura Mercolini (University of Bologna) and Metabolomics Core Technology Platform (EMBL - Germany), we identified several metabolites, whose concentrations were seen altered upon AGC1 silencing. Specifically, these comprise aspartate and NAA, which are less abundant in silenced cells, respect to control one, mimicking the pathological conditions seen in AGC1 deficiency patients (Wibom et al. 2009). A switch towards anaerobic glycolysis was testified by increased concentration of lactate, deriving from conversion of pyruvate, rather than entering the TCA cycle for ATP/acetyl-CoA production (Wu, Lee, and Xiong 2023). This shift, considering also the increased in CoA and NAD levels measured in silenced cells, could be possible through pyruvate

dehydrogenase inhibition, induced by these cofactors (Shurubor et al. 2020). In turn, a more glycolytic metabolism can reduce the availability of other metabolites, as 2-oxoglutarate, a TCA cycle intermediate, essential for glutamine synthesis. This indeed, was found consecutively less abundant - together with glutamate- in siAGC1 Oli-Neu cells, respect to control. These amino acids are crucial for proliferation and OPCs differentiation (Spitzer et al. 2016). Ultimately, reduction of leucine and isoleucine, key ketogenic branched-chain amino acids, was detected in silenced cells. This could impair the replenishment of acetyl-CoA pool of the cells, reducing acetyl moieties availability, for histone acetylation, but also myelin lipids synthesis (Sperringer, Addington, and Hutson 2017a; Bixel and Hamprecht 1995). Taken together, these results highlight a dysregulation of the metabolic profile of silenced Oli-neu cells, upon AGC1 silencing.

One class of enzymes mainly subjected to metabolites availability are sirtuins. They are NAD-dependent deacetylases, involved in a plethora of biological functions (DNA stress repair, metabolism, and cell cycle progression), which are responsible of protein and histones acetylation (Mei et al. 2016; Carafa et al. 2016). Thus, since Poeta et al. (2021) have already analyzed and measured the expression and activity profile of HDACs and given the altered levels of NAD detected in Oli-Neu silenced cells, we decided to investigate sirtuins expression in both our AGC1 deficiency models. Although SIRT1 didn't show any statistical differences in siAGC1 Oli-Neu cells neither in heterozygous spheres, its phosphorylated isoform was seen upregulated in $AGC1^{+/-}$ spheres. Phosphorylation of this sirtuins could activated or inactivated this protein, causing different results. Indeed, previous studies have shown that SIRT1 activation could deacetylases SREBP1 (Walker et al. 2010), causing its ubiquitination and degradation. This in turn could explain the alterations on fatty acids synthesis pathways and hypomyelination seen in patients (Wibom et al. 2009) and mouse models (Profilo et al. 2017) of AGC1 deficiency. In parallel, role of SIRT1 in oligodendrogenesis was confirmed by Rafalski et al. (2013a), which measured a consequently increment in OPCs pool from Neural Precursor Cells, upon its inactivation. This finding is in line with our model of NSCs that, upon increase of p-SIRT1, spontaneously tend to differentiate towards neuronal and astrocytic lineage (Petralla et al. 2019).

Regarding SIRT2, surprisingly, no expression was detected in both control and silenced Oli-Neu cells, whereas it resulted downregulated in heterozygous spheres. This discrepancy could be derived by the differences among the two models, even though SIRT2 is generally more expressed in mature oligodendrocytes rather than OPCs (Ji, Doucette, and Nazarali 2011). However, more in depth analysis are required to clarify its absence or undetectable abundance in Oli-Neu cells. Concerning its expression in $AGC1^{+/-}$ neurospheres instead, all its three distinct isoforms presented a downregulation, but only for the two that are constitutively expressed in cytoplasm, it is statistically

significant; while not for the third one, which has no deacetylase activity and is localized in the nucleus (Rack et al. 2014b). Since compartmentalized NAD pools exist, in mitochondria, cytosol and nucleus, we hypothesized that the different isoforms, residing in different organelles, can be subjected to distinct NAD concentrations, which could affect the sirtuins expression and activity (Zhang et al. 2019). Further experiments will be required, using subcellular fractionation, to validate this hypothesis. Overall, SIRT2 downregulation was however already linked to hypomyelination, and this could also suggest a role of this sirtuin in myelin alterations detected in AGC1 deficiency patients (Wibom et al. 2009; Y. Wang et al. 2019). In silenced Oli-Neu, other alterations were seen for SIRT3 and 5, whose activities are mainly related to glucose metabolism and their upregulation correlated with induction of glycolysis (Mei et al. 2016), a metabolic state already suggested for this AGC1 deficiency model. Conversely, the lightest isoform of SIRT6 was seen less expressed in heterozygous neurospheres, respect to wild-type ones. This protein, with its deacetylase activity, can inhibit SREBP1, through three distinct mechanisms: repressing its transcription, hindering the proteolytic cleavage or activating AMPk, which hampers SREBP1 activity (Elhanati et al. 2013). Overall, these results about sirtuins expression highlight a novel level of metabolic and epigenetic alterations in both AGC1 deficiency models, all traceable to the carrier misfunction.

Since these metabolome and epigenome dysregulations mainly affect the proliferation and differentiation processes in OPCs and NSCs (Poeta et al. 2021), we try to rebalance them, performing supplementations with ketone bodies and branched-chain amino acids. The reasons for this choice reside in the beneficial effects seen in AGC1 deficiency patients, subjected to ketogenic diet (Dahlin et al. 2015) and the ability of these compounds to replenish acetyl-CoA pool and/or TCA cycle intermediates within the cell (Sperringer, Addington, and Hutson 2017a; Poduslo and Miller 1991; Düking et al. 2022). Firstly, we assessed the possible beneficial consequences of these supplementations on proliferation deficits. Thus, using real-time imaging tools, as LiveCyte and Incucyte S3 (Centro di Ricerca Biomedica Applicata, Bologna), we monitor the growth of Oli-Neu and neurospheres respectively, treated with these compounds. In OPCs culture, the most effective concentrations on siAGC1 cells were Bhb 10 mM, AcAc 1 mM, Leu/Ile at 400 mg/l, and Val 200 mg/l. These can recover completely the reduced proliferation of silenced cells, when used alone. Instead, we revealed modest effects for those combinations with lowest concentrations of all compounds. This is probably due to an increase in acidaemia, for what concerns BCAAs supplementations (Sperringer, Addington, and Hutson 2017a); while hyperactivation of OXPHOS and consequent ROS accumulation can reduce the proliferation rate, when too higher concentrations of KBs are added to cell medium (Andreyev, Kushnareva, and Starkov 2005).

Similarly, these supplementations have induced favourable effects on neurospheres proliferation. For this model, two distinct parameters were considered to assess proliferation recovery: the object count and the total area. For ketone bodies, the outcome for object count were just modest, since they seemed not altering the number of cells; whereas a more pronounced increased of total area respect to untreated heterozygous spheres, were detected for Bhb 2,5 mM and AcAc 1 mM. Instead, amino acids induced a peak of objects numbers, even before the 4th day in culture, for AGC1$^{+/-}$ neurospheres, respect to untreated one, which generally show delayed growth. This effect was seen for total area as well, with an increment of spheres size upon treatment with Leu/Ile at 800 mg/l and Val at 200 mg/l. Also, for this model, combinations of KBs or BCAAs just induced modest results. Overall, this testifies a positive outcome of KBs and BCAAs supplementations over Oli-Neu and Neurospheres proliferation defects, probably induced by different contributions of these compounds to cell metabolism. Indeed, ketogenic bodies have already known to have different beneficial effects, from neuroprotective and antioxidant (Imdad et al. 2022) to anti-epileptic ones (Murugan and Boison 2020). More interestingly, KBs can be metabolized more efficiently than glucose, in developing brain, for energy production, sustaining the cell bioenergetics and refurnishing acetyl-CoA pool (Tepavčević 2021). These metabolites could be used for common metabolic pathways but also for fatty acids synthesis or proteins acetylation. Their supplementations were already seen to be effective in AGC1 deficiency models, by Pérez-Liébana et al. (2020), in which acetyl-CoA probably is used to restore NAA production and the metabolic defects. In addition, recent studies have highlighted the role as HDACs inhibitor of Bhb (Newman and Verdin 2017). This, together with recycle of acetyl groups deriving from HDAC activity (Moffett et al. 2013), could increase the level of histone acetylation (Qin, Ma, and Yan 2022), in these AGC1 deficiency models. In parallel, BCAAs are essential anabolic compounds, involved in replenishment of acetyl-CoA and TCA cycle intermediates (as succinyl-CoA) through carbon skeletal catabolism (Sperringer, Addington, and Hutson 2017a) and as nitrogen donors, for other amino acids synthesis (glutamine and glutamate, primarily; Conway et al. 2012). Leucine and isoleucine, since their ketogenic nature, can also be converted to ketones, producing similar beneficial effects of KBs supplementations (Sperringer, Addington, and Hutson 2017a; Bixel and Hamprecht 1995). Furthermore, they can activate mTORC1 complex, one of the most important pathways involved in control of cell proliferation. This would, in turn, induces the transcription of lipogenic genes, such as *SREBP1* (Dong et al. 2018; Condon and Sabatini 2019). The consequential result could be the improvement of myelin lipids synthesis and hypomyelination, seen in AGC1 deficiency patients. Moreover, BCAAs essential role in brain metabolism was seen for other pathologies, such as Alzheimer disease, in which hiPS-derived astrocytes display an altered BCAAs catabolism, with harmful effects also on leucine-derived aspartate production (Salcedo et al. 2021).

In summary, through different mechanisms, as replenishing acetyl moieties availability or sustaining cell metabolism, these compounds can boost the proliferation of AGC1 deficiency models.

Upon screening of KBs and BCAAs for pro-proliferative effects, we tested the most effective concentrations on differentiation analysis. Indeed, especially in OPCs/OLs, balance between proliferation and differentiation is extremely important to achieve the correct maturation and creation of fully functional myelinating oligodendrocytes (Emery 2010; Emery and Lu 2015). From Immunofluorescence analysis, Oli-Neu silenced cells, subjected to KBs and BCAAs, showed a reduction of CNPase, a marker for mature oligodendrocytes (Barateiro and Fernandes 2014), thus, they seemed to favour a shift towards a less differentiated phenotype. Quite similarly, all compounds have induced upregulation of Nestin in heterozygous spheres, marker of stemness (A. R. Kriegstein and Götz 2003), speeded up their self-renewal and proliferative capacity. These results are in line with the increase in proliferation rate, detected by LiveCyte and Incucyte systems, since less differentiated cells generally tend to proliferate more rapidly. Even though with some differences, we noted a more extended effect of some compounds to other lineage-specific markers, as well. For example, combinations of all branched-chain amino acids have induced an increase in DCX, marker of neuronal commitment. This agrees with previous studies in which BCAAs supplementations were added for the complete differentiation of hiPS cells towards mature neuronal cultures, mainly through oxidative metabolism induction (Bifari et al. 2020). Similarly, leucine, isoleucine and valine hold a central role in oligodendrocyte and brain development, and their altered levels can induce Maple Syrup Urine Disease (when in excess; Harris et al. 2005) or leukodystrophy (when they lack; She et al. 2013). Reduced BCAAs availability can affect the myelin lipids formation and oligodendrocyte maturation process (She et al. 2013; Kohnke et al. 2021), hence, their supplementations could rescue the OLs specification marker expression, Olig2, in neurospheres and act on mTORC1 signalling during following steps OL differentiation. Concerning KBs, previous finding has revealed a Bhb-dependent increment in PDGFRα positive cells, with increase in OPC proliferation and differentiation, in Cuprizone-induced demyelinating mouse model of multiple sclerosis (Sun et al. 2022). Even though in NSCs, nor Bhb neither AcAc induced a statistical increment of Olig2 expression, we suggest that this treatment can restore an earlier markers dysregulation, as those related to Nestin and PDGFRα expression, but not the oligodendrocyte specification itself. Moreover, in Cuprizone-related models, Bhb can mainly exert its role as an antioxidant agent, rather than acting on cell metabolism and epigenetics (Zhitian Wang et al. 2023), as required in AGC1 deficiency models. Despite the intrinsic differences, these results support a role of these compounds in recovery of proliferation and differentiation defects in AGC1 deficiency models.

From Poeta et al. (2021), we verified that proliferative and differentiative defects derive from the altered epigenetic regulation. As stated before, this in turn can be affected by the metabolites' availability (Zijun Wang et al. 2018). For this reason, as last analysis, we verified if, upon supplementations, histones acetylation/methylation have been restored. A preliminary analysis with Western Blot was done, at two distinct time-points: one at the initial phase of the treatment, and one at the end of the analysis period. This would help us to understand : i) if KBs and BCAAs supplementations have a role in epigenetic modifications, ii) if the possible modifications induce at the epigenetic landscape, by the treatments, are necessary for the initiation and/or the maintenance of the proliferative/differentiative recovery. In summary, results from supplementations of KBs and BCAAs on siAGC1 Oli-Neu cells reported a different time and mode of action, with statistical differences for Bhb and AcAc effects on histone methylation, whereas BCAAs on histone acetylation, at 72 and 24 hours, after start of the treatment, respectively. This can highlight a differential modality for these compounds to influence the epigenetic modifications but more in-depth analysis is required. From literature, for KBs, controversial data were obtained on their effects on histone acetylation, since the acetyl-CoA, deriving from their catabolism, can be used by the cells for energy production, rather than replenishing the acetyl groups availability, for histone modifications (Dąbek et al. 2020). In addition, respect to glucose, Bhb is able to reduce just two moles of NAD^+, creating an excess, which can be used to activate NAD-dependent enzymes and proteins, such as sirtuins. Since an increment of NAD concentrations was detected in silenced Oli-Neu cells, Bhb supplementation can be harmful, creating a further increase in this metabolite level, that could abrogate the possible effects of this compound on histone acetylation, by activation of sirtuins (Ungaro et al. 2022). On the other hand, KBs supplementations were seen effective on histone methylation at 72 hours. Bhb ability to increase histone methylation status was already assessed by Dąbek et al. (2020), which highlighted the essential role of this compound, together with glycine, in replenishing the acetyl-CoA pool for SAM (S-adenosylmethionine) synthesis. This cofactor is the methyl groups donor, responsible for histone and DNA methylation (Fig. 6.1; He et al. 2023). Therefore, increment of acetyl-CoA and SAM could induce histone methylation, upon KBs supplementation, in siAGC1 cells. In general, histone methylation is associated with repressive chromatin state (Berry, Wang, and Lu 2020) but in OPCs, this modification is crucial in the initial phase of these cells' maturation, to repress the expression of genes involved in myelination (Hernandez and Casaccia 2015b). Moreover, distinct lysine methylations were identified by Liu et al. (2015), in the transition of NSCs to OLs, passing through OPCs stage, suggesting a central role of these modifications respectively: i) in neural stem cells, for the early loss of neurogenic ability; ii) in oligodendrocyte precursors, for the repression of genes involved in excitability and ion channels. Therefore, the increase of histone methylation could

explain the positive effects of KBs supplementation on proliferation and differentiation of OPCs AGC1 deficiency model, by suppressing the transcription of genes related to mature phenotype.

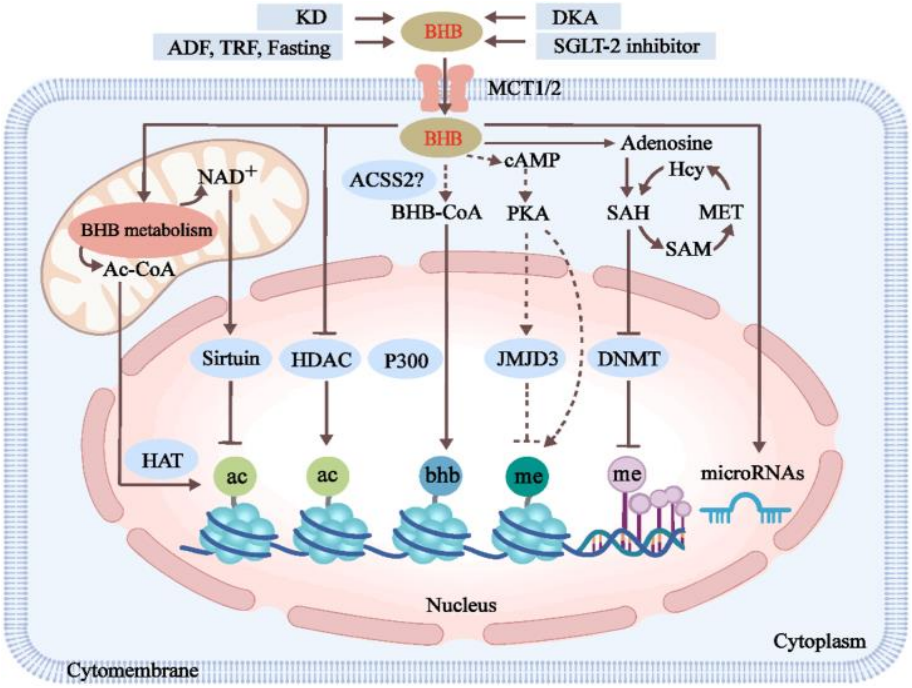

Fig. 6.1 Effect of β-hydroxybutyrate on epigenetic landscape, through action on histone/DNA modifications, microRNAs and metabolism (He et al. 2023)

An opposite situation was instead revealed upon BCAAs supplementations. Indeed, just a slight increase of histone methylation was accompanied by a more profound increment in histone 3 acetylation status of siAGC1 cells, respect to untreated ones, at 24 hours. This could be derived by the ketogenic nature of leucine and isoleucine, which through their catabolism, can be converted to acetyl-CoA (Bixel and Hamprecht 1995; Sperringer, Addington, and Hutson 2017a). Since these compounds induce cells towards a more oxidative metabolism, this can prompt the glucose usage for energy production, whereas acetyl groups, deriving from BCAAs catabolism, directly for histone modifications (Bifari et al. 2020). Given the central role of histone acetylation in OPCs maturation (Hernandez and Casaccia 2015b), their increase at the initial phase of the treatment can explain the beneficial effects of BCAAs supplementations on proliferation and differentiation of siAG1 Oli-Neu cells.

Overall, on OPCs, an epigenetic influence of KBs and BCAAs supplementations, both for induction and maintenance of proliferation/differentiation recovery, was detected. However, why these compounds exert such different effects on epigenetic landscape remains to be clarified. In addition, this preliminary analysis has just verified the possible variations of total histone 3 acetylation/methylation status. It didn't give us more detailed information on the residues-specific histone modifications, for which more focused experiments are required, as mass spectrometry or ChIP-seq. These techniques could also verify if the altered epigenetic profile matches to the promoters

of genes involved in proliferation and differentiation. In addition, further experiments, combining the KBs and BCAAs, could be a promising approach, which fuses the positive outcomes exerted by both classes of compounds. This latter could also be more effective for neurospheres too, which, in this last analysis, didn't show any measurable variations on their histones modifications status, upon KBs neither BCAAs supplementations. This discrepancy can be derived by the highly complex nature of this model, constituted by mixed pool of different neural precursors. Each cell type indeed is characterized by distinct metabolic and proteins set, which affects differently the cell and the whole neurosphere metabolism. Disaggregation of the spheres at single cells and sorting them accordingly to their lineage marker, to verify each cell contribution and epigenetic landscape, can be a valuable tool to better analysed this 3D model.

At the end, preliminary experiments on iPS-derived Neural Progenitors supported the presence of similar proliferation defects also in patients' cell lines, respect to control ones. This opens the way to future experiments to determine if similar alterations at differentiation, epigenetic and metabolic processes are present, in this pathology model, as well. This could justify the possible use of KBs and BCAAs supplementations to recover their defects and give new insights on the potential therapeutic effects of ketogenic diet on AGC1 deficiency patients.

7. CONCLUSION

One of the major features of AGC1 deficiency is the reduced levels of N-acetyl aspartate, which resembles the main myelin precursor (Wibom et al. 2009). This in turn could hamper the myelination process, causing hypomyelination in AGC1 deficiency patients (Falk et al. 2014). From previous studies in our laboratory on OPCs and NSCs AGC1 deficiency models, we identified as the cause of this myelination defects, the altered proliferation and differentiation mechanisms (Petralla et al. 2019). This involves the reduced proliferative rate of both models and the higher tendency to differentiate prematurely, in OLs. While, upstream, a blockage of OPCs specification is present, in neural stem cells model. Poeta et al. (2021) subsequently identified as the causative process of these defects the alteration of epigenetic and transcriptional regulation of proliferation and maturation, which diminishes the fully functional pool of OPCs and myelinating OLs, causing the hypomyelination, seen in patients (Wibom et al. 2009). Here, in this thesis, we demonstrated that AGC1 silencing influences the whole transcriptional and epigenetic profile, through RNA-seq and ATAC-seq, highlighting down/upregulation of genes involved in other pathways, such as the fatty acids and myelin lipids synthesis pathway, always through an aberrant histone and chromatin remodelling process. Then, this analysis was extended to the metabolome, which has revealed different metabolites concentrations, between silenced OPCs and controls, most of which comprise TCA cycle intermediates, amino acids and cofactors (CoA and NAD). These metabolic alterations could also explain the abnormal expression levels -in both AGC1 deficiency models- of sirtuins, NAD-dependent deacetylases, which control proteins/histone deacetylation and directly link to nutrients/metabolites availability. Starting from these discoveries and given the beneficial effects of ketogenic diet/ketones treatment on AGC1 deficiency patients/mouse models (Dahlin et al. 2015; Pérez-Liébana et al. 2020), we performed ketone bodies and branched-chain amino acids supplementation on OPCs and NSCs AGC1 deficiency models. These have brought proliferation and differentiation recovery with specifically: increase in the proliferation rate –at least respect to untreated cells- and induction towards less differentiated phenotype, with increment of Nestin expression (stemness marker), reduced CNPase, DCX and GFAP (marker of mature OLs, neuronal and astrocytic lineage, respectively) and for some compounds, also increase of Olig2 (marker of OPCs specification). To unravel if the mechanistic link between KBs/BCAAs supplementations and the restoration of proliferation/differentiation mechanisms lies in the epigenetic modifications' recovery, upon metabolites rebalance, we quantified the total histone 3 acetylation and methylation status, after treatment. This general analysis gave us essential information on KBs and BCAAs mode and time of action, mainly on OPCs cultures; whereas from the slight differences detected in NSC 3D model, we obtained insights for future analysis, based on more focused, precise and sensible tools,

as mass spectrometry, for the single lysine modifications. These will let us deepen the overall epigenetic landscape and its alterations, upon AGC1 downregulation, on our *in vitro* models and obtained more detailed cues on the possible mechanism of action of ketogenic diet on patients' pathological processes. Moreover, from preliminary experiments of human Induced Pluripotent Stem Cells, differentiated into Neural Progenitors, we discovered a similar slowdown of proliferation in patients' cell lines, respect to controls. This lays the foundation for further experiments with supplementations on this AGC1 deficiency model as well, to detect differences and similarities with mouse-deriving cell lines, but also to find a possible therapeutic intervention that can overcome the ketogenic diet side effects (Qu et al. 2021).

8. REFERENCES

Ahmed, Sohail. 2009. “The Culture of Neural Stem Cells.” *Journal of Cellular Biochemistry* 106 (1): 1–6. https://doi.org/10.1002/jcb.21972.

Amaral, Ana I., Joana M. Tavares, Ursula Sonnewald, and Mark R. N. Kotter. 2016. “Oligodendrocytes: Development, Physiology and Glucose Metabolism.” In , 275–94. https://doi.org/10.1007/978-3-319-45096-4_10.

Amoedo, N.D., G. Punzi, E. Obre, D. Lacombe, A. De Grassi, C.L. Pierri, and R. Rossignol. 2016. “AGC1/2, the Mitochondrial Aspartate-Glutamate Carriers.” *Biochimica et Biophysica Acta (BBA) - Molecular Cell Research* 1863 (10): 2394–2412. https://doi.org/10.1016/j.bbamcr.2016.04.011.

Andreyev, A. Yu., Yu. E. Kushnareva, and A. A. Starkov. 2005. “Mitochondrial Metabolism of Reactive Oxygen Species.” *Biochemistry (Moscow)* 70 (2): 200–214. https://doi.org/10.1007/s10541-005-0102-7.

Antontseva, E. V., and N. P. Bondar. 2021. “Chromatin Remodeling in Oligodendrogenesis.” *Vavilov Journal of Genetics and Breeding* 25 (5): 573–79. https://doi.org/10.18699/VJ21.064.

Arco, Araceli del, and Jorgina Satrústegui. 1998. “Molecular Cloning of Aralar, a New Member of the Mitochondrial Carrier Superfamily That Binds Calcium and Is Present in Human Muscle and Brain.” *Journal of Biological Chemistry* 273 (36): 23327–34. https://doi.org/10.1074/jbc.273.36.23327.

Ariyannur, Prasanth S., John R. Moffett, Chikkathur N. Madhavarao, Peethambaran Arun, Nisha Vishnu, David M. Jacobowitz, William C. Hallows, John M. Denu, and Aryan M.A. Namboodiri. 2010a. “Nuclear-cytoplasmic Localization of Acetyl Coenzyme a Synthetase-1 in the Rat Brain.” *Journal of Comparative Neurology* 518 (15): 2952–77. https://doi.org/10.1002/cne.22373.

———. 2010b. “Nuclear-cytoplasmic Localization of Acetyl Coenzyme a Synthetase-1 in the Rat Brain.” *Journal of Comparative Neurology* 518 (15): 2952–77. https://doi.org/10.1002/cne.22373.

Augustin, Katrin, Aziza Khabbush, Sophie Williams, Simon Eaton, Michael Orford, J Helen Cross, Simon J R Heales, Matthew C Walker, and Robin S B Williams. 2018. “Mechanisms of Action for the Medium-Chain Triglyceride Ketogenic Diet in Neurological and Metabolic Disorders.” *The Lancet Neurology* 17 (1): 84–93. https://doi.org/10.1016/S1474-4422(17)30408-8.

Balboni, N., Babini, G., Poeta, E., Protti, M., Mercolini, L., Magnifico, M. C., Barile, S. N., Massenzio, F., Pignataro, A., Giorgi, F. M., Lasorsa, F. M., & Monti, B. (2024). Transcriptional and metabolic effects of aspartate-glutamate carrier isoform 1 (AGC1) downregulation in mouse oligodendrocyte precursor cells (OPCs). Cellular & molecular biology letters, 29(1), 44. https://doi.org/10.1186/s11658-024-00563-z

Barateiro, Andreia, and Adelaide Fernandes. 2014. “Temporal Oligodendrocyte Lineage Progression: In Vitro Models of Proliferation, Differentiation and Myelination.” *Biochimica et Biophysica Acta, 1843, 1917-1929.*

Beattie, Robert, and Simon Hippenmeyer. 2017. “Mechanisms of Radial Glia Progenitor Cell Lineage Progression.” *FEBS Letters* 591 (24): 3993–4008. https://doi.org/10.1002/1873-3468.12906.

Benjamini, Yoav. 2010. “Discovering the False Discovery Rate.” *J. R. Stat. Soc. Series B Stat. Methodol.* 72 (4): 405–16.

Bergmann, Olaf, Kirsty L. Spalding, and Jonas Frisén. 2015. “Adult Neurogenesis in Humans.” *Cold Spring Harbor Perspectives in Biology* 7 (7): a018994. https://doi.org/10.1101/cshperspect.a018994.

Berry, Kalen, Jiajia Wang, and Q Richard Lu. 2020. “Epigenetic Regulation of Oligodendrocyte Myelination in developmental Disorders and Neurodegenerative Diseases.” *F1000Res.* 9 (February).

Bifari, Francesco, Sissi Dolci, Emanuela Bottani, Annachiara Pino, Marzia Di Chio, Stefania Zorzin, Maurizio Ragni, et al. 2020. “Complete Neural Stem Cell (NSC) Neuronal Differentiation Requires a Branched Chain Amino Acids-Induced Persistent Metabolic Shift towards Energy Metabolism.” *Pharmacological Research* 158 (August): 104863. https://doi.org/10.1016/j.phrs.2020.104863.

Biname, F., D. Sakry, L. Dimou, V. Jolivel, and J. Trotter. 2013. “NG2 Regulates Directional Migration of Oligodendrocyte Precursor Cells via Rho GTPases and Polarity Complex Proteins.” *Journal of Neuroscience* 33 (26): 10858–74. https://doi.org/10.1523/JNEUROSCI.5010-12.2013.

Bixel, Maria Gabriele, and Bernd Hamprecht. 1995. “Generation of Ketone Bodies from Leucine by Cultured Astroglial Cells.” *Journal of Neurochemistry* 65 (6): 2450–61. https://doi.org/10.1046/j.1471-4159.1995.65062450.x.

Boggs, J. M. 2006. “Myelin Basic Protein: A Multifunctional Protein.” *Cellular and Molecular Life Sciences* 63 (17): 1945–61. https://doi.org/10.1007/s00018-006-6094-7.

Bölsterli, Bigna K., Eugen Boltshauser, Luigi Palmieri, Johannes Spenger, Michaela Brunner-Krainz, Felix Distelmaier, Peter Freisinger, et al. 2022. “Ketogenic Diet Treatment of Defects in the Mitochondrial Malate Aspartate Shuttle and Pyruvate Carrier.” *Nutrients* 14 (17): 3605. https://doi.org/10.3390/nu14173605.

Bott, Alex J., I-Chen Peng, Yongjun Fan, Brandon Faubert, Lu Zhao, Jinyu Li, Sarah Neidler, et al. 2015. “Oncogenic Myc Induces Expression of Glutamine Synthetase through Promoter Demethylation.” *Cell Metabolism* 22 (6): 1068–77. https://doi.org/10.1016/j.cmet.2015.09.025.

Broeks, Melissa H., Clara D. M. van Karnebeek, Ronald J. A. Wanders, Judith J. M. Jans, and Nanda M. Verhoeven-Duif. 2021. “Inborn Disorders of the Malate Aspartate Shuttle.” *Journal of Inherited Metabolic Disease* 44 (4): 792–808. https://doi.org/10.1002/jimd.12402.

Camargo, Nutabi, Andrea Goudriaan, Anne-Lieke F. van Deijk, Willem M. Otte, Jos F. Brouwers, Hans Lodder, David H. Gutmann, et al. 2017. “Oligodendroglial Myelination Requires Astrocyte-Derived Lipids.” *PLOS Biology* 15 (5): e1002605. https://doi.org/10.1371/journal.pbio.1002605.

Camargo, Nutabi, August B Smit, and Mark H G Verheijen. 2009. “SREBPs: SREBP Function in Glia-Neuron Interactions.” *FEBS J.* 276 (3): 628–36.

Carafa, Vincenzo, Dante Rotili, Mariantonietta Forgione, Francesca Cuomo, Enrica Serretiello, Gebremedhin Solomon Hailu, Elina Jarho, Maija Lahtela-Kakkonen, Antonello Mai, and Lucia Altucci. 2016. "Sirtuin Functions and Modulation: From Chemistry to the Clinic." *Clinical Epigenetics* 8 (1): 61. https://doi.org/10.1186/s13148-016-0224-3.

Castelo-Branco, Gonçalo, Tobias Lilja, Karolina Wallenborg, Ana M. Falcão, Sueli C. Marques, Aileen Gracias, Derek Solum, et al. 2014. "Neural Stem Cell Differentiation Is Dictated by Distinct Actions of Nuclear Receptor Corepressors and Histone Deacetylases." *Stem Cell Reports* 3 (3): 502–15. https://doi.org/10.1016/j.stemcr.2014.07.008.

Cavicchioli, Maria Vittoria, Mariangela Santorsola, Nicola Balboni, Daniele Mercatelli, and Federico Manuel Giorgi. 2022. "Prediction of Metabolic Profiles from Transcriptomics Data in Human Cancer Cell Lines." *Int. J. Mol. Sci.* 23 (7).

Chakrabarty, Ram Prosad, and Navdeep S. Chandel. 2021. "Mitochondria as Signaling Organelles Control Mammalian Stem Cell Fate." *Cell Stem Cell* 28 (3): 394–408. https://doi.org/10.1016/j.stem.2021.02.011.

Chen, Li, Zhigang Miao, and Xingshun Xu. 2017. "β-Hydroxybutyrate Alleviates Depressive Behaviors in Mice Possibly by Increasing the Histone3-Lysine9-β-Hydroxybutyrylation." *Biochemical and Biophysical Research Communications* 490 (2): 117–22. https://doi.org/10.1016/j.bbrc.2017.05.184.

CHEN, Q.W., X.Y. ZHU, Y.Y. LI, and Z.Q. MENG. 2014. "Epigenetic Regulation and Cancer (Review)." *Oncology Reports* 31 (2): 523–32. https://doi.org/10.3892/or.2013.2913.

Choi, Hyun Woo, Yean Ju Hong, Jong Soo Kim, Hyuk Song, Ssang Gu Cho, Hojae Bae, Changsung Kim, Sung June Byun, and Jeong Tae Do. 2017. "In Vivo Differentiation of Induced Pluripotent Stem Cells into Neural Stem Cells by Chimera Formation." *PLOS ONE* 12 (1): e0170735. https://doi.org/10.1371/journal.pone.0170735.

Condon, Kendall J., and David M. Sabatini. 2019. "Nutrient Regulation of MTORC1 at a Glance." *Journal of Cell Science* 132 (21). https://doi.org/10.1242/jcs.222570.

Conway, Gregory D., Melanie A. O'Bara, Bansi H. Vedia, Suyog U. Pol, and Fraser J. Sim. 2012. "Histone Deacetylase Activity Is Required for Human Oligodendrocyte Progenitor Differentiation." *Glia* 60 (12): 1944–53. https://doi.org/10.1002/glia.22410.

Cope, Elise C., and Elizabeth Gould. 2019. "Adult Neurogenesis, Glia, and the Extracellular Matrix." *Cell Stem Cell* 24 (5): 690–705. https://doi.org/10.1016/j.stem.2019.03.023.

Dąbek, Arkadiusz, Martyna Wojtala, Luciano Pirola, and Aneta Balcerczyk. 2020. "Modulation of Cellular Biochemistry, Epigenetics and Metabolomics by Ketone Bodies. Implications of the Ketogenic Diet in the Physiology of the Organism and Pathological States." *Nutrients* 12 (3): 788. https://doi.org/10.3390/nu12030788.

Dahlin, Maria, Daniel A Martin, Zandra Hedlund, Monica Jonsson, Ulrika von Döbeln, and Anna Wedell. 2015. "The Ketogenic Diet Compensates for AGC1 Deficiency and Improves." *Epilepsia* 56 (11): e176–81.

Darnell, Diana, and Scott F. Gilbert. 2017. "Neuroembryology." *WIREs Developmental Biology* 6 (1). https://doi.org/10.1002/wdev.215.

Delsite, Robert, Sushant Kachhap, Ramaswamy Anbazhagan, Edward Gabrielson, and Keshav K Singh. 2002. “Nuclear Genes Involved in Mitochondria-to-Nucleus Communication in Breast Cancer Cells.” *Molecular Cancer* 1 (1): 6. https://doi.org/10.1186/1476-4598-1-6.

Dimas, Penelope, Laura Montani, Jorge A Pereira, Daniel Moreno, Martin Trötzmüller, Clay F Gerber Joanne and Semenkovich, Harald C Köfeler, and Ueli Suter. 2019. “CNS Myelination and Remyelination Depend on Fatty Acid by Oligodendrocytes.” *Elife* 8 (May).

Dong, X., Z. Zhou, L. Wang, B. Saremi, A. Helmbrecht, Z. Wang, and J.J. Loor. 2018. “Increasing the Availability of Threonine, Isoleucine, Valine, and Leucine Relative to Lysine While Maintaining an Ideal Ratio of Lysine:Methionine Alters Mammary Cellular Metabolites, Mammalian Target of Rapamycin Signaling, and Gene Transcription.” *Journal of Dairy Science* 101 (6): 5502–14. https://doi.org/10.3168/jds.2017-13707.

Düking, Tim, Lena Spieth, Stefan A. Berghoff, Lars Piepkorn, Annika M. Schmidke, Miso Mitkovski, Nirmal Kannaiyan, et al. 2022. “Ketogenic Diet Uncovers Differential Metabolic Plasticity of Brain Cells.” *Science Advances* 8 (37). https://doi.org/10.1126/sciadv.abo7639.

Dutta, Dipankar J., Andleeb Zameer, John N. Mariani, Jingya Zhang, Linnea Asp, Jimmy Huynh, Sean Mahase, et al. 2014. “Combinatorial Actions of Tgfβ and Activin Ligands Promote Oligodendrocyte Development and CNS Myelination.” *Development* 141 (12): 2414–28. https://doi.org/10.1242/dev.106492.

Eberlé, Delphine, Bronwyn Hegarty, Pascal Bossard Pascale and Ferré, and Fabienne Foufelle. 2004. “SREBP Transcription Factors: Master Regulators of Lipid.” *Biochimie* 86 (11): 839–48.

Elbaz, Benayahu, and Brian Popko. 2019. “Molecular Control of Oligodendrocyte Development.” *Trends in Neurosciences* 42 (4): 263–77. https://doi.org/10.1016/j.tins.2019.01.002.

Elhanati, Sivan, Yariv Kanfi, Alexander Varvak, Asael Roichman, Ilana Carmel-Gross, Shaul Barth, Gilad Gibor, and Haim Y. Cohen. 2013. “Multiple Regulatory Layers of SREBP1/2 by SIRT6.” *Cell Reports* 4 (5): 905–12. https://doi.org/10.1016/j.celrep.2013.08.006.

Emery, Ben. 2010. “Regulation of Oligodendrocyte Differentiation and Myelination.” *Science* 330 (6005): 779–82. https://doi.org/10.1126/science.1190927.

Emery, Ben, and Q Richard Lu. 2015. “Transcriptional and Epigenetic Regulation of Oligodendrocyte and Myelination in the Central Nervous System.” *Cold Spring Harb. Perspect. Biol.* 7 (9): a020461.

Falk, Marni J, Dong Li, Xiaowu Gai, Elizabeth McCormick, Emily Place, Francesco M Lasorsa, Frederick G Otieno, et al. 2014. “AGC1 Deficiency Causes Infantile Epilepsy, Abnormal, and Reduced N-Acetylaspartate.” *JIMD Rep.* 14 (February): 77–85.

Fancy, Stephen P.J., Chao Zhao, and Robin J.M. Franklin. 2004. “Increased Expression of Nkx2.2 and Olig2 Identifies Reactive Oligodendrocyte Progenitor Cells Responding to Demyelination in the Adult CNS.” *Molecular and Cellular Neuroscience* 27 (3): 247–54. https://doi.org/10.1016/j.mcn.2004.06.015.

Fruttiger, Marcus, Linda Karlsson, Anita C. Hall, Alexandra Abramsson, Andrew R. Calver, Hans Boström, Karen Willetts, et al. 1999. “Defective Oligodendrocyte Development and Severe

Hypomyelination in PDGF-A Knockout Mice." *Development* 126 (3): 457–67. https://doi.org/10.1242/dev.126.3.457.

Garcia Corrales, Aida V., Mansour Haidar, Jeroen F. J. Bogie, and Jerome J. A. Hendriks. 2021. "Fatty Acid Synthesis in Glial Cells of the CNS." *International Journal of Molecular Sciences* 22 (15): 8159. https://doi.org/10.3390/ijms22158159.

Gibson, Erin M., David Purger, Christopher W. Mount, Andrea K. Goldstein, Grant L. Lin, Lauren S. Wood, Ingrid Inema, et al. 2014. "Neuronal Activity Promotes Oligodendrogenesis and Adaptive Myelination in the Mammalian Brain." *Science* 344 (6183). https://doi.org/10.1126/science.1252304.

Gil-Perotín, Sara, María Duran-Moreno, Arantxa Cebrián-Silla, Mónica Ramírez, Paula García-Belda, and José Manuel García-Verdugo. 2013. "Adult Neural Stem Cells From the Subventricular Zone: A Review of the Neurosphere Assay." *The Anatomical Record* 296 (9): 1435–52. https://doi.org/10.1002/ar.22746.

Grandi, Fiorella C., Hailey Modi, Lucas Kampman, and M. Ryan Corces. 2022. "Chromatin Accessibility Profiling by ATAC-Seq." *Nature Protocols* 17 (6): 1518–52. https://doi.org/10.1038/s41596-022-00692-9.

Greer, Judith M, and Marjorie B Lees. 2002. "Myelin Proteolipid Protein—the First 50 Years." *The International Journal of Biochemistry & Cell Biology* 34 (3): 211–15. https://doi.org/10.1016/S1357-2725(01)00136-4.

Harris, Robert A., Mandar Joshi, Nam Ho Jeoung, and Mariko Obayashi. 2005. "Overview of the Molecular and Biochemical Basis of Branched-Chain Amino Acid Catabolism." *The Journal of Nutrition* 135 (6): 1527S-1530S. https://doi.org/10.1093/jn/135.6.1527S.

He, Yanqiu, Xi Cheng, Tingting Zhou, Dongze Li, Juan Peng, Yong Xu, and Wei Huang. 2023. "β-Hydroxybutyrate as an Epigenetic Modifier: Underlying Mechanisms and Implications." *Heliyon* 9 (11): e21098. https://doi.org/10.1016/j.heliyon.2023.e21098.

Hernandez, Marylens, and Patrizia Casaccia. 2015a. "Interplay between Transcriptional Control and Chromatin in the Oligodendrocyte Lineage." *Glia* 63 (8): 1357–75.

———. 2015b. "Interplay between Transcriptional Control and Chromatin Regulation in the Oligodendrocyte Lineage." *Glia* 63 (8): 1357–75. https://doi.org/10.1002/glia.22818.

Hisahara, Shin, Naotoshi Iwahara, Takashi Matsushita, Syuuichirou Suzuki, Akihiro Matsumura, Mai Fujikura, Kazuki Yokokawa, et al. 2021. "SIRT1 Decelerates Morphological Processing of Oligodendrocyte Cell Lines and Regulates the Expression of Cytoskeleton-Related Oligodendrocyte Proteins." *Biochemical and Biophysical Research Communications* 546 (March): 7–14. https://doi.org/10.1016/j.bbrc.2021.01.095.

Hochstim, Christian, Benjamin Deneen, Agnès Lukaszewicz, Qiao Zhou, and David J. Anderson. 2008. "Identification of Positionally Distinct Astrocyte Subtypes Whose Identities Are Specified by a Homeodomain Code." *Cell* 133 (3): 510–22. https://doi.org/10.1016/j.cell.2008.02.046.

Imdad, Kaleem, Turki Abualait, Ammara Kanwal, Ziyad Tareq AlGhannam, Shahab Bashir, Anum Farrukh, Sahir Hameed Khattak, Raidah Albaradie, and Shahid Bashir. 2022. "The Metabolic

Role of Ketogenic Diets in Treating Epilepsy." *Nutrients* 14 (23): 5074. https://doi.org/10.3390/nu14235074.

Jalil, Md. Abdul, Laila Begum, Laura Contreras, Beatriz Pardo, Mikio Iijima, Meng Xian Li, Milagros Ramos, et al. 2005. "Reduced N-Acetylaspartate Levels in Mice Lacking Aralar, a Brain- and Muscle-Type Mitochondrial Aspartate-Glutamate Carrier." *Journal of Biological Chemistry* 280 (35): 31333–39. https://doi.org/10.1074/jbc.M505286200.

Jensen, Josephine B., and Malin Parmar. 2006. "Strengths and Limitations of the Neurosphere Culture System." *Molecular Neurobiology* 34 (3): 153–62. https://doi.org/10.1385/MN:34:3:153.

Ji, S., J. R. Doucette, and A. J. Nazarali. 2011. "Sirt2 Is a Novel in Vivo Downstream Target of Nkx2.2 and Enhances Oligodendroglial Cell Differentiation." *Journal of Molecular Cell Biology* 3 (6): 351–59. https://doi.org/10.1093/jmcb/mjr009.

Knaap, Jan A. van der, and C. Peter Verrijzer. 2016. "Undercover: Gene Control by Metabolites and Metabolic Enzymes." *Genes & Development* 30 (21): 2345–69. https://doi.org/10.1101/gad.289140.116.

Kohnke, Sara, Sophie Buller, Danae Nuzzaci, Katherine Ridley, Brian Lam, Helena Pivonkova, Marie A. Bentsen, et al. 2021. "Nutritional Regulation of Oligodendrocyte Differentiation Regulates Perineuronal Net Remodeling in the Median Eminence." *Cell Reports* 36 (2): 109362. https://doi.org/10.1016/j.celrep.2021.109362.

Koper, Jan W., Elly C. Zeinstra, Matthijs Lopes-Cardozo, and Lambert M.G. Van Golde. 1984. "Acetoacetate and Glucose as Substrates for Lipid Synthesis by Rat Brain Oligodendrocytes and Astrocytes in Serum-Free Culture." *Biochimica et Biophysica Acta (BBA) - Lipids and Lipid Metabolism* 796 (1): 20–26. https://doi.org/10.1016/0005-2760(84)90233-9.

Kouzarides, Tony. 2007. "Chromatin Modifications and Their Function." *Cell* 128 (4): 693–705. https://doi.org/10.1016/j.cell.2007.02.005.

Kriegstein, Arnold, and Arturo Alvarez-Buylla. 2009. "The Glial Nature of Embryonic and Adult Neural Stem Cells." *Annual Review of Neuroscience* 32 (1): 149–84. https://doi.org/10.1146/annurev.neuro.051508.135600.

Kriegstein, Arnold R., and Magdalena Götz. 2003. "Radial Glia Diversity: A Matter of Cell Fate." *Glia* 43 (1): 37–43. https://doi.org/10.1002/glia.10250.

Kumar, Ashutosh, Vikas Pareek, A Muneeb Faiq, K Sanjib Ghosh, and Chiman Kumari. 2019. "ADULT NEUROGENESIS IN HUMANS: A Review of Basic Concepts, History, Current Research, and Clinical Implications." *Innovations in Clinical Neuroscience*.

Kunji, Edmund R. S., Martin S. King, Jonathan J. Ruprecht, and Chancievan Thangaratnarajah. 2020. "The SLC25 Carrier Family: Important Transport Proteins in Mitochondrial Physiology and Pathology." *Physiology* 35 (5): 302–27. https://doi.org/10.1152/physiol.00009.2020.

Lahunta, Alexander de, Eric N. Glass, and Marc Kent. 2016. "Embryonic Development of the Central Nervous System." *Veterinary Clinics of North America: Small Animal Practice* 46 (2): 193–216. https://doi.org/10.1016/j.cvsm.2015.10.011.

Laule, Cornelia, Irene M. Vavasour, Shannon H. Kolind, David K.B. Li, Tony L. Traboulsee, G.R. Wayne Moore, and Alex L. MacKay. 2007. “Magnetic Resonance Imaging of Myelin.” *Neurotherapeutics* 4 (3): 460–84. https://doi.org/10.1016/j.nurt.2007.05.004.

LI, LIAN TAO, GUAN JIANG, QIAN CHEN, and JUN NIAN ZHENG. 2015. “Ki67 Is a Promising Molecular Target in the Diagnosis of Cancer (Review).” *Molecular Medicine Reports* 11 (3): 1566–72. https://doi.org/10.3892/mmr.2014.2914.

Lim, Daniel A., and Arturo Alvarez-Buylla. 2016. “The Adult Ventricular–Subventricular Zone (V-SVZ) and Olfactory Bulb (OB) Neurogenesis.” *Cold Spring Harbor Perspectives in Biology* 8 (5): a018820. https://doi.org/10.1101/cshperspect.a018820.

Lin, Huai-Peng, Zhou-Li Cheng, Ruo-Yu He, Meng-Xin Song Lei and Tian, Li-Sha Zhou, Beezly S Groh, Wei-Ren Liu, et al. 2016. “Destabilization of Fatty Acid Synthase by Acetylation Inhibits De Novo Lipogenesis and Tumor Cell Growth.” *Cancer Res.* 76 (23): 6924–36.

Liu, Jia, and Patrizia Casaccia. 2010. “Epigenetic Regulation of Oligodendrocyte Identity.” *Trends in Neurosciences* 33 (4): 193–201. https://doi.org/10.1016/j.tins.2010.01.007.

Liu, Jia, Laura Magri, Fan Zhang, Nidaa O. Marsh, Stefanie Albrecht, Jimmy L. Huynh, Jasbir Kaur, et al. 2015. “Chromatin Landscape Defined by Repressive Histone Methylation during Oligodendrocyte Differentiation.” *The Journal of Neuroscience* 35 (1): 352–65. https://doi.org/10.1523/JNEUROSCI.2606-14.2015.

López-Muguruza, Eneritz, and Carlos Matute. 2023. “Alterations of Oligodendrocyte and Myelin Energy Metabolism in Multiple Sclerosis.” *International Journal of Molecular Sciences* 24 (16): 12912. https://doi.org/10.3390/ijms241612912.

Love, Michael I, Charlotte Soneson, Peter F Hickey, Lisa K Johnson, N Tessa Pierce, Lori Shepherd, Martin Morgan, and Rob Patro. 2020. “Tximeta: Reference Sequence Checksums for Provenance in RNA-Seq.” *PLoS Comput. Biol.* 16 (2): e1007664.

Luong, A, V C Hannah, M S Brown, and J L Goldstein. 2000. “Molecular Characterization of Human Acetyl-CoA Synthetase, an enzyme Regulated by Sterol Regulatory Element-Binding Proteins.” *J. Biol. Chem.* 275 (34): 26458–66.

Malatesta, Paolo, Eva Hartfuss, and Magdalena Götz. 2000. “Isolation of Radial Glial Cells by Fluorescent-Activated Cell Sorting Reveals a Neuronal Lineage.” *Development* 127 (24): 5253–63. https://doi.org/10.1242/dev.127.24.5253.

Matilainen, Olli, Pedro M. Quirós, and Johan Auwerx. 2017. “Mitochondria and Epigenetics – Crosstalk in Homeostasis and Stress.” *Trends in Cell Biology* 27 (6): 453–63. https://doi.org/10.1016/j.tcb.2017.02.004.

Mei, Zhen, Xian Zhang, Jiarong Yi, Junjie Huang, Jian He, and Yongguang Tao. 2016. “Sirtuins in Metabolism, DNA Repair and Cancer.” *Journal of Experimental & Clinical Cancer Research* 35 (1): 182. https://doi.org/10.1186/s13046-016-0461-5.

Menn, Bénédicte, Jose Manuel Garcia-Verdugo, Cynthia Yaschine, Oscar Gonzalez-Perez, David Rowitch, and Arturo Alvarez-Buylla. 2006. “Origin of Oligodendrocytes in the Subventricular Zone of the Adult Brain.” *The Journal of Neuroscience* 26 (30): 7907–18. https://doi.org/10.1523/JNEUROSCI.1299-06.2006.

Menzies, Keir J., Hongbo Zhang, Elena Katsyuba, and Johan Auwerx. 2016. “Protein Acetylation in Metabolism — Metabolites and Cofactors.” *Nature Reviews Endocrinology* 12 (1): 43–60. https://doi.org/10.1038/nrendo.2015.181.

Meyer, Niklas, and Johanne Egge Rinholm. 2021. “Mitochondria in Myelinating Oligodendrocytes: Slow and Out of Breath?” *Metabolites* 11 (6): 359. https://doi.org/10.3390/metabo11060359.

Moffett, John R., Peethambaran Arun, Prasanth S. Ariyannur, and Aryan M. A. Namboodiri. 2013. “N-Acetylaspartate Reductions in Brain Injury: Impact on Post-Injury Neuroenergetics, Lipid Synthesis, and Protein Acetylation.” *Frontiers in Neuroenergetics* 5. https://doi.org/10.3389/fnene.2013.00011.

Moffett, John R, Brian Ross, Peethambaran Arun, Chikkathur N Madhavarao, and Aryan M A Namboodiri. 2007. “N-Acetylaspartate in the CNS: From Neurodiagnostics To.” *Prog. Neurobiol.* 81 (2): 89–131.

Monnerie, Hubert, Micah Romer, Brigid K Jensen, John S Millar, Kelly L Jordan-Sciutto, Sangwon F Kim, and Judith B Grinspan. 2017. “Reduced Sterol Regulatory Element-Binding Protein (SREBP) Processing through Site-1 Protease (S1P) Inhibition Alters Differentiation in Vitro.” *J. Neurochem.* 140 (1): 53–67.

Montani, Laura. 2021. “Lipids in Regulating Oligodendrocyte Structure and Function.” *Seminars in Cell & Developmental Biology* 112 (April): 114–22. https://doi.org/10.1016/j.semcdb.2020.07.016.

Murugan, Madhuvika, and Detlev Boison. 2020. “Ketogenic Diet, Neuroprotection, and Antiepileptogenesis.” *Epilepsy Research* 167 (November): 106444. https://doi.org/10.1016/j.eplepsyres.2020.106444.

Narine, Mohanlall, and Holly Colognato. 2022. “Current Insights Into Oligodendrocyte Metabolism and Its Power to Sculpt the Myelin Landscape.” *Frontiers in Cellular Neuroscience* 16 (April). https://doi.org/10.3389/fncel.2022.892968.

Newman, John C., and Eric Verdin. 2017. “β-Hydroxybutyrate: A Signaling Metabolite.” *Annual Review of Nutrition* 37 (1): 51–76. https://doi.org/10.1146/annurev-nutr-071816-064916.

Nishiyama, Akiko, Takahiro Shimizu, Amin Sherafat, and William D. Richardson. 2021. “Life-Long Oligodendrocyte Development and Plasticity.” *Seminars in Cell & Developmental Biology* 116 (August): 25–37. https://doi.org/10.1016/j.semcdb.2021.02.004.

Noctor, Stephen C, Verónica Martínez-Cerdeño, Lidija Ivic, and Arnold R Kriegstein. 2004. “Cortical Neurons Arise in Symmetric and Asymmetric Division Zones and Migrate through Specific Phases.” *Nature Neuroscience* 7 (2): 136–44. https://doi.org/10.1038/nn1172.

Noctor, Stephen C., Verónica Martínez-Cerdeño, and Arnold R. Kriegstein. 2008. “Distinct Behaviors of Neural Stem and Progenitor Cells Underlie Cortical Neurogenesis.” *Journal of Comparative Neurology* 508 (1): 28–44. https://doi.org/10.1002/cne.21669.

Nowakowski, Tomasz J., Alex A. Pollen, Carmen Sandoval-Espinosa, and Arnold R. Kriegstein. 2016. “Transformation of the Radial Glia Scaffold Demarcates Two Stages of Human Cerebral Cortex Development.” *Neuron* 91 (6): 1219–27. https://doi.org/10.1016/j.neuron.2016.09.005.

Obernier, Kirsten, and Arturo Alvarez-Buylla. 2019. “Neural Stem Cells: Origin, Heterogeneity and Regulation in the Adult Mammalian Brain.” *Development* 146 (4). https://doi.org/10.1242/dev.156059.

Ormazabal, Aida, Mercedes Casado, Marta Molero-Luis, Julio Montoya, Shamima Rahman, Sophie-Beth Aylett, Iain Hargreaves, Simon Heales, and Rafael Artuch. 2015. “Can Folic Acid Have a Role in Mitochondrial Disorders?” *Drug Discovery Today* 20 (11): 1349–54. https://doi.org/10.1016/j.drudis.2015.07.002.

Palazuelos, J., M. Klingener, and A. Aguirre. 2014. “TGF Signaling Regulates the Timing of CNS Myelination by Modulating Oligodendrocyte Progenitor Cell Cycle Exit through SMAD3/4/FoxO1/Sp1.” *Journal of Neuroscience* 34 (23): 7917–30. https://doi.org/10.1523/JNEUROSCI.0363-14.2014.

Palmieri, Ferdinando. 2013. “The Mitochondrial Transporter Family SLC25: Identification, Properties and Physiopathology.” *Molecular Aspects of Medicine* 34 (2–3): 465–84. https://doi.org/10.1016/j.mam.2012.05.005.

Palmieri, L., B. Pardo, F.M. Lasorsa, A. del Arco, K. Kobayashi, M. Iijima, M.J. Runswick, et al. 2001. “Citrin and Aralar1 Are Ca2+-Stimulated Aspartate/Glutamate Transporters in Mitochondria.” *The EMBO Journal* 20 (18): 5060–69. https://doi.org/10.1093/emboj/20.18.5060.

Pardo, Beatriz, Eduardo Herrada-Soler, Jorgina Satrústegui, Laura Contreras, and Araceli del Arco. 2022. “AGC1 Deficiency: Pathology and Molecular and Cellular Mechanisms of the Disease.” *International Journal of Molecular Sciences* 23 (1): 528. https://doi.org/10.3390/ijms23010528.

Patro, Rob, Geet Duggal, Michael I Love, Rafael A Irizarry, and Carl Kingsford. 2017. “Salmon Provides Fast and Bias-Aware Quantification of Transcript.” *Nat. Methods* 14 (4): 417–19.

Pebay-Peyroula, Eva, and Gérard Brandolin. 2004. “Nucleotide Exchange in Mitochondria: Insight at a Molecular Level.” *Current Opinion in Structural Biology* 14 (4): 420–25. https://doi.org/10.1016/j.sbi.2004.06.009.

Pérez-Liébana, Irene, María José Casarejos, Andrea Alcaide, Eduardo Herrada-Soler, Irene Llorente-Folch, Laura Contreras, Jorgina Satrústegui, and Beatriz Pardo. 2020. “BOHB Protective Pathways in Aralar-KO Neurons and Brain: An Alternative to Ketogenic Diet.” *The Journal of Neuroscience* 40 (48): 9293–9305. https://doi.org/10.1523/JNEUROSCI.0711-20.2020.

Petralla, Sabrina, Luis Emiliano Peña-Altamira, Eleonora Poeta, Francesca Massenzio, Marco Virgili, Simona Nicole Barile, Luigi Sbano, et al. 2019. “Deficiency of Mitochondrial Aspartate-Glutamate Carrier 1 Leads to Oligodendrocyte Precursor Cell Proliferation Defects Both In Vitro and In Vivo.” *Int. J. Mol. Sci.* 20 (18).

Pfeiffer, Brian, Kuntal Sen, Shagun Kaur, and Kara Pappas. 2020. “Expanding Phenotypic Spectrum of Cerebral Aspartate-Glutamate Isoform 1 (AGC1) Deficiency.” *Neuropediatrics* 51 (2): 160–63.

Pietrocola, Federico, Lorenzo Galluzzi, José Manuel Bravo-San Pedro, Frank Madeo, and Guido Kroemer. 2015. “Acetyl Coenzyme A: A Central Metabolite and Second Messenger.” *Cell Metabolism* 21 (6): 805–21. https://doi.org/10.1016/j.cmet.2015.05.014.

Pino, Annachiara, Guido Fumagalli, Francesco Bifari, and Ilaria Decimo. 2017. “New Neurons in Adult Brain: Distribution, Molecular Mechanisms and Therapies.” *Biochemical Pharmacology* 141 (October): 4–22. https://doi.org/10.1016/j.bcp.2017.07.003.

PODUSLO, S, and K MILLER. 1991. “Ketone Bodies as Precursors for Lipid Synthesis in Neurons, Astrocytes, and Oligodendroglia (Myelin) in Hyperthyroidism, Hyperketonemia and Hypoketonemia.” *Neurochemistry International* 18 (1): 85–88. https://doi.org/10.1016/0197-0186(91)90040-K.

Poeta, Eleonora, Sabrina Petralla, Giorgia Babini, Brunaldo Renzi, Luigi Celauro, Simona Nicole Magnifico Maria Chiara and Barile, Martina Masotti, et al. 2021. “Histone Acetylation Defects in Brain Precursor Cells: A Potential Mechanism Causing Proliferation and Differentiation in Mitochondrial Aspartate-Glutamate Carrier 1 Deficiency.” *Front. Cell. Neurosci.* 15: 773709.

Poitelon, Yannick, Ashley M. Kopec, and Sophie Belin. 2020. “Myelin Fat Facts: An Overview of Lipids and Fatty Acid Metabolism.” *Cells* 9 (4): 812. https://doi.org/10.3390/cells9040812.

Profilo, Emanuela, Luis Emiliano Peña-Altamira, Mariangela Corricelli, Alessandra Castegna, Alberto Danese, Gennaro Agrimi, Sabrina Petralla, et al. 2017. “Down-Regulation of the Mitochondrial Aspartate-Glutamate Carrier Isoform 1 AGC1 Inhibits Proliferation and N-Acetylaspartate Synthesis in Neuro2A Cells.” *Biochimica et Biophysica Acta (BBA) - Molecular Basis of Disease* 1863 (6): 1422–35. https://doi.org/10.1016/j.bbadis.2017.02.022.

Protti, Michele, Marco Cirrincione, Sarah Palano, Eleonora Poeta, Giorgia Babini, Maria Chiara Magnifico, Simona Nicole Barile, et al. 2023. “Targeted Quantitative Metabolic Profiling of Brain-Derived Cell Cultures by Semi-Automated MEPS and LC-MS/MS.” *Journal of Pharmaceutical and Biomedical Analysis* 236 (November): 115757. https://doi.org/10.1016/j.jpba.2023.115757.

Prozorovski, Tim, Jens Ingwersen, Denise Lukas, Peter Göttle, Barbara Koop, Jonas Graf, Reiner Schneider, et al. 2019. “Regulation of Sirtuin Expression in Autoimmune Neuroinflammation: Induction of SIRT1 in Oligodendrocyte Progenitor Cells.” *Neuroscience Letters* 704 (June): 116–25. https://doi.org/10.1016/j.neulet.2019.04.007.

Qin, Luye, Kaijie Ma, and Zhen Yan. 2022. “Rescue of Histone Hypoacetylation and Social Deficits by Ketogenic Diet in a Shank3 Mouse Model of Autism.” *Neuropsychopharmacology* 47 (6): 1271–79. https://doi.org/10.1038/s41386-021-01212-1.

Qu, Changbo, Jaap Keijer, Merel J.W. Adjobo-Hermans, Melissa van de Wal, Tom Schirris, Clara van Karnebeek, Yihang Pan, and Werner J.H. Koopman. 2021. “The Ketogenic Diet as a Therapeutic Intervention Strategy in Mitochondrial Disease.” *The International Journal of Biochemistry & Cell Biology* 138 (September): 106050. https://doi.org/10.1016/j.biocel.2021.106050.

Rack, Johannes G.M., Magali R. VanLinden, Timo Lutter, Rein Aasland, and Mathias Ziegler. 2014a. “Constitutive Nuclear Localization of an Alternatively Spliced Sirtuin-2 Isoform.” *Journal of Molecular Biology* 426 (8): 1677–91. https://doi.org/10.1016/j.jmb.2013.10.027.

———. 2014b. “Constitutive Nuclear Localization of an Alternatively Spliced Sirtuin-2 Isoform.” *Journal of Molecular Biology* 426 (8): 1677–91. https://doi.org/10.1016/j.jmb.2013.10.027.

Rae, Caroline, Aurélie D. Fekete, Mohammed A. Kashem, Fatima A. Nasrallah, and Stefan Bröer. 2012. “Metabolism, Compartmentation, Transport and Production of Acetate in the Cortical Brain Tissue Slice.” *Neurochemical Research* 37 (11): 2541–53. https://doi.org/10.1007/s11064-012-0847-5.

Rafalski, Victoria A., Peggy P. Ho, Jamie O. Brett, Duygu Ucar, Jason C. Dugas, Elizabeth A. Pollina, Lionel M. L. Chow, et al. 2013a. “Expansion of Oligodendrocyte Progenitor Cells Following SIRT1 Inactivation in the Adult Brain.” *Nature Cell Biology* 15 (6): 614–24. https://doi.org/10.1038/ncb2735.

———. 2013b. “Expansion of Oligodendrocyte Progenitor Cells Following SIRT1 Inactivation in the Adult Brain.” *Nature Cell Biology* 15 (6): 614–24. https://doi.org/10.1038/ncb2735.

Ramos, Milagros, Beatriz Pardo, Irene Llorente-Folch, Takeyori Saheki, Araceli Del Arco, and Jorgina Satrústegui. 2011. “Deficiency of the Mitochondrial Transporter of aspartate/Glutamate Aralar/AGC1 Causes Hypomyelination and neuronal Defects Unrelated to Myelin Deficits in Mouse Brain.” *J. Neurosci. Res.* 89 (12): 2008–17.

Ritchie, Matthew E, Belinda Phipson, Di Wu, Charity W Hu Yifang and Law, Wei Shi, and Gordon K Smyth. 2015. “Limma Powers Differential Expression Analyses For-Sequencing and Microarray Studies.” *Nucleic Acids Res.* 43 (7): e47.

Rosko, Lauren, Victoria N. Smith, Reiji Yamazaki, and Jeffrey K. Huang. 2019. “Oligodendrocyte Bioenergetics in Health and Disease.” *The Neuroscientist* 25 (4): 334–43. https://doi.org/10.1177/1073858418793077.

Rowitch, David H., and Arnold R. Kriegstein. 2010. “Developmental Genetics of Vertebrate Glial–Cell Specification.” *Nature* 468 (7321): 214–22. https://doi.org/10.1038/nature09611.

Ruan, Hai-Bin, and Peter A. Crawford. 2018. “Ketone Bodies as Epigenetic Modifiers.” *Current Opinion in Clinical Nutrition & Metabolic Care* 21 (4): 260–66. https://doi.org/10.1097/MCO.0000000000000475.

Ruijtenberg, Suzan, and Sander van den Heuvel. 2016. “Coordinating Cell Proliferation and Differentiation: Antagonism between Cell Cycle Regulators and Cell Type-Specific Gene Expression.” *Cell Cycle* 15 (2): 196–212. https://doi.org/10.1080/15384101.2015.1120925.

Russell, Oliver M., Gráinne S. Gorman, Robert N. Lightowlers, and Doug M. Turnbull. 2020. “Mitochondrial Diseases: Hope for the Future.” *Cell* 181 (1): 168–88. https://doi.org/10.1016/j.cell.2020.02.051.

Sakurai, Takeshi, Nicolas Ramoz, Marta Barreto, Mihaela Gazdoiu, Nagahide Takahashi, Michael Gertner, Nathan Dorr, et al. 2010. “Slc25a12 Disruption Alters Myelination and Neurofilaments: A Model for a Hypomyelination Syndrome and Childhood Neurodevelopmental Disorders.” *Biological Psychiatry* 67 (9): 887–94. https://doi.org/10.1016/j.biopsych.2009.08.042.

Salcedo, Claudia, Jens V. Andersen, Kasper Tore Vinten, Lars H. Pinborg, Helle S. Waagepetersen, Kristine K. Freude, and Blanca I. Aldana. 2021. “Functional Metabolic Mapping Reveals Highly Active Branched-Chain Amino Acid Metabolism in Human Astrocytes, Which Is

Impaired in IPSC-Derived Astrocytes in Alzheimer's Disease." *Frontiers in Aging Neuroscience* 13 (September). https://doi.org/10.3389/fnagi.2021.736580.

Satrústegui, Jorgina, Beatriz Pardo, and Araceli del Arco. 2007. "Mitochondrial Transporters as Novel Targets for Intracellular Calcium Signaling." *Physiological Reviews* 87 (1): 29–67. https://doi.org/10.1152/physrev.00005.2006.

SCHONBERGER, S. 2004. "Dysmyelination in the Brain of Adolescents and Young Adults with Maple Syrup Urine Disease." *Molecular Genetics and Metabolism* 82 (1): 69–75. https://doi.org/10.1016/j.ymgme.2004.01.016.

She, Pengxiang, Piyawan Bunpo, Judy K. Cundiff, Ronald C. Wek, Robert A. Harris, and Tracy G. Anthony. 2013. "General Control Nonderepressible 2 (GCN2) Kinase Protects Oligodendrocytes and White Matter during Branched-Chain Amino Acid Deficiency in Mice." *Journal of Biological Chemistry* 288 (43): 31250–60. https://doi.org/10.1074/jbc.M113.498469.

Shen, Siming, Juan Sandoval, Victoria A Swiss, Jiadong Li, Jeff Dupree, Robin J M Franklin, and Patrizia Casaccia-Bonnefil. 2008. "Age-Dependent Epigenetic Control of Differentiation Inhibitors Is Critical for Remyelination Efficiency." *Nature Neuroscience* 11 (9): 1024–34. https://doi.org/10.1038/nn.2172.

Shurubor, Yevgeniya I., Arthur J. L. Cooper, Andrey B. Krasnikov, Elena P. Isakova, Yulia I. Deryabina, M. Flint Beal, and Boris F. Krasnikov. 2020. "Changes of Coenzyme A and Acetyl-Coenzyme A Concentrations in Rats after a Single-Dose Intraperitoneal Injection of Hepatotoxic Thioacetamide Are Not Consistent with Rapid Recovery." *International Journal of Molecular Sciences* 21 (23): 8918. https://doi.org/10.3390/ijms21238918.

Silbereis, John C., Sirisha Pochareddy, Ying Zhu, Mingfeng Li, and Nenad Sestan. 2016. "The Cellular and Molecular Landscapes of the Developing Human Central Nervous System." *Neuron* 89 (2): 248–68. https://doi.org/10.1016/j.neuron.2015.12.008.

Soldán, M., and Istvan Pirko. 2012. "Biogenesis and Significance of Central Nervous System Myelin." *Seminars in Neurology* 32 (01): 009–014. https://doi.org/10.1055/s-0032-1306381.

Sperringer, Justin E., Adele Addington, and Susan M. Hutson. 2017a. "Branched-Chain Amino Acids and Brain Metabolism." *Neurochemical Research* 42 (6): 1697–1709. https://doi.org/10.1007/s11064-017-2261-5.

———. 2017b. "Branched-Chain Amino Acids and Brain Metabolism." *Neurochemical Research* 42 (6): 1697–1709. https://doi.org/10.1007/s11064-017-2261-5.

Spitzer, Sonia, Katrin Volbracht, Iben Lundgaard, and Ragnhildur T. Káradóttir. 2016. "Glutamate Signalling: A Multifaceted Modulator of Oligodendrocyte Lineage Cells in Health and Disease." *Neuropharmacology* 110 (November): 574–85. https://doi.org/10.1016/j.neuropharm.2016.06.014.

Sugimoto, Yoshihiko, Masahiko Taniguchi, Takeshi Yagi, Yoshio Akagi, Yoshiaki Nojyo, and Nobuaki Tamamaki. 2001. "Guidance of Glial Precursor Cell Migration by Secreted Cues in the Developing Optic Nerve." *Development* 128 (17): 3321–30. https://doi.org/10.1242/dev.128.17.3321.

Sun, Wei, Min Wen, Min Liu, Qingpeng Wang, Quiqin Liu, Lanjie Li, Hans-Christian Siebert, Gabriele Loers, Ruiyan Zhang, and Ning Zhang. 2022. “Effect of β-Hydroxybutyrate on Behavioral Alterations, Molecular and Morphological Changes in CNS of Multiple Sclerosis Mouse Model.” *Frontiers in Aging Neuroscience* 14 (December). https://doi.org/10.3389/fnagi.2022.1075161.

Takahashi, Kazutoshi, and Shinya Yamanaka. 2006. “Induction of Pluripotent Stem Cells from Mouse Embryonic and Adult Fibroblast Cultures by Defined Factors.” *Cell* 126 (4): 663–76. https://doi.org/10.1016/j.cell.2006.07.024.

Taormina, Giusi, Antonio Russo, Mario A. Latteri, and Mario G. Mirisola. 2019. “Mitochondrion at the Crossroad Between Nutrients and Epigenome.” *Frontiers in Endocrinology* 10 (October). https://doi.org/10.3389/fendo.2019.00673.

Tepavčević, Vanja. 2021. “Oligodendroglial Energy Metabolism and (Re)Myelination.” *Life* 11 (3): 238. https://doi.org/10.3390/life11030238.

Thangaratnarajah, Chancievan, Jonathan J. Ruprecht, and Edmund R. S. Kunji. 2014. “Calcium-Induced Conformational Changes of the Regulatory Domain of Human Mitochondrial Aspartate/Glutamate Carriers.” *Nature Communications* 5 (1): 5491. https://doi.org/10.1038/ncomms6491.

Tsai, Hui-Hsin, Jianqin Niu, Roeben Munji, Dimitrios Davalos, Junlei Chang, Haijing Zhang, An-Chi Tien, et al. 2016. “Oligodendrocyte Precursors Migrate along Vasculature in the Developing Nervous System.” *Science* 351 (6271): 379–84. https://doi.org/10.1126/science.aad3839.

Ungaro, Paola, Immacolata Cristina Nettore, Fabiana Franchini, Giuseppe Palatucci, Giovanna Muscogiuri, Annamaria Colao, and Paolo Emidio Macchia. 2022. “Epigenome Modulation Induced by Ketogenic Diets.” *Nutrients* 14 (15): 3245. https://doi.org/10.3390/nu14153245.

Urenjak, J, SR Williams, DG Gadian, and M Noble. 1993. “Proton Nuclear Magnetic Resonance Spectroscopy Unambiguously Identifies Different Neural Cell Types.” *The Journal of Neuroscience* 13 (3): 981–89. https://doi.org/10.1523/JNEUROSCI.13-03-00981.1993.

Walker, Amy K., Fajun Yang, Karen Jiang, Jun-Yuan Ji, Jennifer L. Watts, Aparna Purushotham, Olivier Boss, et al. 2010. “Conserved Role of SIRT1 Orthologs in Fasting-Dependent Inhibition of the Lipid/Cholesterol Regulator SREBP.” *Genes & Development* 24 (13): 1403–17. https://doi.org/10.1101/gad.1901210.

Waly, Bilal El, Magali Macchi, Myriam Cayre, and Pascale Durbec. 2014. “Oligodendrogenesis in the Normal and Pathological Central Nervous System.” *Frontiers in Neuroscience* 8 (June). https://doi.org/10.3389/fnins.2014.00145.

Wang, Yan, Jingqi Yang, Tingting Hong, Xiongjin Chen, and Lili Cui. 2019. “SIRT2: Controversy and Multiple Roles in Disease and Physiology.” *Ageing Research Reviews* 55 (November): 100961. https://doi.org/10.1016/j.arr.2019.100961.

Wang, Zhitian, Tian Li, Miaoyu Du, Lei Zhang, Linling Xu, Hao Song, and Junjian Zhang. 2023. “β-Hydroxybutyrate Improves Cognitive Impairment Caused by Chronic Cerebral Hypoperfusion via Amelioration of Neuroinflammation and Blood-Brain Barrier Damage.”

Brain Research Bulletin 193 (February): 117–30. https://doi.org/10.1016/j.brainresbull.2022.12.011.

Wang, Zijun, Hai Long, Christopher Chang, Ming Zhao, and Qianjin Lu. 2018. "Crosstalk between Metabolism and Epigenetic Modifications in Autoimmune Diseases: A Comprehensive Overview." *Cellular and Molecular Life Sciences* 75 (18): 3353–69. https://doi.org/10.1007/s00018-018-2864-2.

Wellen, Kathryn E, and Craig B Thompson. 2012. "A Two-Way Street: Reciprocal Regulation of Metabolism And." *Nat. Rev. Mol. Cell Biol.* 13 (4): 270–76.

Wiame, Elsa, Donatienne Tyteca, Nathalie Pierrot, François Collard, Mustapha Amyere, Gaëtane Noel, Jonathan Desmedt, et al. 2010. "Molecular Identification of Aspartate N-Acetyltransferase and Its Mutation in Hypoacetylaspartia." *Biochemical Journal* 425 (1): 127–39. https://doi.org/10.1042/BJ20091024.

Wibom, Rolf, Francesco M Lasorsa, Michela Töhönen Virpi and Barbaro, Fredrik H Sterky, Karin Kucinski Thomas and Naess, Monica Jonsson, Ciro L Pierri, Ferdinando Palmieri, and Anna Wedell. 2009. "AGC1 Deficiency Associated with Global Cerebral Hypomyelination." *N. Engl. J. Med.* 361 (5): 489–95.

Wu, Anika, Daehoon Lee, and Wen-Cheng Xiong. 2023. "Lactate Metabolism, Signaling, and Function in Brain Development, Synaptic Plasticity, Angiogenesis, and Neurodegenerative Diseases." *International Journal of Molecular Sciences* 24 (17): 13398. https://doi.org/10.3390/ijms241713398.

Xie, Zhongyu, Di Zhang, Dongjun Chung, Zhanyun Tang, He Huang, Lunzhi Dai, Shankang Qi, et al. 2016. "Metabolic Regulation of Gene Expression by Histone Lysine β-Hydroxybutyrylation." *Molecular Cell* 62 (2): 194–206. https://doi.org/10.1016/j.molcel.2016.03.036.

Xin, Wendy, Yevgeniya A. Mironova, Hui Shen, Rosa A.M. Marino, Ari Waisman, Wouter H. Lamers, Dwight E. Bergles, and Antonello Bonci. 2019. "Oligodendrocytes Support Neuronal Glutamatergic Transmission via Expression of Glutamine Synthetase." *Cell Reports* 27 (8): 2262-2271.e5. https://doi.org/10.1016/j.celrep.2019.04.094.

Xu, Sutong, Xi Zhang, Chenming Liu, Qiulu Liu, Huazhen Chai, Yuping Luo, and Siguang Li. 2021. "Role of Mitochondria in Neurodegenerative Diseases: From an Epigenetic Perspective." *Frontiers in Cell and Developmental Biology* 9 (August). https://doi.org/10.3389/fcell.2021.688789.

Yan, Jing, Xiaole Tang, Zhi-qiang Zhou, Jie Zhang, Yilin Zhao, Shiyong Li, and Ailin Luo. 2022. "Sirtuins Functions in Central Nervous System Cells under Neurological Disorders." *Frontiers in Physiology* 13 (August). https://doi.org/10.3389/fphys.2022.886087.

Zhang, Jingpu, Jie Tao, Yun Ling, Feng Li, Xuewei Zhu, Li Xu, Mei Wang, Shuye Zhang, Charles E. McCall, and Tie Fu Liu. 2019. "Switch of NAD Salvage to de Novo Biosynthesis Sustains SIRT1-RelB-Dependent Inflammatory Tolerance." *Frontiers in Immunology* 10 (October). https://doi.org/10.3389/fimmu.2019.02358.

Zhao, Xianghui, Xuelian He, Xiaolei Han, Yang Yu, Feng Ye, Ying Chen, ThaoNguyen Hoang, et al. 2010. “MicroRNA-Mediated Control of Oligodendrocyte Differentiation.” *Neuron* 65 (5): 612–26. https://doi.org/10.1016/j.neuron.2010.02.018.

Zhao, Xianghui, Jiang Wu, Minhua Zheng, Fang Gao, and Gong Ju. 2012. “Specification and Maintenance of Oligodendrocyte Precursor Cells from Neural Progenitor Cells: Involvement of MicroRNA-7a.” *Molecular Biology of the Cell*.

Zhou, Qiao, Gloria Choi, and David J. Anderson. 2001. “The BHLH Transcription Factor Olig2 Promotes Oligodendrocyte Differentiation in Collaboration with Nkx2.2.” *Neuron* 31 (5): 791–807. https://doi.org/10.1016/S0896-6273(01)00414-7.

Zhou, Wenjuan, Tiantian Zhao, Jingyi Du, Guangyu Ji, Xinyue Li, Shufang Ji, Wenyu Tian, Xu Wang, and Aijun Hao. 2019. “TIGAR Promotes Neural Stem Cell Differentiation through Acetyl-CoA-Mediated Histone Acetylation.” *Cell Death & Disease* 10 (3): 198. https://doi.org/10.1038/s41419-019-1434-3.